A modelling study on the residual circulation in the North Sea, with the focus on water fluxes through the Strait of Dover

by

Rens van der Linden

June 2014

Committee members:
Prof. dr. Julie D. Pietrzak
Ir. Theo van der Kaaij
Dr. ir Gerben J. de Boer
Dr. ir. Martin Verlaan
Dr. ir. Marcel Zijlema

In order to obtain the academical degree of Master of Science in Hydraulic Engineering

Section of Environmental Fluid Mechanics,
Department of Hydraulic Engineering,
Faculty of Civil Engineering & Geosciences,
Delft University of Technology

Abstract

In this master thesis the residual circulation in the North Sea is investigated. It has been shown that the numerical models used in this thesis (DCSMv5 and DCSMv6) give a rather low representation of the actual circulation pattern in the North Sea. The dominating forces which cause residual currents in the North Sea are the tidal forcings, meteorological forcings and density variations. Their variability over the whole domain, as well as their interaction with bottom topography and the earth's rotation, leads to a variety of different processes. Since it is difficult to quantify to total transport over the whole North Sea, the focus in this thesis lies on the transports through the Strait of Dover.

Studies on fluxes through the Strait of Dover date back to the late 1920's, where in situ velocity profiles were measured and integrated over the crosssection to make an estimate on residual flows. In later studies different methods were used to obtain valuable information on transports. Use was made of electric potentials through a telephone cable, high frequency radars and modelling studies. Because the magnitude of residual transports is an order of magnitude smaller than short scale movements like tidal oscillations, the estimated transports lack accuracy. They vary between 87000 to 235000 m^3s^{-1}. Dutch ecologists suggests an annual inflow in the order of 100000 m^3s^{-1}.

In this thesis the state-of-the-art numerical DCSM models of Deltares have been computed in Delft3D-FLOW to investigate the dominant processes in the Strait of Dover. The models cover the complete northwest European continental shelf and calculate depth averaged barotropic flow. The representation of the general North Sea circulation is qualitatively well, except for some highly stratified and density driven areas. However, the in- and outflow of water at the North Sea boundaries is considerably low. The leakage of the radioactive nuclide Antimony-125 from La Hague in 1985 till 1994 has been simulated to give an indication of the spatial varying transit time of the current model. It is shown that in the southern region transit times are simulated to be two times larger than other modelling studies and measurements suggest.

The daily varying residual flow through the Strait of Dover has been investigated by applying a Low-Pass frequency filter to the modelled fluxes. The contribution of tidal residuals are found to be very significant with an average annual flow of 45000 m^3s^{-1}. When meteorological forcings are also taken into account the annual inflow for the year of 2007 equals 56000 m^3s^{-1}. Since meteorological forcings vary throughout the years, a quasi-linear approximation is formulated where the daily residual flow is a function of the wind induced shear stress and wind direction. A correlation of 0.79 is found for this linear approximation. For rapidly varying surface elevations differences between the North Sea and English Channel the approximation fails to give proper estimates.

During the research, model adjustments were made to (1) assess the sensitivity of the fluxes and (2) look for candidate solutions to improve the amount of transport through the Strait of Dover. Physical adjustments have been made by implementing density differences, residual surface level boundaries and a varying bottom roughness. The numerical adjustments were for the largest part based on different discretization methods. In addition, a preliminary computation has been performed in DFlow-FM; a recently developed simulation package which computes on an unstructured grid. Although there are notable differences for each adjustment, the effects are small in comparison with tide and wind induced residuals.

Preface

The thesis in front of you is performed as conclusion of the Master of Science program Hydraulic Engineering at the Faculty of Civil Engineering and Geosciences, Delft University of Technology, the Netherlands. The research has been conducted in collaboration with Deltares, who provided me a workplace, guidance and the needed equipment. The project is funded by the Port of Rotterdam Authority within the framework of the MoS^2 project.

I would like to thank my graduation committee for their supervision during this project. Especial expressions of gratitude go to prof. dr. J.D. Pietrzak, ir. T. van der Kaaij and dr. ir. G.J. de Boer for their continuous guidance and dedication to this project. I also thank dr. ir. M. Verlaan and dr. ir. M. Zijlema for their involvement and interest in this project. All members of Deltares who gave me any kind of support and input are thanked for their available time.

I am very grateful to my brother Tim van der Linden and stepbrother Job Bleeker for an extensive spell and grammar check. I really appreciate the time you took to critically read my thesis.

I thank my close family for their understanding, support and encouragement during the whole period. At last, I thank my fellow musicians for the appropriate distraction during this project.

Rens van der Linden,
June 2014, Delft

Contents

1 Introduction

1.1 Framework

A continual growth in demand of harbour facilities at the Port of Rotterdam has led to several extensions in the past. Because of the scarcity of available land in this area, two extensions were done by reclaiming land from the North Sea. In the 1960's, Maasvlakte 1 was constructed. From 2008 till present another extension called Maasvlakte 2 (MV2) is being build. The sand used for these land reclamations is dredged from the North Sea. The construction process has significant influences on the water quality of the Dutch coastal zone, and in particular the adjacent Rhine ROFI (Region of Freshwater Influence, as defined by Simpson et al. (1993)). Therefore, monitoring the possible affected areas in the Southern North Sea was set as an additional requirement to the Port of Rotterdam for constructing MV2.

The silt and clay material in suspension, together with the particles of biological origin like algae and detritus in the water, are referred to as Suspended Particulate Matter (SPM). The MoS^2 project (Model-Supported Monitoring of SPM) of Deltares aims to provide the Port of Rotterdam with novel and improved means to monitor SPM in the Dutch coastal zone in relation to the construction of MV2 (Blaas et al. (2012)). A series of nested numerical models has been developed to obtain optimal results in an efficient manner. The hydrodynamic structure of the North Sea is computed by the three-dimensional ZUNO-DD model (Zuidelijke Noordzee Domain Decomposition), which covers the whole southern North Sea, including a part of the English Channel. Boundary forcings are obtained from the larger Dutch Continental Shelf Model (DCSM) which covers the whole northwest European continental shelf. The hydrodynamics which are computed with the ZUNO-DD model are linked to the SPM with the use of DELWAQ; an application specialized in water quality and ecology modelling.

The SPM distribution which originates from MV2 is noticeable in a large part of the North Sea, and has an important effect on the ecology. To guarantee quality and accuracy of the model output, proper knowledge on the physics of the North Sea is essential. For the past decade, several studies have been executed on the physics in the Rhine ROFI which are of significant influence on the local SPM distribution. An extensive study on the interaction of tides and stratification in the ROFI area has been performed by De Boer (2009). An extension on this research was done by Van Wiechen (2011), who added the interaction and competition of wind to this system. The North Sea as a whole has been a widely studied subject for the last decades. This is mainly due to the complexity of the hydrodynamics in the North Sea. A thorough review on the North Sea properties is published by Otto et al. (1990). SPM travels along with the general circulation pattern which is present in the North Sea. A proper understanding on this residual circulation is of major importance for the monitoring of possible affected areas by MV2.

Residual currents are in general described as water movements which have specially large characteristic times of variation and can often be approximated by time independent flows over any reasonable period (Nihoul and Ronday (1975)). Residual currents are often an order of magnitude smaller than currents with shorter time scales, like tidal oscillations. This makes it a challenge to properly monitor or simulate the correct residual current. Several disciplines have a different interpretation of a residual current so that it can be properly reproduced. An experimentalist often prefers to regard the residual currents as the residuary flow obtained by subtracting the (computed) main tidal currents from the actual fluid motion. For this interpretation, one can object the large errors which arise due to the uncertainty of the calculated currents. Since the short-scale tidal currents are an order of magnitude larger than the resulting residuals, their possible errors are also significantly larger. However, with the subtraction of these tidal currents their related errors are not removed. The remaining residuals still contain errors which are relatively large, which makes the accuracy of these results rather low. From a mathematical point of view, it is tempting to define the residual currents as the steady state solution of the equations which describe the flow pattern. In other words, all derivatives with respect to time are considered to be zero. This is fundamentally correct, as long as the equations are fully linear. However, this is not the case for oceanic circulation. A better way would be to take a time average of these terms, since the non-linearity's could leave some substantial forcings. Prandle (1978b) did

such a time-averaging for tide induced residuals. However, this mathematical approach is only feasible for very simple or simplified situations, otherwise the computations become too complex to solve. Hydrodynamicists have a still different notion. They define the residual currents as mean currents over a time sufficiently long to cover several tidal periods and thus cancel out most of the tidal contributions. The latter seems to be the most reliable and practical method, with the use of a numerical model a time average can easily be taken while the computational effort stays relatively low. Errors induced by short-scale fluctuations are removed and the desired impact of non-linearity's is still present in the results.

1.2 Objective and approach

The three-dimensional ZUNO-DD model (fig. 1.1) is used to monitor the transport of SPM, nutrients and other dissolved and suspended matters. For a proper age distribution it is essential for the residual circulation to be correct. However, when model results are compared with measurements or other modelling studies, the propagation of these substances appears to be rather low. This indicates the general North Sea circulation, as simulated by ZUNO-DD, to be slower than the actual circulation rate. One of the indicators for the general circulation pattern is the inflow of nutrients form the English Channel through the Strait of Dover. Since the modelled inflow of nutrients is smaller than needed, this problem is generally solved by raising the water level at the southern boundary of the ZUNO-DD model. As a result, the transport through the Strait of Dover increases. However, this method is not desired. A demand arises for a more proper solution to this problem.

The main objective of this thesis is to get a better understanding in the dominating forces causing the large scale residual circulation pattern in the North Sea. Hereby the focus lies on the residual transport through the Strait of Dover and the corresponding processes which are involved. The variability as a function of time is investigated, taking into account the (in)accuracy from the obtained transports. Available theory, measurements and modelling results from past studies are investigated as a starting point. This knowledge is combined with the knowledge gained from numerical modelling. The gained knowledge is used to increase the accuracy and reproduction of the residual flow through the Strait of Dover in the present model.

The dominating forces causing residual currents in the North Sea are the tidal forcings, meteorological forcings, barotropic pressure gradients and baroclinic pressure gradients. Their variability over the whole domain, as well as their interaction with bottom topography and the earth's rotation, leads to a variety of processes. This makes the North Sea circulation a complex system. For the past century a wide range of studies has been performed on the important processes which induce this large scale circulation. These studies are based upon tracer trials, current measurements, theoretical approaches and numerical modelling (see e.g. Davies et al. (1997), Prandle (1978a), Otto et al. (1990), Holt and Proctor (2008)). The dominating processes in the North Sea differ, dependent on the time and location. Therefore the first aim of this thesis is to get a better insight into the presence and significance of the dominating processes at different locations in the North Sea.

Based on theory and analytical solutions an understanding on the circulation is provided. However, there is a certain limit to the knowledge which can be gained from this approach. Non-linearity's and high complexity are very difficult or impossible to solve in this way. Numerical models are the answer to this problem, since they can deal with highly complex systems. However, it should be kept in mind that these models give errors to a certain amount. These errors are based on the numerical computation method and on assumptions made to decrease the computation time. Both errors are inevitable, it is up to the user to find the proper balance between computation time and accuracy. In general, the computation time becomes smaller when the amount of physical assumptions increases.

The ZUNO-DD model is a three dimensional model which covers the whole southern North Sea, including a part of the English Channel. Due to its fine structure and vertical layers, it is able to reproduce a large part of the important physical processes. At first sight this model would be perfect to model residual flow. However, a large part of the residual circulation originates from outside the ZUNO-DD domain. These residuals are implemented as boundary conditions, gained from a larger continental shelf model. Before any reliable computations can be done in ZUNO-DD, the boundary values need to be correct. For

this reason, the model as used for this project is the large continental shelf model. The state-of-the-art model is known as the Dutch Continental Shelf Model version 6 (DCSMv6). It is a large scale model, covering the complete northwest European continental shelf. It ranges from the continental margin west of the British Isles up to the Baltic Sea, and from south France up to the Norwegian Sea. The model domain is shown in figure 1.1. It is a barotropic, depth averaged, model designed for storm surge predictions on the Dutch coast. Due to data assimilation it is unique in its kind, errors in water levels are only up to a few centimetres. The model has never been used for large scale residuals before, even though it provides important boundary conditions to the ZUNO-DD model. This makes it a challenge to obtain proper results, since the model never has been calibrated or validated on residual flows. Since the model is depth averaged, vertical stratification cannot be taken into account during the computations. In addition, a grid size of 2 x 2 km (which is in fact very fine for such a large model) can be to course to reproduce small scale processes. Therefore one should keep in mind that several important processes can't be reproduced properly by the continental shelf model. In addition to the DCSMv6 model its previous version, DCSMv5, also has been used for this research. It has a courser grid structure and covers a smaller area. At the expense of the accuracy of the output, the computation time becomes much smaller. Especially at periods during this project where several adjustments were made, this relatively low computation time was very useful to execute preliminary simulations.

A qualitative analysis on residual circulation will be performed by comparing the general flow pattern with North Sea Circulation studies from the past. For a quantitative analysis this area is too large and complex to compare. Besides, the magnitude and direction of the currents fluctuates as a function of time. It has a time scale in the order of months, seasons or even years. A better result is gained by looking at the water balance of the North Sea. For the present model, the only water based-boundaries of the southern North Sea are in the North between Scotland and Norway, and in the south at the Strait of Dover. The annual residual flow of the latter is relatively small compared to the Northern boundary, only 7% of the total Atlantic inflow comes from the Southern Boundary. Because of its large variability it still has significant influence on the general flow pattern in the North Sea. Therefore, an extensive investigation will be done into residuals through the Strait of Dover.

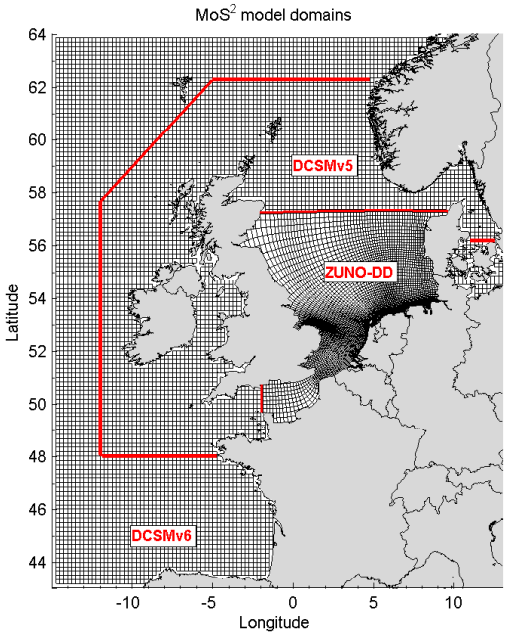

Figure 1.1: Model domains of the MoS^2 project, for DCSMv6 every tenth of a grid cell is shown.

1.3 Outline of this thesis

In Chapter 2 a thorough literature survey is performed. The general, most important, North Sea characteristics are described. In addition, the large scale circulation pattern is treated based on various studies done in the past. For the Strait of Dover, a comprehensive overview of the available measurements and modelling studies is given. Chapter 3 gives a theoretical background for the most relevant processes related to residual circulation. A mathematical description of the relevant processes for both the North Sea and Strait of Dover is given. In Chapter 4 a clear overview of the DCSM properties is given. The initial and boundary conditions are treated, as well as some important numerical approaches behind this computation. In Chapter 5 the model results are analysed in a qualitative way for the whole North Sea, and in a more extensive, quantitative way for the Strait of Dover. A comparison is made with other measurements and modelling studies is done. Adjustments, which are done on the present models during the project, are described in Chapter 6. These adjustments are either based on physical processes, or numerical approaches. Conclusions and recommendations are described in Chapter 7.

2 Literature study

2.1 Scales and scope

The main topic of this thesis is to obtain a better understanding on the residual circulation in the North Sea. To get here, it is chosen to focus on the residual flow through the Strait of Dover as an indicator of this circulation. Altough subsequent chapters will mainly deal with this small entrance of the North Sea, this chapter also looks at the North Sea as a whole. This is done for two reasons. First of all to fit the impact of the flow through the Strait of Dover into the overall domain. Thereafter to give an idea on the main residual structures in the North Sea. The scope of this chapter is therefore to give a brief review on the important physical properties and processes of the complete North Sea.

For general circulation in large water bodies, the main circulation patterns have a large spatial scale. In other words, patterns become noticeable when one looks at the big picture. Therefore the smallest spatial scale considered in this thesis will be in the order of 1 km, up to the complete area in the order of 1000 km. Over the vertical the flow patterns can vary on a much smaller scale. This is mainly due to the possibility of a stratified flow. Therefore all variations in the vertical are considered. The dynamic behaviour of residual patterns is relatively slow; a timescale of 1 day is small enough to monitor the complete dynamic residual structure. Hydrodynamic structures with a smaller time-scale, like tidal fluctuations, are not directly taken into account. Only their impact on the large scale circulation is of importance for this thesis.

The main forcings responsible for residual flow in the North Sea are tidal fluctuations, meteorological forcings, density differences and the earth's rotation. A qualitative view on the impact of these forcings on the residual circulation in the North Sea will be treated in this chapter. Section 2.2 deals with the main characteristics of the North Sea to get the reader familiar with the topic. Also the general North Sea circulation pattern and its variation over time is given as obtained from a literature study. Thereafter section 2.3 gives a thorough literature survey of all important researches done in the past on residual flow through the Strait of Dover.

2.2 Large scale North Sea characteristics

2.2.1 Main characteristics

The North Sea is part of the northwest European continental shelf. It is for the largest part enclosed by land boundaries from the British Isles, Scandinavia and the European continent. Therefore it is usually classified as a marginal sea: A partially enclosed sea adjacent to the open ocean. It is a shallow area since two third of the region has depths of less than 100 m. Along the Norwegian coast a deeper channel-like part is present with depths exceeding 700 m, also known as the Norwegian Trench. A length of around 1000 km and a width of 600 km gives it a surface area of 575.000 km^2 and a volume of 40.000 km^3.

The North Sea is adjacent to the North Atlantic Ocean in the North, between Scotland and Norway. A relative small second connection is in the south via the English Channel through the Strait of Dover. Based on in- and outflow patterns these two water boundaries can be divided into five different sites as shown in figure 2.1. Four of them are responsible for the annual inflow of Atlantic Ocean water, namely the Orkneys-Shetland section(1), the Shetland shelf area (2), the western part of the Norwegian Trench (3) and the Strait of Dover (5). The eastern part of the Norwegian Trench (4) is the only region where North Sea water leaves the shelf sea. A small connection with the Baltic Sea exists via the Skagerrak and Kattegat (6). From here a large amount of brackish water enters the North Sea. The residence time of this water is short though, the major part directly leaves the North Sea through the Norwegian Trench into the Norwegian Sea and North Atlantic Ocean. Various fresh-water bodies debouch in the North Sea. Outflows which are worth mentioning come from the river Rhine, Elbe and lake IJsel with an average annual outflow of 2000 m^3/s, 700 m^3/s and 500 m^3/s respectively[1]. An overview of water transports in and out of the North

[1]River loads were calculated from original monthly flow and nutrient data, supplemented with daily flow data where possible. Mean values were taken from data representing 2002 till 2009. Data was processed from raw data provided by the Environment Agency, the Scottish Environment Protection Agency and the

Section	Mean flow 10^3 m^3s^{-1}
Orkneys-Shetland inflow	490
Shetland shelf inflow	500
Norwegian channel inflow	1230
Norwegian channel outflow	2303
Strait of Dover inflow	160
Kattegat inflow	15
River-based inflow	11

Table 2.1: Annual in- and outflows in at the North Sea boundaries, values obtained from Winther and Johannessen (2006)

Sea is given in table 2.1, these values are based on measurements and model outputs from various authors (Winther and Johannessen (2006)).

Tidal forcing is one of the dominant features in the North Sea. Tidal motions are induced by planetary movements and the earth's rotation. Although this has some direct impact on the water level and currents in the North Sea, the main tidal forcings arise via the boundaries with the Atlantic Ocean. The prevailing tidal constituents are the semi-diurnal 'M2' tide with an amplitude of about 1 m and the semi-diurnal 'S2' with an amplitude of about 10 cm. The tidal propagation in the North Sea can be described as a rotary or amphidromic system; at the North West boundaries tidal waves enter the North Sea and travel as so-called Kelvin waves along the land boundaries of the British Isles to the South, here they turn direction to the east and propagate to the North along the Dutch

National River Flow Archive, UK; S.M. van Leeuwen, Cefas, pers. comm.

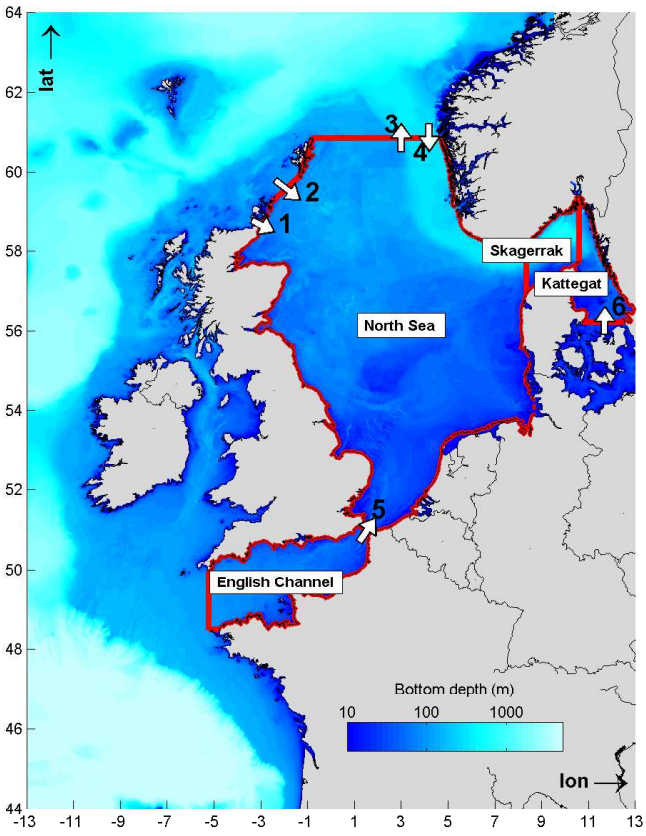

Figure 2.1: Water bodies on the European Continental Shelf. The North Sea is adjacent to the Atlantic Ocean at five different side namely the Orkneys-Shetland section(1), Shetland shelf area (2), Norwegian Trench (3,4) and Strait of Dover (5). Further water sources are the Baltic Water via the Kattegat (6) and river inflow (various locations along the coast)

coast. Maximum water levels are observed directly at the boundaries, and decrease when going further offshore. At certain points in the North Sea the tidal amplitude equals zero, this is called the amphidromic point. Kelvin waves rotate around these points. During their propagation the amplitude of the boundary tidal waves is further adapted by the local geometry. In addition, new constituents with higher frequencies are introduced due to bottom friction. The first tidal map originates back to the early 20th century by Proudman and Doodson (1924). This map is shown in figure 2.2a. Here, only the tidal amplitude of the dominating M2 constituent is shown. The co-tidal and co-range lines are based on observational data only.

At the surface level several meteorological effects influence (a part of) the underlying water column. From these effects, wind forcing is responsible for the largest currents after tides over most of the North Sea. Especially at locations where tidal influences are weak (for example Norway), wind dominates the current structure. The largest storms occur in winter when the water-column is in general well-mixed. Other effects are the atmospheric pressure with its corresponding inverse barometer effect and solar heating which increases the surface temperature. Time scales of typical meteorological effects vary from a couple of hours (storm conditions) to a couple of years (North Atlantic Oscillation).

The spreading of water types often is used as an indicator of residual circulation. Since surface temperature is not a conservative property, salinity is the only large scale indicator of water types which has been extensively measured. Other indicators like chemicals and optical properties are also used in many studies, but have in the overall picture two disadvantages. First, most of the time they only are restricted to smaller areas which do not cover the whole North Sea. Second, they are almost never conservative. Still, they can give a good qualitative image. Lee (1980) divided the North Sea in a couple of 'hydrographical regions' as shown in figure 2.2b. These regions are based upon nearly a century of measured water properties such as salinity, radionuclides, residual current data and numerical modelling.

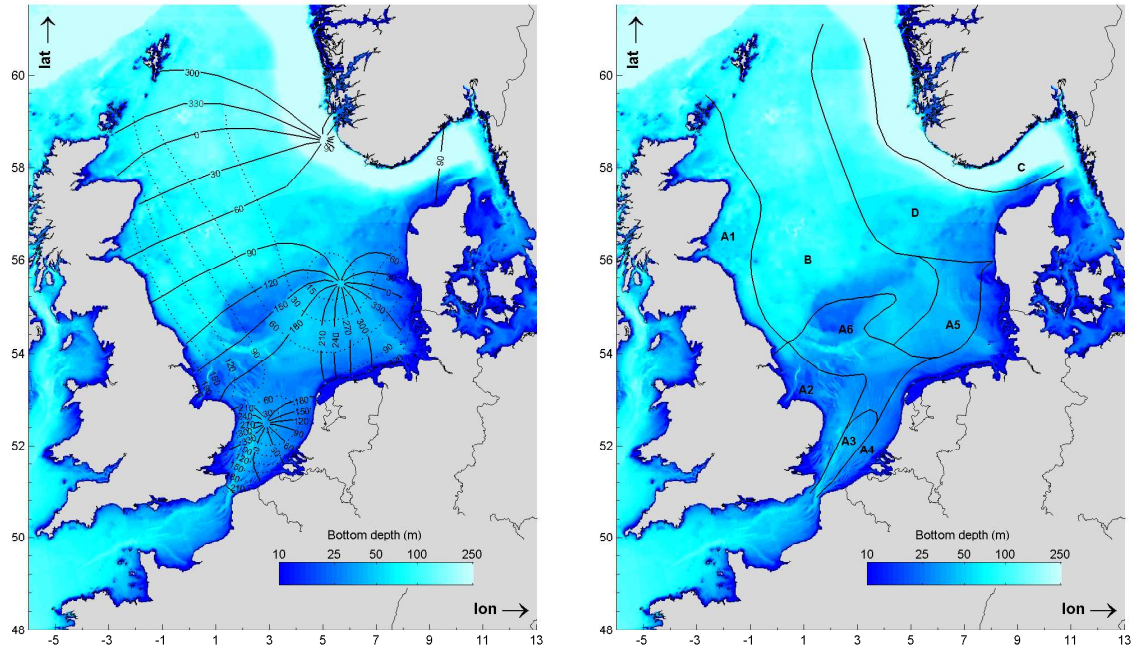

(a) Amphidromic system of the North Sea for the semi-diurnal M2 tide. Co-tidal (solid) lines in degrees and co-range (dashed) lines in cm. [after Proudman and Doodson (1924)]

(b) Classification of the different North Sea water masses [after Lee (1980) Fig. 14.13]. The water types are A1 (Scottish coastal water), A2 (English coastal water), A3 (Channel water), A4 (continental coastal water), A5 and A6 are transitional areas between A4 and B (Northern North Sea water), D is transitional water to C (Skagerrak and the Norwegian Rinne).

Figure 2.2: Amphidromic system (left) and hydrographical regions (right) of the North Sea

2.2.2 Large scale circulation

Currents in the North Sea occur in response to the forcing by tides, winds and pressure gradients. These forcings have large seasonal variations; the largest storms mainly occur in winter, river discharges have annual cycles and the Northern North Sea stratifies during summer. Still, a general circulation pattern can be found in the North Sea. This pattern is illustrated in figure 2.3, here the basic pattern of an amphidromic system is clearly visible. Starting in the north, the North Atlantic Current flows in easterly direction along the Northern North Sea boundary. Due to topographic steering a small part of this current deflects to the right into the North Sea indicated as the Fair Isle Current. While it continues flowing to the south, a large part deflects to the left known as the Dooley current in the direction of the Skagerrak. The remaining part flows along the British Isles southwards, where it meets the Atlantic inlet from the Strait of Dover. From there it follows the topography to the North-East and in the end also enters the Skagerrak. Within the Skagerrak, the dense Atlantic water meets the brackish water from the Baltic Sea. Stratification occurs where at the surface the brackish water flows along the Scandinavian coast to the north where it leaves the North Sea known as the Norwegian Coastal Current (NCC). At this point it joins the North Atlantic current. During the circulation, several fresh water inlets debouch into the North Sea introducing so-called Regions of Freshwater Influence (ROFI). Due to thermal wind effects local currents can increase with a factor 40 solely due to these density variations.

2.2.3 Density structure

The behaviour of currents highly depends on whether the water column is well mixed or stratified. Both the heating of the water surface as well as buoyancy input from fresh water river inlets increase the amount of stratification in the North Sea. In contrast, the different water bodies are mixed due to the available energy from tides and wind shear. For the southern North Sea, where depths are shallow and tidal currents strong, the situation tends to remain well mixed throughout the year. Solar heat input causes most of the northern North Sea to stratify between April/May and October/December, with a well-mixed surface layer of about 30-40m deep. At several locations along the shoreline fresh

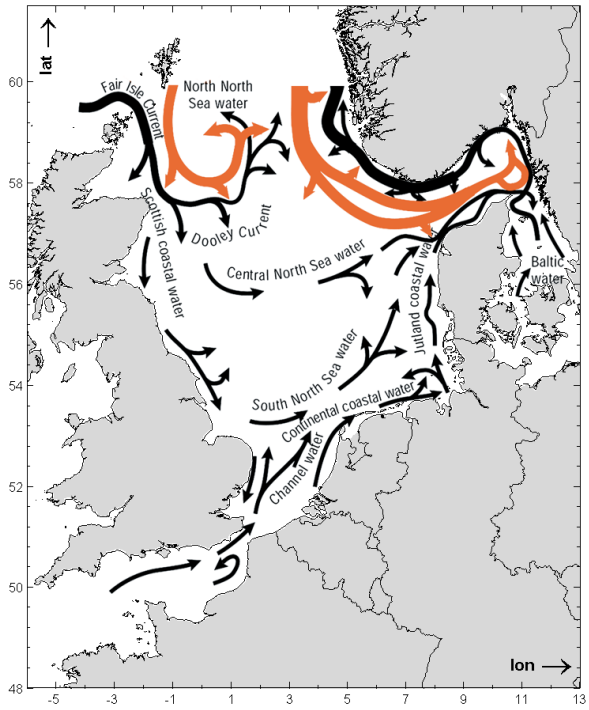

Figure 2.3: Schematic diagram of the circulation of the North Sea. The thickness of the lines is indicative of the magnitude of volume transport. [after Howarth (2001)]

water bodies enter the North Sea, which locally stratify the water column. In case of the Rhine river, its Region of Freshwater Influence (ROFI) can have a width of 20 - 40 km (De Boer (2009)). Stratification affects the current profile basically in two ways. Horizontal density gradients let the currents tend to flow along density fronts according to the thermal wind balance. Vertical density gradients can decouple the vertical velocity profile; surface currents can have significant different directions and magnitudes than the currents in deeper water layers.

2.2.4 Meteorological forcings

The North Sea experiences pronounced seasonal changes in meteorological conditions. In general, from September to April, it is exposed to the effect of a series of storms. Dominant winds come from the west, southwest and northwest. However, several events occur where winds could blow from any direction. On average, the atmospheric pressure is higher in the South than in the North. This affects the sea surface level with a gradient with low water levels at the South. After seasonal variations, a variability with a time scale of several years can be noticed, known as the North Atlantic Oscillation (NAO). The NAO describes the large scale variability of atmospheric pressure at sea level of the North Atlantic Ocean. The longitude boundaries are the Icelandic low and the Azores high. It effects the large scale circulation in two major cases. First, the strength of westerly winds is partly determined by the NAO. Second, an average increase or decrease in atmospheric pressure causes the surface level to rise or fall. This results in an annual in- or outflow at the Atlantic boundaries. The NAO can be quantified by the NAO index (NAOI). It is generally based on seasonal average air pressure between different stations in the NAO domain. For further knowledge about the NAO one is referred to Wanner et al. (2001), who gives a comprehensive review of related studies and concepts concerning the North Atlantic Oscillation. Concerning the North Sea, an estimate on the influence of the NAO on the sea-level is given by Tsimplis et al. (2006). It is based on satellite data, in situ measurements near Den Helder and model results. The sensitivity of the sea-level to the NAO index is in the order of 5 cm per unit. Although the NAOI does not vary that much over the relative small North Sea, a change in water level can have significant influence on the residual flow in and out of the North Sea. For an increase of $\Delta\eta = 5$ cm over the whole North Sea with surface area $A = 5.75 \cdot 10^{11}\text{m}^2$, this results in an inflow of $\Delta\eta A = 0.05 \cdot 5.75 \cdot 10^{11} = 2.88 \cdot 10^{10}$ m^3. The continual change in atmospheric pressure brings strong trade winds with it. Winther and Johannessen (2006) extensively studied the link between the NAO induced winds and the in- and outflow of Atlantic Ocean water. Results show that the maximum Atlantic inflow at the northern boundary coincides with a local maximum in the NAO index. Subsequently, a minimum inflow occurs when the NAO index reaches a local minimum. These results indicate that the annual cycle of Atlantic inflow to the North Sea is strongly influenced by westerly winds. For the Orkneys and Shetland and for the Shetland shelf region, the connection between wind forcing and magnitude of flow is on a weekly time scale. The deeper Norwegian Trench is less sensitive to weekly changes, but is more dependent on monthly averaged winds. The relation between NAOI and Atlantic inflow at the Northern boundary is shown in figure 2.4. It should also be noted that the correlation in winter is much stronger than during summer.

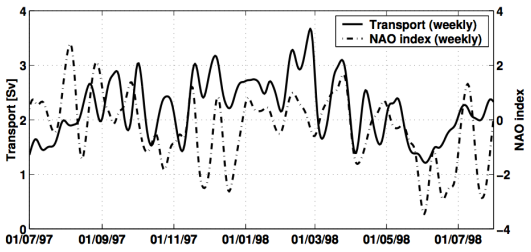

Figure 2.4: Weekly filtered time series of Atlantic inflow at northern boundary and NAO. From Winther and Johannessen (2006)

2.3 Transports through the Strait of Dover

After the large 400 km wide connection in the North, the Strait of Dover is the second boundary were Atlantic Ocean water can enter the North Sea. It forms the boundary between the North Sea and the English Channel, which has a direct connection with the Atlantic Ocean (see figure 2.1). With an oversea span of approximately 35 km between the cities of Calais (France) and Dover (England) it can be considered as a narrow entrance compared to the spatial scale of the large-scale circulation in the North Sea. For this reason, the residual flow through the Strait of Dover can be considered as an indicator of magnitude of residual flow through the North Sea, which still is possible to measure to a certain extent. However, since the gross transport through the strait is an order larger than the net transport, it is difficult to obtain accurate measurements of the residual flow. In addition, long term in situ data is scarce, due to the intense traffic through the Channel. Therefore alternative methods have been used to monitor the flow pattern. Below, a literature survey is given with the most important measurements done in the past.

2.3.1 In situ data

The first measurements on currents through the Strait of Dover date back to the late 1920's. In 1928 a few thousand drift bottles were set loose in the center of the Strait of Dover, which were collected again after a few months up to a year. By dividing the North Sea and English channel into separate sections, the main direction of the residual flow could be monitored. Based on this experiment a strong east northeast flow was stated. The first release on this experiment was published by Carruthers (1928). Carruthers also measured velocities at 10m depth from a vessel for 5 subsequent years. He made an estimate on the total flow through the Strait by assuming this velocity to be (1) equal to the depth averaged velocity and (2) representative for the whole section of the Strait of Dover. Based on this velocity an yearly averaged residual flow of 164000 m^3s^{-1} was found. He stated seasonal differences by the following relation: Spring : summer : autumn : winter = 77,3 : 83,3 : 100 : 88,9.

A few years later, Van Veen (1938) was the first to measure the current profile over the whole water depth. Measurements were executed in 1934 till 1936 with the use of a so-called 'heavy Ott' current-meter on board of a large vessel. An Ott is a propeller-type measuring device, it measured the horizontal velocity as a function of the vertical with an interval of 2 up to 5 meters distance. Every half hour such a series of measurements was executed with a total duration of several weeks. The direction of the stream was monitored with a hollow, pyramid shaped, object (Jacobsen meter) near the water surface. Taking into account turbulent motions, a calibration was done with the use of submerged floating sea-weed. The calibration showed the results measured by the Ott to be fairly accurate even in heavy weather conditions. Between Dover and Gris-Nez, just below Calais, 18 different places were used as measuring sight. This led to a time dependent velocity profile over the whole Strait. Surface elevations over the whole section were obtained from measurements at Dover and Gris-Nez. Based on these data sets, the total flow was estimated during a meteorological period which was considered as more or less "normal". Van Veen calculated the mass flux during a flood tide and an ebb tide. A simple transformation gives an residual flow of 100000 m^3s^{-1} during the measured time span. Since the annual inflow into the North Sea varies over time, Van Veen adjusted the measured output by adding 12,5% to the measurements to take into account seasonal variability. Leading to an annual residual inflow of 112500 m^3s^{-1}.

2.3.2 Cable voltage data

In the mid 50's the average flow velocity through the whole channel was obtained with the use of a cross-channel telephone cable between Dover and Calais. The measured electric potential differences through this cable can be translated to an average velocity based on Faraday's law of induction. Water flowing through a channel acts as a moving conductor. This flow generates a certain magnetic flux dependent on among others the velocity and crosssections area. When these properties change in time a so-called geomagnetic induction is introduced, which results in an electromotive force. This forces translates into electric currents which could be measured with the use of a cable. By assuming an elliptical shaped

channel, the potential difference Φ may be written as a function of the velocity by

$$\Phi = \hat{U} Z L \left(1 + \frac{\kappa_0}{\kappa_1} \frac{L}{2D}\right)^{-1} \times 10^{-8} \tag{2.1}$$

Where $\hat{U}$ is the amplitude of the spatial averaged water velocity in the channel. Z is the vertical component of the Earth's magnetic field, L and 2D are the major and minor axis of the ellipse respectively. κ_0 and κ_1 are the specific conductivities of the water and the channel bed. The specific conductivity of water dependent on the fluids dissolved substances and temperature, this conductivity was determined based on vessel measurements. Knowledge on the conductivity of the channel bed is scarce, therefore this factor is determined by calibration.

Since the cable lies on the bottom of the channel, and monitoring stations are land based, measurements could be done in all weather conditions. Compared to the former measurements this is already a big advantage, since storm weather now also can be monitored. Records from February 1953 till June 1954 were analysed by Bowden (1956). Bowden stated the average velocity $\langle U \rangle$ to have a relation with the wind velocity W and surface elevation $\Delta\eta$ in the form $\langle U \rangle = 0.37 W^2 \cos\theta + 0.7\Delta\eta$ where θ is the angle between wind direction and normal direction of the crosssection. Cartwright (1961) extended this research by investigating the average 'back-voltage', which represents the residual flow. This was obtained by applying an X_0 filter on the measured signal; this is a set of weighting factors for hourly data. Hereby tidal constituents drop out of the signal. This resulted in an yearly averaged flow of 235000 m^3s^{-1}. In a more recent analysis, Alcock and Cartwright (1977) analysed the potential difference in the submarine cable for a much longer period; December 1955 till March 1965. A smaller back-voltage was found, which is equivalent to 168000 m^3s^{-1}. An additional data analysis was executed in the second half of 1973 by Prandle and Harrison (1975). During this period wind stresses were small and considered to have no significant effect on measured potentials. Therefore, a voltage was measured purely based on tidal en surface elevations induced residuals, which correspond to 129000 m^3s^{-1}.

2.3.3 High frequency radar data

Starting from the beginning of the 90's, a new measuring device was introduced for monitoring flow velocities. High frequency radar (HFR) observations made it possible to observe a complete, spatial and time varying, surface current structure. The first to use this method was Prandle (1993) from October 1990 up to January 1991. Data was obtained from four HFR's placed around the Strait of Dover. Simultaneous deployment of a bottom-mounted ADCP provided knowledge on the vertical structure of the observed currents. Tidal ellipses were calculated for the dominating constituents. Based on these ellipses, tide induced residuals could be defined by

$$Q_r^{\text{tide}} = \frac{1}{2} \hat{U} \hat{\eta} \cos(\theta) \tag{2.2}$$

Where θ is the phase difference between the horizontal and vertical tide. This resulted in a residual current of 36000 m^3s^{-1} with the greater proportion on the French side. It is almost entirely determined by the M2 tide. A least-square fitting was executed to compare measured wind data with discharge through the channel. An expression was found for the total discharge by $Q_r^{\text{wind}} = 1432 \alpha w^2 \cos(\theta - 193)$. Where α is the ratio between surface and depth averaged currents; ADCP data provided a value of $\alpha = 0.75$. Based on the above formulation and the monitored tidal residuals, the annual mean residual flow was estimated to be 87000 m^3s^{-1}. By combining new observational results, **?** made a new estimate for the years 1990 till 1991 of 94000 m^3s^{-1}.

2.3.4 Modelling studies

For the past decade, a wide range of modelling studies have been done on residual flows. Below, a brief overview is given of the most important, innovative, studies. An extensive modelling study has been executed by Prandle (1978a). A fully non-linear model was used to solve the depth averaged Navier-Stokes equations. The model was forced by M2 tidal

oscillations and a uniform, time varying, wind field for 5 subsequent years. Prandle found a mean residual flow of 160000 m^3s^{-1}. The largest residuals are found to occur in autumn and the smallest residuals during winter. By leaving out wind forcings, a tidal residual was found of 82000 m^3s^{-1}. In addition, a linearized model has been applied to examine the impact of non-tidal forcing phenomena. Residuals due to wind and sea-surface gradients were found to be responsible for 37000 m^3s^{-1} and 41000 m^3s^{-1} respectively. The effect of density gradients appeared to be negligible, since the water column is in general well mixed, except for certain river inlets.

When one is purely interested in residual circulation patterns, short scale motions are out of interest and only introduce undesired high frequency noise. Instead of solving the fundamental Navier-Stokes equations for a fixed coordinate system, Salomon et al. (1993) introduced the so-called barycentric coordinates. Here, the system follows the mean trajectory of a certain particle set loose at a location x_0 and time t_0. Different simulations were executed with each a different, stationary and uniform, wind field. A tidal residual was found of 37400 m^3s^{-1}. Salomon and Breton (1993) made a formulation for residual flow due to tidal and wind driven effects as

$$Q_r = 37400 + 1.1 \times 10^6 \tau \cos(\theta - 186) \tag{2.3}$$

This formulation has been applied on monthly mean wind values from 1983 up to 1991. A mean value of 114000 m^3s^{-1} was found with a standard deviation of 52 m^3s^{-1}. The largest residuals occur in December and January.

2.3.5 Concluding remarks

Through the last century many attempts have been done to monitor the residual flow into the North Sea from the English Channel. Obtained results still have a wide variety, ranging from 87000 m^3s^{-1} to 235000 m^3s^{-1}. Below (table 2.2), a brief overview is given of the most important measurements and modelling studies in the past.

Source	Year	Method	Tidal	Wind	Other	Total
Carruthers (1928)	1926-1934	(I)	-	-	-	164
Van Veen (1938)	1934-1936	(I)	-	-	-	112.5
Cartwright (1961)	1957-1958	(II)	50	-	-	235
Prandle and Harrison (1975)	1973	(II)	-	-	-	129
Alcock and Cartwright (1977)	1955-1965	(II)	-	-	-	168
Prandle (1978a)	1978	(IV)	82	37	41	160
Prandle (1984)	1951-1975	(IV)	50	-	-	90
Prandle (1993)	1990	(III)	36	45	6	87
Salomon and Breton (1993)	1983-1991	(IV)	37	-	-	114
Prandle et al. (1996)	1990-1991	(III)	41	47	6	94

Table 2.2: Residual flows based on historical measurements and numerical modelling. Flows are given in $10^3 m^3s^{-1}$. Data obtained from (I) in situ measurements, (II) cable measurements (III) HFR & ADCP and (IV) model simulations.

3 Theoretical background

In this chapter, a theoretical background is given on the dominating processes which cause residual flow in the North Sea. Here, especially the important processes around the Strait of Dover are described in more detail. In section the governing equations are described which are used to describe all relevant processes. Section executes a scale analysis to examine which processes are important, or irrelevant for this thesis. In section the barotropic wave propagation is treated. In the last section the effect of wind and density is taken into consideration.

3.1 Governing equations

The North Sea can be considered as a shallow sea, were horizontal length scales are much larger than vertical scales. Hydrodynamic processes can be described with the three-dimensional shallow water equations. They are derived from the 3D Navier-Stokes equations under the assumption that vertical pressure gradients are fully hydrostatic. They consist of a single continuity equation based on mass conservation and three momentum equations based on Newton's second law as applied on a fluid motion. In this section the general processes, which are relevant for large scale circulations, are elaborated based on this set of equations. The four equations are given below.

$$\frac{\partial u}{\partial x} + \frac{\partial v}{\partial y} + \frac{\partial w}{\partial z} = 0 \tag{3.1}$$

$$\frac{\partial u}{\partial t} + u\frac{\partial u}{\partial x} + v\frac{\partial u}{\partial y} + w\frac{\partial u}{\partial z} = -\frac{1}{\rho}\frac{\partial p}{\partial x} + fv + \nu_H\left(\frac{\partial^2 u}{\partial x^2} + \frac{\partial^2 u}{\partial y^2}\right) - \nu_V\frac{\partial^2 u}{\partial z^2} + \frac{\tau_x}{\rho h} \tag{3.2}$$

$$\frac{\partial v}{\partial t} + u\frac{\partial v}{\partial x} + v\frac{\partial v}{\partial y} + w\frac{\partial v}{\partial z} = -\frac{1}{\rho}\frac{\partial p}{\partial y} - fu + \nu_H\left(\frac{\partial^2 v}{\partial x^2} + \frac{\partial^2 v}{\partial y^2}\right) - \nu_V\frac{\partial^2 v}{\partial z^2} + \frac{\tau_y}{\rho h} \tag{3.3}$$

$$\frac{\partial p}{\partial z} = -\rho g \tag{3.4}$$

With:

t	time
x, y, z	spatial coordinates
u, v, w	x, y and z components of currents, respectively
ρ	density of water
g	gravitational acceleration
h	water depth
p	pressure
f	Coriolis parameter
$\nu_{H,V}$	eddy viscosity
$\tau_{x,y}$	stress tensor

The left hand side of the horizontal momentum equations consist of the material derivatives of mass and the three velocity components, respectively. Here the first term represents inertia, whereas the others are convective terms in three dimensions. The right hand side from the momentum equations consist of body forces and stresses. The ∇p terms are known as the isotropic pressure gradients and act as a surface stress. Gravity acts as a body force, shown with the term ρg. Note that this term only present in the vertical momentum equation, since the reference frame is perpendicular to the gravity field and therefore zero in the horizontal plane. The influence of a rotating earth lies in the Coriolis terms fv and fu, where the Coriolis parameter f is a function of the latitude φ as in $f = 2\Omega\sin(\varphi)$ in which $\Omega = 7.292 \cdot 10^5$ rad s^{-1} is the earth's angular velocity. Based on the Boussinesq hypothesis, viscous stresses can be described by a so-called eddy viscosity $\nu_{H,V}$. The last term is the anisotropic, non-linear, stress tensor which represents bottom shear and wind stresses.

3.2 Dominant processes

To get a better insight in the important processes in the North Sea, it is wise to apply some rough scaling to the governing equations. For this reason, several terms of the equations

Quantity	Symbol	Scale	Unit
Horizontal velocity scale	U	$\mathcal{O}[10^{-2}$ - $10^{-1}]$	ms^{-1}
Horizontal length scale	L	$\mathcal{O}[10^{4}$ - $10^{5}]$	m
Vertical length scale	H	$\mathcal{O}[10^{2}]$	m
Time scale	T	$\mathcal{O}[10^{1}]$	days
Coriolis	f	$\mathcal{O}[10^{-4}]$	s^{-1}
Horizontal eddy viscosity	ν_H	$\mathcal{O}[10^{3}]$	m^2s^{-1}

Table 3.1: Typical scale factors for the North Sea

will be compared to each other, neglecting all other terms. By filling in typical values for the North Sea (see table 3.1) the importance of all terms in the equations becomes clear. In subsequent sections all processes will be described in more detail.

For large water bodies the effect of Coriolis is highly significant. One way to show this importance is with the use of the dimensionless Rossby number (Ro). It gives the relation between Coriolis and convection. The definition of this number is the ratio between these two terms gained from the momentum balance.

$$\mathrm{Ro} = \frac{U}{Lf} \tag{3.5}$$

For the North Sea this number varies between $\mathcal{O}[10^{-3}]$ in area's with low, large scale, velocities and $\mathcal{O}[10^{-1}]$ in area's with concentrated high velocities. For the former, Coriolis is dominant over convection, which is the case in the center of the North Sea. A higher Rossby number indicates the non-linear advection term being more important. However, even for rapidly varying flows like the currents in the Strait of Dover the Rossby number stays small ($\mathcal{O}[10^{-1}]$). Still, advection becomes notable at these places.

The Rossby radius of deformation is the length scale at which the rotation of the earth has a significant influence on the hydrodynamic structure in relation to buoyancy and inertial propagation. It gives the distance over which a long gravity wave can travel in the time $1/f$.

$$L_{\mathrm{Ro}} = \frac{c}{f} \tag{3.6}$$

Here c is the wave celerity. For barotropic flow in shallow water the external Rossby radius is calculated with $c = \sqrt{gH}$. When buoyancy should be taken into account the celerity becomes more complicated to notate. In case of a two layered system, which is the case by a single pycnocline, the celerity becomes $c = \sqrt{g' \frac{H_1 H_2}{H}}$ where $H_{1,2}$ are the depths for layer one and two, and g' is the reduced gravity given by $g = \frac{\Delta\rho}{\rho_0}$. In case of baroclinic flow, the characteristic length scale is called the internal Rossby radius. In the southern North Sea, where the water column is in general well mixed, the Rossby radius is determined by its barotropic structure. It has a typical length of $L_{\mathrm{Ro}} = 250km$. When one looks at for example the Norwegian trench, the water column is stratified in a two layered system and the radius becomes much smaller; $L_{\mathrm{Ro}} = 14km$. For the Rhine ROFI it is approximately 5 km.

Whether friction is important with respect to Coriolis can be shown with the horizontal Ekman number, which is the ratio between the friction term and Coriolis term from the momentum balance. The friction term is in this case described as a function of horizontal eddy viscosity and the second derivative of velocity, $\nu_H \frac{\partial^2 u}{\partial x^2}$. When u and x are replaced by their related scaling parameters the Ekman number becomes:

$$\mathrm{Ek} = \frac{\nu_H}{fL^2} \tag{3.7}$$

Again, in the center of the North Sea the Ekman number is small due to the larger length scale of flow circulation ($\mathcal{O}[10^{-3}]$). Coriolis is dominant over the bottom friction. Near the land boundaries the horizontal scale becomes smaller (and therefore also the eddy viscosity), and velocity increases. The Ekman number increases up to $\mathcal{O}[10^{-1}]$, indicating that friction becomes important.

3.3 Barotropic wave propagation

The propagation of long waves can be described by the governing equations 3.1 till 3.4. In order to find relative manageable analytical solutions to these equations, non-linear terms should not be taken into consideration. In other words, the advective terms and non-linearity's inside the friction terms should be neglected or linearized. Solutions to these linear equations approximate reality for small Rossby and Ekman numbers, since in that case Coriolis dominates the non-linear advection and friction terms. As indicated in previous section, this is true for the largest part of the North Sea. For this section only the linearized barotropic situation will be treated, so density differences are not taken into consideration. Therefore the governing equations can be reduced to their two-dimensional form, all $\partial/\partial z$ terms drop out, and for the continuity equation the Leibniz rule needs to be applied.

$$\frac{\partial \eta}{\partial t} + h\left(\frac{\partial u}{\partial x} + \frac{\partial v}{\partial y}\right) = 0 \tag{3.8}$$

$$\frac{\partial u}{\partial t} - fv = g\frac{\partial \eta}{\partial x} + \frac{ku}{h} \tag{3.9}$$

$$\frac{\partial v}{\partial t} + fu = g\frac{\partial \eta}{\partial y} + \frac{ku}{h} \tag{3.10}$$

Here the water depth h is a function of the bottom depth and surface elevation as $h = d + \eta$. The friction term is represented by the linear friction coefficient k. The above, linear, shallow water equations are the basis of the following paragraphs.

Vorticity A rotating water body contains a certain amount of vorticity. In case of a frictionless flow, this vorticity is conserved. It can have a significant influence on the directions and magnitude of oceanic flow patterns. Vorticity of a water body can be split up in two types; planetary vorticity and relative vorticity. The former has already been introduced by the Coriolis parameter f, which is a function of the rotation speed of the earth and the local latitude. Relative vorticity ω_r is the rotation speed of the water body itself relative to the earth's rotation, defined as:

$$\omega_r = \frac{\partial v}{\partial x} - \frac{\partial u}{\partial y} \tag{3.11}$$

The absolute vorticity is the sum of the planetary and relative vorticity, defined as $\omega_a = f + \omega_r$. The governing equations can be rewritten as a function of the relative vorticity. For this reason, the $\partial/\partial y$ of equation 3.9 is subtracted from the $\partial/\partial x$ of equation 3.10. After some algebraic manipulations the resulting equation of vorticity becomes:

$$\frac{D}{Dt}(\omega_r + f) + (\omega_r + f)\left(\frac{\partial u}{\partial x} + \frac{\partial v}{\partial y}\right) = 0 \tag{3.12}$$

Here $\frac{D}{Dt}$ is called the Langrangian derivative which equals $\frac{D}{Dt} = \frac{\partial}{\partial t} + u\frac{\partial}{\partial x} + v\frac{\partial}{\partial y}$. Equation 3.8 can be rewritten by applying the product rule on the second and third term.

$$\frac{Dh}{Dt} + h\left(\frac{\partial u}{\partial x} + \frac{\partial v}{\partial y}\right) = 0 \tag{3.13}$$

Substituting eq. 3.13 in eq. 3.12 gives

$$\frac{D}{Dt}(\omega_r + f) - \frac{(\omega_r + f)}{h}\frac{Dh}{Dt} = 0 \tag{3.14}$$

This can be rewritten, using the reversed quotient rule, as the Lagrangian derivative of the potential vorticity Π:

$$\frac{D\Pi}{Dt} = \frac{D}{Dt}\left(\frac{f + \omega_r}{h}\right) = 0 \tag{3.15}$$

Here h is the water depth as a function of bottom depth d and surface elevation η. According to Stewart (2009), the relative vorticity in ocean's is rather small compared to

Coriolis ($\omega_r \ll f$). Equation 3.15 therefore requires f/h to be constant, since the RHS of the equations equals zero. In case of a significant topographic decrease in bottom depth, the water depth decreases with it. This will results in a flow to deflect to the right (Northern Hemisphere) since its potential vorticity has to remain constant. This can only happen when the Coriolis parameter decreases. The opposite will happen in case of a deepening of the bottom topography, where the flow will deflect to the left. This phenomena is called topographic steering. It can for example be seen at the northern boundary of the North Sea. Here the Atlantic water flows from the deep ocean on to the northwest European continental shelf. Due to this large decrease in depth, the flow deflects to the right into the North Sea.

Kelvin Wave A Kelvin wave is a tidal wave, forced by Coriolis to propagate along a lateral boundary. This can occur along a coastline where the land acts as the boundary, or along the equator. Although the behaviour is similar, from now on only the coastal Kelvin wave will be treated. Below the terms coastline (parallel to the x-axis) and cross-shore (parallel to y-axis) are used. The most simplified Kelvin wave can be described by taking a straight coastline with uniform depth over the whole domain and friction is neglected. The boundary condition at the coastline requires the cross-shore velocity v to be zero. A first attempt on finding a solution is done by assuming the cross-shore velocity component to be zero over the whole domain. The equations of motion therefore reduce to:

$$\frac{\partial \eta}{\partial t} = -h\frac{\partial u}{\partial x} \tag{3.16}$$

$$\frac{\partial u}{\partial t} = g\frac{\partial \eta}{\partial x} \tag{3.17}$$

$$fu = g\frac{\partial \eta}{\partial y} \tag{3.18}$$

These set of equations can be solved by substituting a general wave solution of the form $\vec{A} = \hat{A}e^{i(kx+ly-\omega t)}$ into the equations. Here $\vec{A}$ is a vector which represents the variables η, u and v. The wave number are given in 2 dimensions by k and l, ω is the wave frequency. When the determinant of the set of equations is set to zero, the general solution can now be found

$$\eta = \Re\left\{\hat{\eta}e^{i(kx-\omega t)-y/L_{\mathrm{Ro}}}\right\} \tag{3.19}$$

$$u = \Re\left\{-\hat{\eta}\sqrt{\frac{g}{h}}e^{i(kx-\omega t)-y/L_{\mathrm{Ro}}}\right\} \tag{3.20}$$

$$v = 0 \tag{3.21}$$

Here the wave properties are described as the real part $\Re\{\}$ of two complex formulations. $\hat{\eta}$ is the tidal amplitude and L_{Ro} the external Rossby radius. The Kelvin wave has its largest amplitude at the boundary and decays exponentially away from the coast over the length scale of the Rossby radius. The water level and velocity are in phase; maximum velocities occur during high and low water.

Poincaré Wave When the lateral boundaries are removed a more general case of the wave description arises. Again the general wave solution of the form $\hat{A} = \hat{A}e^{i(kx+ly-\omega t)}$ is assumed. After the determinant of equations 3.8 till 3.10 is set to zero, the following condition needs to be fulfilled:

$$\omega(\omega^2 - f^2 - ghK^2) = 0 \tag{3.22}$$

Where $K = \sqrt{k^2 + l^2}$. This condition is known as the dispersion relation. The first root of this condition ($\omega = 0$) is the steady state motion and describes geostrophic flow; the balance between pressure gradients and Coriolis. The two remaining roots are known as Poincaré waves:

$$\omega = \sqrt{f^2 + ghK^2} \tag{3.23}$$

The wave speed depends on the wave number and is therefore called dispersive. This is in contrast with Kelvin waves, were the wave speed solely depends on the water depth.

Amphidromic System In marginal seas a rotary tidal system can be seen. A tidal wave which enters the sea is deflected by Coriolis and propagates along the lateral boundaries until it leaves the sea at the other side of the sea. Dependent on the side of the hemisphere this rotation is clockwise (SH) or anti-clockwise (NH). This system was first discussed by Taylor (1922), who described the situation as a superposition of a Kelvinwave and an infinite number of Poincaré waves. Taylor considered a simplified marginal sea; a wide channel connected to the ocean on one side and a closed end on the other side. Its spatial dimensions are sufficiently large that the influence of Coriolis becomes notable. The depth is uniform, unstratified, and friction is not taken into account. When a tidal wave enters the marginal sea it propagates as a Kelvin wave along the land boundary. When it comes close to the end the Kelvin wave needs to be reflected, and therefore a crossshore velocity arises. At this point Poincaré waves become important since the Kelvin wave itself does not contain crossshore velocities. The Kelvin wave can be completely reflected at the closed end as long as its period is large enough compared to the geometry's eigen frequency.

Figure 3.1 shows the amphidromic system as treated by Taylor. Here a highly simplified basin is considered with a width of B=550km and depth of h=80m. These are they are typical values for the North Sea. Only the M2 tide is considered, and friction is neglected. It can be clearly seen that the surface elevation is at its largest at the boundaries. The amphidromic system is a superposition of both Kelvin and Poincaré waves. It rotates in an anti-clockwise manner around the amphidromic points. When friction is implemented in the system the amphidromic points shift to the south, also energy dissipation due to bottom friction causes the amplitude to decrease. The general pattern can be seen in figure 3.2.

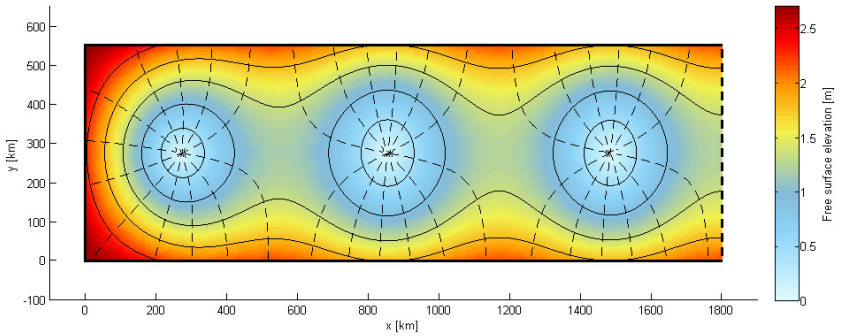

Figure 3.1: Superposition of free surface elevation amplitudes of the wave solutions with co-phase lines (dashed lines) and co-range lines (solid lines) without bottom friction. Geometry typical for the North Sea (B = 550km, h = 80m) and tidal amplitude of ζ_0 = 2m. [after Velema (2010)]

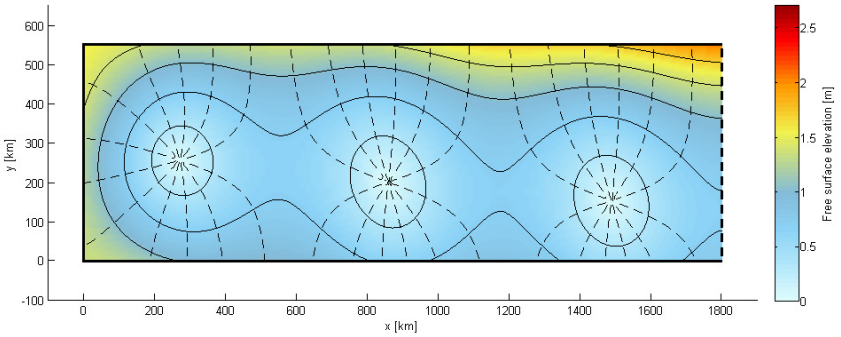

Figure 3.2: Superposition of free surface elevation amplitudes of the wave solutions with co-phase lines (dashed lines) and co-range lines (solid lines) with bottom friction. Geometry typical for the North Sea (B = 550km, h = 80m) and tidal amplitude of ζ_0 = 2m. [after Velema (2010)]

Barotropic tidal residuals Tidal residuals are introduced by the non-linear interaction between the horizontal and vertical tide. In case of a phase difference, a radiation stress is introduced which causes causes an excess of momentum flux. This results in a mean current in the direction of the wave propagation. The mathematical derivation was introduced in the mid 70's by different authors. Nihoul and Ronday (1975) introduced the concept of "tidal stress", which is in addition to wind stress a term causing residual flow. Another way to find tidal residuals is to rewrite the depth-averaged Navier-Stokes equations in terms of mass transport and taking its average. The latter is done by e.g. Prandle (1978a) and will be elaborated below. It should be noted that both approaches give the same results.

For the mathematical description, a single tidal constituent is considered with a flow velocity $u(t)$ and a surface elevation $\eta(t)$. Both velocity and surface elevation can be written as a function of time containing a non-tidal part and a time dependent fluctuating part:

$$u = \overline{u} + \hat{u}\cos(\omega t + \theta_h) \tag{3.24}$$

$$\eta = \overline{\eta} + \hat{\eta}\cos(\omega t + \theta_v) \tag{3.25}$$

Here, the overbar stands for an averaged variable and the hat for the amplitude of a sinusoidal function with rotating speed ω and phase θ. The mass flux is given as the product of the velocity and water depth $h(\eta)$ where d is the local water depth:

$$q = uh, \text{ and } h = d + \eta \tag{3.26}$$

Filling in equations 3.24 and 3.25 in equation 3.26 gives:

$$q = \overline{u}(d+\overline{\eta}) + (d+\overline{\eta})\hat{u}\cos(\omega t + \theta_h) + \overline{u}\hat{\eta}\cos(\omega t + \theta_v) + \hat{u}\hat{\eta}\cos(\omega t + \theta_v)\cos(\omega t + \theta_h) \tag{3.27}$$

The last term can be rewritten as:

$$\hat{u}\hat{\eta}\cos(\omega t + \theta_v)\cos(\omega t + \theta_h) = \frac{1}{2}\hat{u}\hat{\eta}(\cos(2\omega t + \theta_h + \theta_v) + \cos(\theta_h - \theta_v)) \tag{3.28}$$

The residuals induced by the mass flux q can be calculated by taking the average with respect to time. As a result, al terms containing $cos(\omega t)$ drop out. The remaining time averaged mass flux, also known as the Lagrangian transport (Longuet-Higgins (1969)), becomes:

$$\overline{q} = \overline{u}(d+\overline{\eta}) + \frac{1}{2}\hat{u}\hat{\eta}\cos(\theta_h - \theta_v) \tag{3.29}$$

The first term on the RHS is called the Eulerian transport, which is also present in case of non-tidal forcing. The second term is introduced by the non-linear interaction, it is known as the stokes transport. Note that the latter is not present in case of a standing wave, were the velocity and surface elevation are exactly 90°'s out of phase.

3.4 Meteorological processes

The response of oceanic currents to the wind can be separated into an ageostrophic (frictional) and a geostrophic (Ekman) component. The frictional forcing is simply the drag which is introduced by the shear stress between the water and atmosphere. After the fluid starts to flow, Coriolis will deflect the current to the right, resulting in a so-called Ekman-spiral. The corresponding Ekman layer is the surface layer in which the wind shear has direct influence on the water column. In a well mixed water column, this is generally between 50 and 200 m. For a stratified column, the layer is as thick as the layer above the first pycnoclyne. For a thin layer, currents become larger, the total mass transport however stays equal (3.30).

$$Q_{xE} = \frac{\tau_y}{f\rho_0},\ Q_{yE} = -\frac{\tau_x}{f\rho_0} \tag{3.30}$$

Here Q_{xE} and Q_{yE} stand for the Ekman volume flux in x and y direction respectively. The wind stress τ is at surface level. The density ρ_0 is the mean value of the upper layer were the actual flow takes place. Note that the direction of the Ekman transport is exactly 90°'s deflected to the right. When there is a horizontal variability in the wind field, the Ekman

transport will also differ in space. For a growing Ekman transport, the gross horizontal transport is larger than zero and the Ekman layer becomes thinner. The deeper layer comes closer to the surface, this process is called upwelling. For a reducing flow the result is called downwelling. The same reasoning applies to a coastal region, where an alongshore wind stress will cause either up- or downwelling.

4 Model set-up

4.1 Introduction

In this thesis an extensive modeling study has been performed to simulate and visualize the residual circulation in the North Sea. For this reason the Dutch Continental Shelf Model version 6 (DCSMv6) is used; a numerical model which covers the whole northwest European Continental Shelf (NWECS). DCSMv6 is an application of SIMONA, a framework for hydrodynamic modeling of free-surface water systems. Computations are done with Delft3D-FLOW module on a Linux cluster. A simulation of one year takes about seven days to calculate the spatial and time varying hydrodynamic structure. During this study several small adjustments have been made to test the sensitivity of the model. For this reason a computation time of 7 days is rather large since the implementation of these adjustments is an interactive process. Therefore a much shorter computation time is desired. An older version of the Dutch Continental Shelf Model (DCSMv5) has been used in addition to the first model, since its computation time is only a couple of hours for a complete year. This is mainly due to a courser grid structure and larger time step. Since the grid is more courser, detailed flow structures can't be simulated. This could result in a less accurate output, which should be kept in mind during the analysis. In this chapter a short description will be given on the simulation module Delft3D, which is used for the computations of the numerical models. Thereafter the most important features of the models are discussed. Finally some test runs have been done, which were used to determine the computation time step and spin-up time.

4.2 Simulation module

The modeling system used for simulations is the depth-averaged module of Delft3D-FLOW. It solves the 2D shallow water equations derived from the three dimensional Navier-Stokes equations for incompressible free surface flow (eq. 3.1 till eq. 3.4). In case of variable density the Boussinesq approximation holds; density variations are small and therefore density is assumed to be constant in all terms except for the gravitational pressure term. Furthermore the pressure is assumed to be hydrostatic; vertical accelerations are neglected. For a complete overview of the numerical aspects one is referred to the user manual (Deltares (2013)). Below the basic concepts are briefly discussed.

4.2.1 Governing equations

The shallow water equations are discretized to a finite difference scheme and solved on a staggered computational grid. In Delft3D the ADI solver is chosen for discretization. See for example Stelling and Leendertse (1992) for a full elaboration of this process. For convenience, the infinite depth averaged shallow water equations are shown below

$$\frac{\partial U}{\partial t} + U\frac{\partial U}{\partial x} + V\frac{\partial U}{\partial y} = -\frac{1}{\rho_0}\frac{\partial p}{\partial x} + fV + \nu_H\left(\frac{\partial^2 U}{\partial x^2} + \frac{\partial^2 U}{\partial y^2}\right) - \frac{\tau_x}{\rho h} + 0.69g\frac{\partial \phi}{\partial \lambda} \tag{4.1}$$

$$\frac{\partial V}{\partial t} + U\frac{\partial V}{\partial x} + V\frac{\partial V}{\partial y} = -\frac{1}{\rho_0}\frac{\partial p}{\partial y} - fU + \nu_H\left(\frac{\partial^2 V}{\partial x^2} + \frac{\partial^2 V}{\partial y^2}\right) - \frac{\tau_y}{\rho h} + 0.69g\frac{\partial \phi}{\partial \varphi} \tag{4.2}$$

$$\frac{\partial \eta}{\partial t} + \frac{\partial hU}{\partial x} + \frac{\partial hV}{\partial y} = 0 \tag{4.3}$$

Here the horizontal eddy viscosity ν_H is introduced as a user defined constant. It represents a virtual viscosity based on a superposition of three processes which can't be simulated by the other terms. These processes are sub-grid scale turbulence, 3D turbulence and dispersion. Frictional effects such as bottom shear $\vec{\tau_b}$ and wind shear $\vec{\tau_w}$ are represented in the frictional terms $\vec{\tau}/\rho h$ and $\vec{\tau}/\rho h$ with $\vec{\tau} = \vec{\tau_b} - \vec{\tau_w}$. The final term of equations 4.1 and 4.2 represents the tide generating forces.

Bottom friction A shear stress in opposite direction of the current is added to the momentum equations to implement the effect of bottom friction. Delft3D-FLOW assumes

this stress to have an quadratic relation with the depth averaged velocity via

$$\vec{\tau}_b = \rho g \frac{\vec{U}|\vec{U}|}{C_{2D}^2} \tag{4.4}$$

The two dimensional Chézy coefficient C_{2D} is a variable based on the Chézy formulation ($C_{2D} = C$) or Manning's formulation ($C_{2D} = \sqrt[6]{h}/n$). Where C and n are the Chézy and Manning coefficient, respectively.

Wind stress For the calculation of wind stresses, the widely used quadratic expression for wind shear is used

$$\vec{\tau}_w = \rho_a C_D \vec{W}_{10}|\vec{W}_{10}| \tag{4.5}$$

Where ρ_a is the local atmospheric density, $\vec{W}_{10}$ is the wind speed at 10m above surface level and C_D is the wind-drag coefficient. The latter is derived from the Smith and Banke relation as formulated by Smith and Banke (1975). The wind-drag coefficient linearly varies from 0.63x10^{-3} to 7.23x10^{-3} for a wind speed of 0 to 100 ms^{-1} respectively.

Tide generating forces In coastal areas, it is sufficient to generate the proper tidal motion by imposing the tidal forcing only along the open boundaries by means of either changing water levels, velocities, or both. For larger areas, the direct influence of tide generating forces induced by the rotation of the planetary system can't be neglected anymore. For this case, the derivative of the tidal potential ϕ for equilibrium tide is taken to the latitude φ and longitude λ. These terms are based on the equilibrium tide (assuming the earth is covered entirely with water), with a 31% reduction by the earth tide (displacement of the earth's crust). For the North Sea, this gives a water level amplitude of 10 cm throughout the whole model domain. See Deltares (2013) for more detail on this derivation.

4.2.2 Boundary conditions

To obtain singular results, boundary conditions are imposed at the open "water-water" and closed "land-water" boundaries. For closed boundaries the flow velocity component perpendicular to the land boundary is set to zero. Since the grid is relatively coarse, flow parallel to the boundary is still allowed via a free-slip condition (Deltares (2013)). At the open boundaries, a time dependent water level is prescribed at various boundary stations. In case of water inflow, the tangential velocity component is set to zero. As a results, inflow is always perpendicular to the boundary.

4.2.3 Transport equations

In addition to the flow velocities and surface elevation other fluid properties can be modelled with the use of additional transport equations. For a certain property c the transport equation is defined as

$$\frac{\partial c}{\partial t} + \frac{\partial Uc}{\partial x} + \frac{\partial Vc}{\partial y} = D_H \left(\frac{\partial^2 c}{\partial x^2} + \frac{\partial^2 c}{\partial y^2} \right) + Q_c \tag{4.6}$$

$$\tag{4.7}$$

Here the property c can be for example salinity, temperature or any dissolved particle. D_H is the horizontal diffusivity and Q_c is any source or sink of the given property. In case of baroclinic modeling, the density ρ in equations 4.1 and 4.2 is calculated with the equation of state as formulated by Eckart (1958)

$$\rho = \frac{P_0}{\lambda + \alpha_0 P_0} \tag{4.8}$$

with

$$\lambda = 1779.5 + 11.25T - 0.0745T^2 - (3.80 + 0.01T)S \tag{4.9}$$

$$\alpha_0 = 0.6980 \tag{4.10}$$

$$P_0 = 5890 + 38T - 0.375T^2 + 3S \tag{4.11}$$

Here T and S are the temperature and salinity as calculated with equation 4.6.

4.3 Model description

4.3.1 Domain

The DCSMv6 model domain covers the area between 15°W to 13°E and 43°N to 64°N. The complete northwest European Continental shelf (NWECS) lies within the model domain. For this reason, all open boundaries are located in deep water. It computes on a spherical grid with a uniform cell size of 1.5' in east-west direction and 1.0' in north-south direction, corresponding to a grid size of about 2 by 2 km^2 over the whole domain (see fig. 1.1). The DCSMv5 model covers a smaller area, it still covers the whole NWECS domain. However, especially at the western boundary, the domain almost lies on the continental shelf edge. This could result in some numerical problems. The grid size is courser than the former model, namely 7.5' in east-west direction and 5.0' in north-south direction, corresponding to a grid size of about 10 by 10 km^2. Within both model boundaries lies the ZUNO-DD domain, ranging from the western part of the English Channel up to around the northern boundary of the southern bight. The focus on residual circulation lies in particular on the area within this domain for two reasons. Because (1) artificial boundary currents are assumed to be negligible within this area and (2) the original reason of this research was to define proper boundary conditions for the ZUNO-DD model, including both currents as surface elevations. The bathymetry is based on the NOOS gridded bathymetry data set. Since this grid does not cover the complete domain, missing parts are gained from NOAA's ETOPO2 bathymetry data. Along the open boundaries the bathymetry has been smoothed to prevent instabilities. The final bathymetric data set is shown in figure 4.1). To account for bottom friction, the Manning coefficient is used for DCSMv6 and the Chézy coefficient for DCSMv5. Together with the obtained bathymetry data a calibration has been executed to improve the water level representation and tidal propagation (Zijl (2013)). For this reason the bathymetric data has been adapted as well as the roughness coefficients, resulting in a specially varying bottom friction.

4.3.2 Boundary conditions

At the edges of the model grid several boundary stations are located. Each station prescribes a time varying water level $\eta(\varphi, \lambda, t)$. Between the boundary stations water levels are linearly interpolated. The water level prescribed at the open boundaries consists of three components, namely the astronomical tidal constituents $\eta_t(\varphi, \lambda, t)$, the effect of local air pressure $\eta_a(\varphi, \lambda, t)$ via the so-called inverse barometer effect (IBM) and other global residual surface elevations $\eta_r(\varphi, \lambda, t)$ with for example density induced height differences, known as the steric height. Although wind set-up could be a forth component to the surface elevations, in this case these heights are assumed to be negligible, since the open sea boundaries are located in deep water. Finally, a bias in surface level could occur due to a wrong reference in the vertical datum (Slobbe (2013)). It is assumed that the mean bias is much larger than the spatial variety. Therefore the impact on residual flows is considered as negligible.

Tidal constituents The water level $\eta_t(\varphi, \lambda, t)$ represents the astronomical Atlantic tides. Main diurnal and semi-diurnal constituents are gained from the GOT00.2 global tidal model. These eight constituents are in order of increasing frequency Q1, O1, P1, K1, N2, M2, S2 and K2. For the North Sea, the semi-diurnal M2 constituent is the dominating tidal frequency (see e.g. Prandle (1978a) and Otto et al. (1990)). Its mean amplitude at the model boundaries is 0.64 m with a standard deviation of 0.28 m. Smaller (semi-)diurnal constituents were derived from the eight main constituents. Finally the annual constituent Sa has been added. Other low frequency constituents appeared to have a low sensitivity to the model output and are not implemented in the current (Zijl (2013)). The total tidal water level is a superposition of n tidal waves via

$$\eta_t(\varphi, \lambda, t) = \sum_{j=1}^{n} \hat{\eta}_j \cos(\omega_j t - \theta_j) \tag{4.12}$$

Where $\hat{\eta}_j$ is the amplitude, ω_j the frequency, and θ_j the phase of the tidal constituent j.

Inverse barometer The effect of local air pressure $p_a(\varphi, \lambda, t)$ on surface elevation is implemented on the open boundaries based on the so-called inverted barometer effect (Ponte and Gaspar (1999)):

$$\eta_a(\varphi, \lambda, t) = -\frac{p_a(\varphi, \lambda, t) - \langle p_a(t) \rangle}{\rho g} \tag{4.13}$$

Here $\langle p_a(t) \rangle$ is the spatial average of $p_a(\varphi, \lambda, t)$ over the Northeast Atlantic Ocean. For the present simulations, the effect of temporal varying mean atmospheric pressure is assumed to be negligible, since they are rather small compared to differences with the local air pressure. Therefore the atmospheric pressure is also averaged into time, resulting in a both spatial and time averaged atmospheric pressure for the simulation year. Note that only the atmospheric pressure above water based surfaces is taken into account for calculating the average. The pressure fields are provided by the meteorological High-Resolution Limited Area Model (HiRLAM). It has a spatial resolution of 5 - 15 km with an temporal adjustment every 6 hours. On first approximation, an increase in air pressure by 1 mbar causes a decrease of 1 cm in sea surface elevation.

Residual surface elevations Steric height anomaly is the difference between the height of a given water column and the height of an ideal reference column with a temperature of 0°and salinity of 35 PPT. Both columns are considered to experience the same surface pressure. The steric height over the whole vertical can be expressed as

$$\eta_{steric}(\varphi, \lambda, t) = \frac{\rho_{ref} - \rho(T, S)}{\rho_{ref}} h(\varphi, \lambda, t) \tag{4.14}$$

Where ρ_{ref} is the density of the reference column. Steric heights can reach up to 10cm. Large elevation differences occur for example in the Norwegian Trench which is highly stratified. Implementation of steric heights is not possible in the Delft3D-FLOW module.

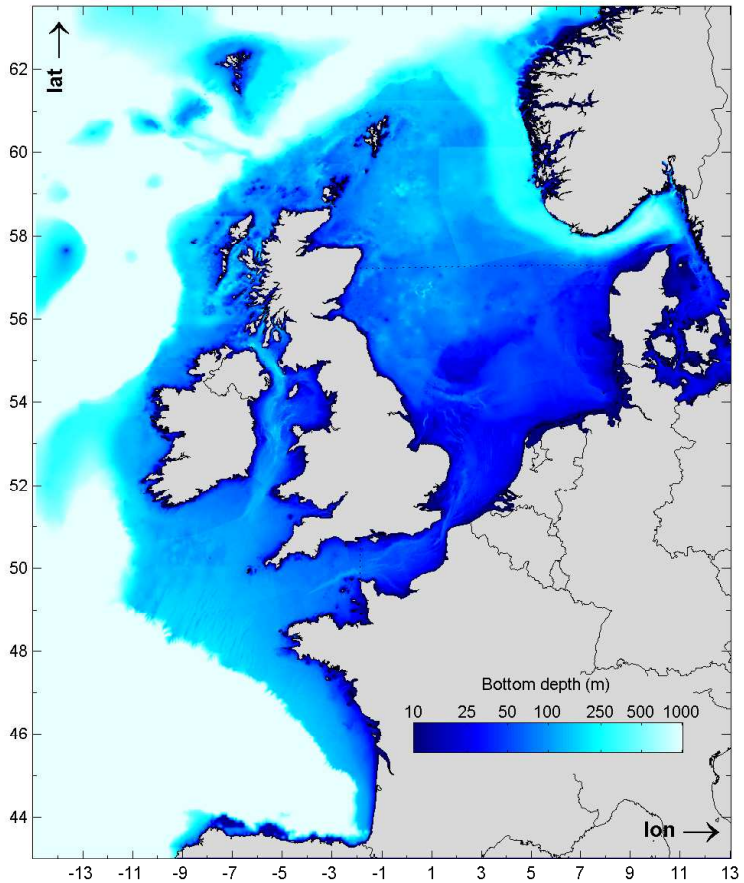

Figure 4.1: DCSM bathymetry, relative to MSL

Therefore its impact is implemented in an alternative, more indirect, manner. Along the boundaries of the model a so-called tidal zero-frequency component 'A0' is implemented. this is in fact a spatial varying residual surface elevation. Mean water levels are obtained from altimeter data acquired by the joint venture TOPEX/Poseidon. Altimeter data is available for the period of October 1992 till November 2010. The dataset contains a monthly varying sea surface topography with respect to the geoid on grid cells of 1 degree. For each boundary station, its A0 component is obtained from the closest TOPEX/Poseidon grid cell. A smoothing function is used with the 5 surrounding stations to minimize water level gradients at the boundaries. Figure 4.2 shows the magnitude of the A0 components for 2007 as obtained from TOPEX/Poseidon for both models.

Meteorological forcing A spatially and time varying wind field is imposed over the whole domain for the simulation of meteorological induced flow. These fields are provided by HiRLAM. It has a spatial resolution of 5 - 15 km with and adjusts every 6 hours. In chapter 5.3 some simulations were done for 1984 up to 1993. However, HiRLAM does not provide data prior to 2002. Therefore another source is used for these specific simulations. The publicly available data of the interim reanalysis project ERA-Interim provided by the European Centre for Medium-Range Weather Forecasts (ECMWF) is used. It has a spatial resolution of 1.5°x 1.5°and adjusts every 24 hours.

4.4 Time Frame

Before valuable results can be obtained, some test simulations have been done to determine the time step needed for both models. For DCSMv5 a time step of 10 minutes is used; DCSMv6 requires a smaller time step of 1 minute. Although the time discretization is implicit, the model becomes unstable for larger time steps. With the correct time step, the hydrodynamic behaviour was monitored to investigate the time needed for the model to adjust the imposed initial conditions to its dynamic equilibrium.

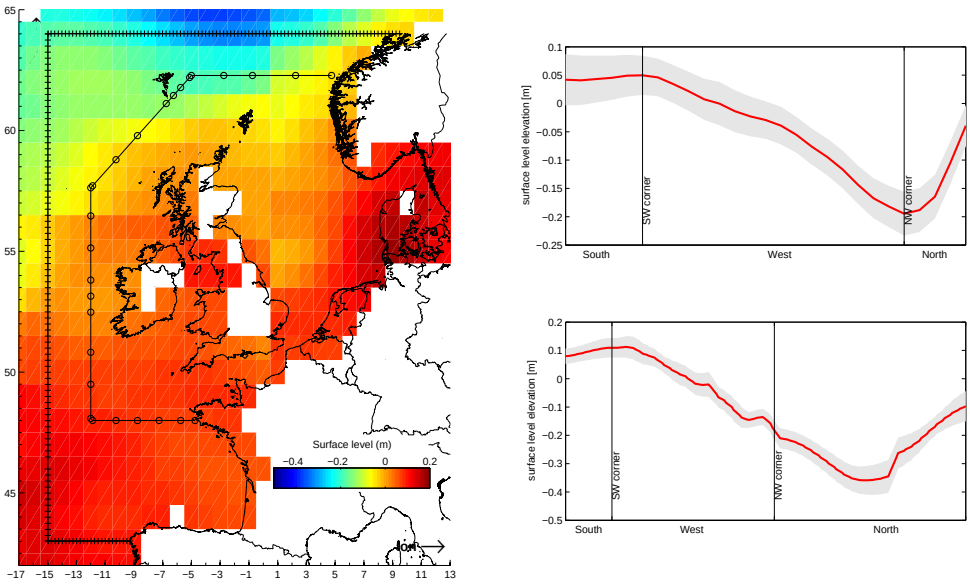

(a) Spatial variation

(b) Boundary values

Figure 4.2: A0 component for 2007, data obtained from TOPEX/Poseidon. An overview of spatial variability is given (left) with the boundary locations indicated with a '+' symbol for DCSMv6 and 'o' symbol for DCSMv5. The values at the boundaries for both versions is shown on the right. The annual mean A0 component (red line) is implemented on the models. The corresponding standard deviation is shown as indicator of monthly variability (grey area).

Barotropic calculations are executed with a so-called cold start; knowledge of the computational variables (surface level and velocity) are not implemented on the initial conditions. Therefore the computation needs some time to reach its dynamic equilibrium, defined as the spin-up time. For the barotropic calculations the initial conditions η_i, U_i and V_i are all set to zero. The spin-up time depends on the time needed for disturbances enforced at the boundaries to reach the whole model domain. In addition, numerical wiggles, which are induced by the large gradients between boundary and initial values, should have travelled outside the model domain or be damped out. For the former, the furthest point in the model domain to be reached from the model boundaries is the Kattegat. Based on the shallow water approximation, the propagation of (e.g. tidal) disturbances equals $\sqrt{gh}$. By assuming a uniform water depth, it takes about a day for the boundary conditions to reach the Kattegat. The presence of numerical wiggles is more difficult to estimate and can be of a much larger time scale. It depends on the type of boundary conditions, the amount of numerical damping and the amount of physical damping. Numerical wiggles could even be for an infinite time be present inside the model domain.

The discharge through the Strait of Dover has been used as test case for the time needed to get rid of, or at least minimize, all numerical wiggles. Four simulations are compared with different spin-up times; namely 7, 14 and 31 days are compared with a 4 months spin-up. For the latter it is assumed all numerical wiggles are either damped out or have left the model domain. Furthermore a relative error of 1% between a single simulation and reference simulation is considered to be satisfactory. A comparison of the different simulations is shown in figure 4.3 where it is clear that the 14 days spin-up is long enough for numerical wiggles to disappear.

In case of the computation of dissolved substances, such as temperature T and salinity S, the rate of displacement of these properties should be taken into account. Where a surface perturbation travels with a speed of $\mathcal{O}(10\ \mathrm{ms}^{-1})$ in shallow water, dissolved matter travels together with the fluids motion $\mathcal{O}(0.1\ \mathrm{ms}^{-1})$. Therefore, in contrast to the non-conserved fluid properties for barotropic flow (η,u and v), temperature, salinity and other dissolved matter have a much larger age distribution. A modeling study on the residence time of various inflow sources into the North Sea has been executed by De Ruijter et al. (1987). For example, it takes about one year for the fresh river Rhine water to reach the coast of Denmark. For this reason, a similar cold start as used for the barotropic case will result in a spin-up time in the order of years. To reduce this large amount of computation time a so-called hot start is performed. A hot start computes with initial values (ζ,u and v, T, S) which correspond to the dynamic equilibrium of the model. These initial variables are obtained in two steps. First, the temperature and salinity distributions within the North Sea are used from NOOS temperature and salinity distributions. Since the spatial domain of the models is larger than the obtained density maps, the initial conditions outside the NOOS area are set equal to the salinity and temperature conditions of the

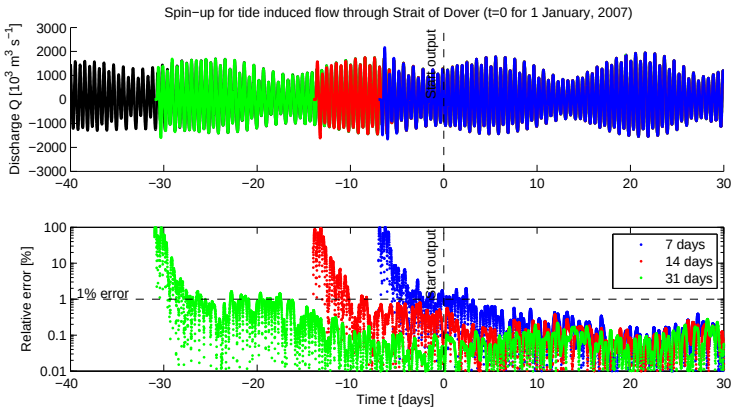

Figure 4.3: (top) Tide induced discharge through the Strait of Dover with a cold start of 7 days spin-up (blue), 14 days spin-up (red), 31 days spin-up (green) and reference case of 120 days spin-up (black). (bottom) relative error with reference case.

	DCSMv5	DCSMv6	Units
Number of grid cells	201 x 173	1121 x 1261	[n x n]
Gridcell size	10 x 10	2 x 2	[km^2]
Time step	10	1	[min]
Modelling year	2007	2007	[year]
Barotropic initial conditions	Uniform^a	Uniform^a	[-]
Baroclinic initial conditions	Diagnostic^b	Diagnostic^b	[-]
Barotropic spin-up	14	14	[days]
Baroclinic spin-up	365 (hot start)	365 (hot start)	[days]
Boundary condition	$\eta(\varphi, \lambda, t)$	$\eta(\varphi, \lambda, t)$	[m]
Number of boundary stations	27	208	[-]

Table 4.1: General DCSM properties.

[a] All parameters are initially set to zero over the whole domain, hence $U(\varphi, \lambda, t_0) = 0$, $V(\varphi, \lambda, t_0) = 0$, $\eta(\varphi, \lambda, t_0) = 0$.

[b] Temperature and Salinity distributions are obtained from NOOS maps from January 2007. Another year has been simulated to let the model reach its dynamic equilibrium.

closest boundary conditions. Figure 4.4 shows the implementation of both temperature and salinity distributions into the initial conditions. Even though the missing data is for the largest part outside the NWECS where density variations are small, the deviations in density still could result in some undesired wiggles. Another preliminary simulation of 1 year has been executed to let the model reach its proper dynamic equilibrium. The obtained fluid properties (S,T,U,V,η) after one year are used as initial conditions for the baroclinic hot start.

4.5 Summarized model properties

For clarity all important properties of both models are summarized in table 4.1. It should be noted that these properties are the starting point of all model simulations. During this thesis, several properties have been modified to obtain better, or other, results.

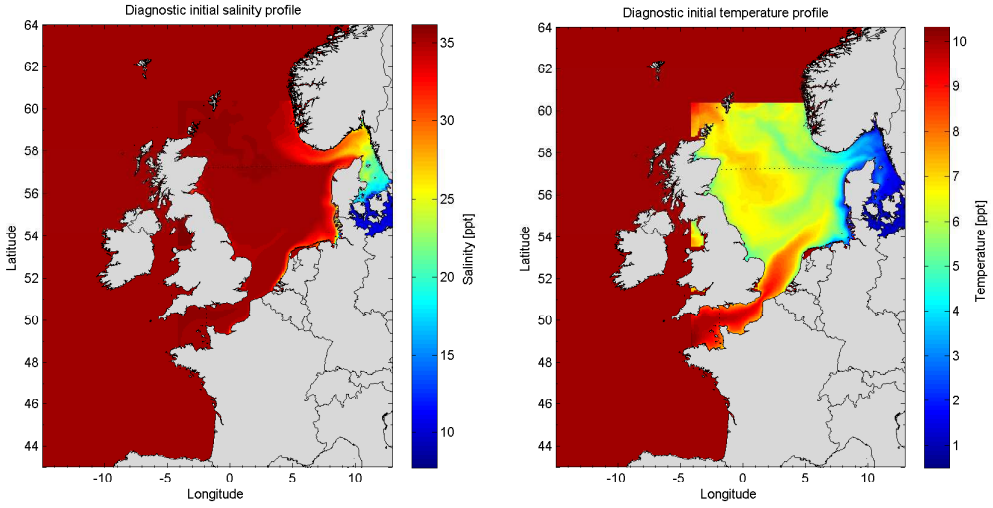

(a) Salinity

(b) Temperature

Figure 4.4: Diagnostic salinity and temperature profile based on NOOS density maps in January 2007.

5 Output analysis

5.1 Introduction

In this chapter, the original DCSM models will be analysed. The complete North Sea circulation will for the largest part only be investigated in a qualitative way. Its general circulation pattern is compared with available literature. Fluxes through the Strait of Dover are examined in much more detail and also in a quantitative way; the amount of water flowing through the Strait of Dover is compared with available measurements and modelling studies. The uncertainty on the North Sea circulation, as well as the fluxes through the Strait of Dover, are quite significant. Therefore, this section will put the computed residual flow in perspective with known stream patterns, measured data and other modelling studies.

The boundary and miscellaneous properties of the models used in this section are a direct copy from the models used by Zijl (2013). Zijl calibrated the model on water level variations; model results were compared with available measurements. The model computes barotropic flow, hence density variations are not taken into account. River inflows, as well as the Baltic inflow, are not present in the present models.

In the first section the annual large scale circulation pattern is investigated in a qualitative manner for the whole North Sea. Both versions of DCSM are used and showed similar results. Therefore only DCSMv6 is presented. In section 5.3 the so-called Cap de la Hague experiment is simulated. Based on measurements and modeling studies, mean trajectories and time scales can be defined in relation to the circulation pattern in the English channel and southern North Sea. Due to lack of time, in combination with many desired simulations, most simulations are only done in DCSMv5. The first part of this experiment was also simulated in DCSMv6 and showed comparable results. In the final section the residual flow through the Strait of Dover is investigated in much more detail for both model versions.

5.2 General North Sea circulation

In this section a qualitative impression will be given on the circulation pattern of the present model (DCSMv6). This is done with a Fourier analysis on the spatial velocity distribution for the zero-frequency component. Results obtained in this way are compared to known circulation patterns from a variety of authors. Figure 2.3 illustrates the large scale North Sea circulation, it is desired for the present model to give similar circulation structures. The model is forced by tidal water elevations and atmospheric pressure at the boundaries and meteorological forcings at the water surface. Results are shown in figure 5.1, the general structure is similar as known circulation patterns, some important aspects are discussed below.

At the North-western boundary of Atlantic water enters the North sea and splits up into two distinct branches. The largest part flows to towards the East, known as the Dooley current. It is clearly present at a latitude of 58°N, it follows more or less the 100m isobath to conserve potential vorticity. At the edge of the Norwegian trench it joins the large Atlantic inflow from the North and moves south along the same isobath to enter the Skagerrak. Once at the Skagerrak it meets the Jutland coastal current, which flows along the Danish coast to the North. A third current which should meet the other two currents at the Skagerrak is missing in the present simulation. This is the density driven current along the Dogger bank located at a latitude of 55°N (see e.g. Holt and Proctor (2008)) with a shallow depth of 40m. The fact that the present model simulates barotropic flow makes it logical that the latter current is missing in the present simulation. Currents in the Skagerrak and Kattegat, as well as the Norwegian Coastal Current are highly stratified due to the Baltic inflow. Even though the present simulation does not include density variations, the circulation pattern still shows similar circulation patterns. It follows the edge of the Norwegian trench and turns in an opposite direction. From here it flows along the Norwegian coast in Northern direction. Around 59°N two counter rotating eddy's are present along the coastal boundary, as also stated by Johannessen et al. (1989). The strong Norwegian Coastal current flows around these eddy's and leaves the model domain. On the Western side of the model domain the other, smaller, branch of Atlantic inflow flows along the British coast up to a latitude of 52,5°N. From here the majority of the current turns easterly towards the Dutch coast. From here a wide branch of 200 km flows along the Waddenzee and German coast where

it reaches Denmark. A much smaller part continues to flow South towards the English Channel. Here it meets the inflow at the Strait of Dover and travels along the Dutch coast.

A second Fourier analysis has been executed on the specific discharge, defined as the velocity integrated over the vertical $q = \vec{u}h$. They give a useful indication on the transport of suspended or dissolved materials. Results are shown in figure 5.2. Here it can be seen that the largest transports occur in the Northern North Sea by among others the Dooley current and Norwegian Coastal current. When boundary in- and outflows are compared with table 2.1 two large differences can be observed. First of all, the Strait of Dover inflow is almost three times smaller than estimated by Winther and Johannessen (2006), who assumed the inflow to be 160000 m^3s^{-1}. Second, the large in- and outflow in the Norwegian trench are two times smaller. For the latter, this is known to be a high density driven current, and therefore the lower in- and outflows are not surprising. The inflow with the Fair Isle Current shows similar values as table 2.1.

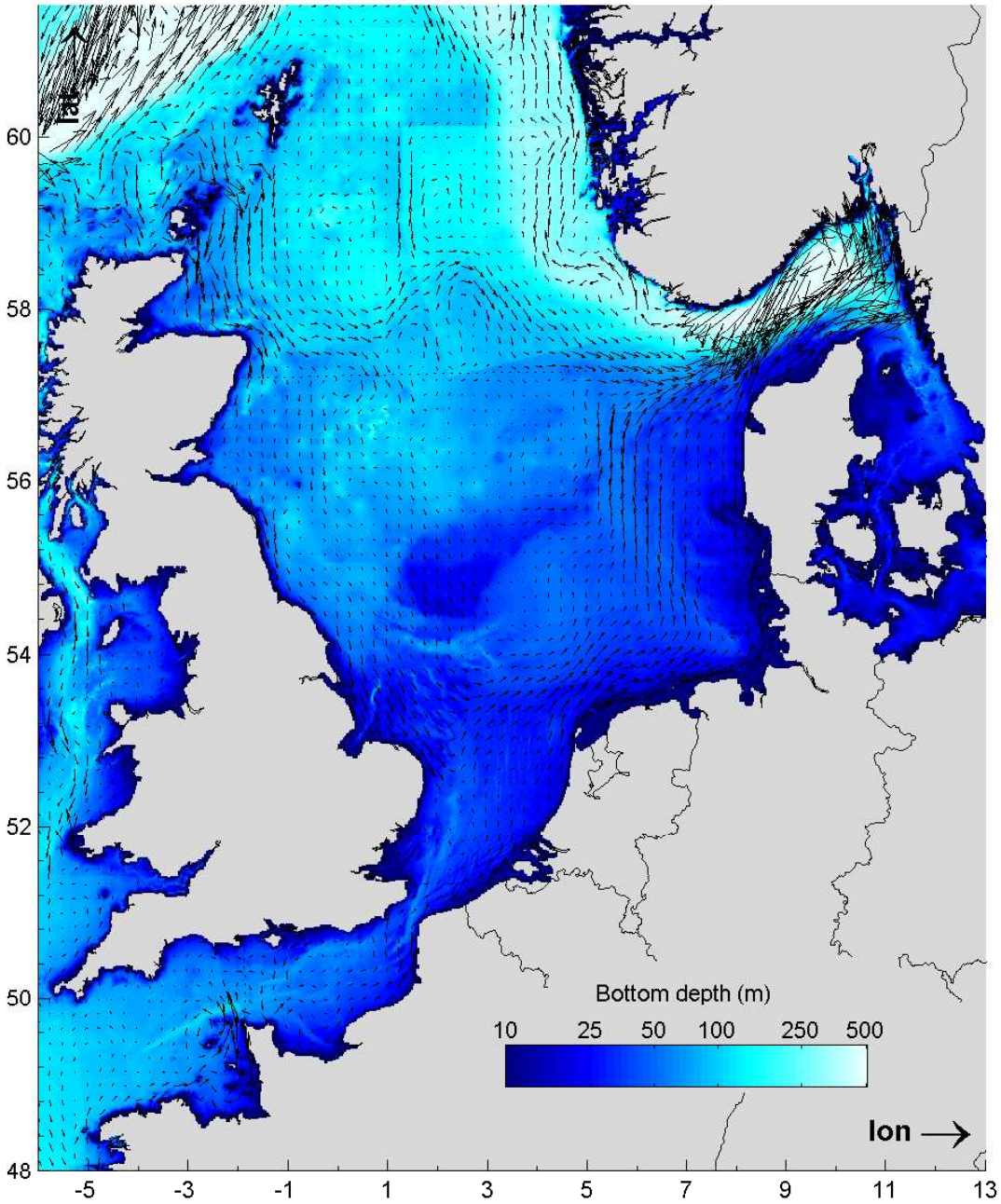

Figure 5.1: Annual mean, depth averaged, horizontal velocities for barotropic flow. For clarity only vectors are shown at every tenth grid cell. Magnitude is indicated with the vector length on square root scale. Bottom depth is plotted on logarithmic scale.

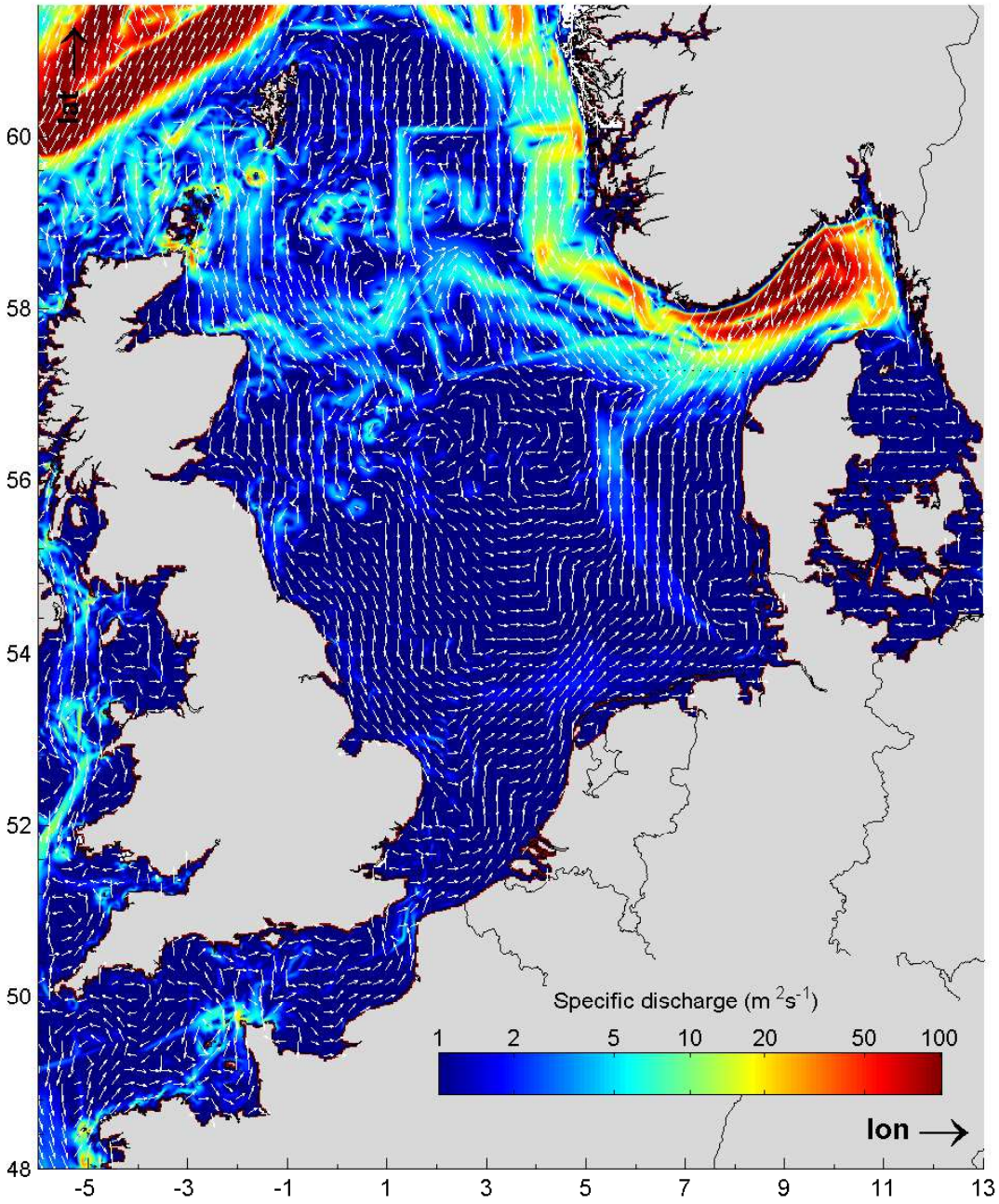

Figure 5.2: Annual mean, depth integrated, horizontal velocities for barotropic flow. For clarity only vectors are shown at every tenth grid cell. Magnitude is indicated with the color map, direction is shown by the corresponding vectors.

5.3 Cap de la Hague experiment

The English Channel is the southern connection between the Atlantic Ocean and the North Sea. On average, it takes about a year for a water particle to travel from its western boundary with the Atlantic Ocean to its northern boundary with the North Sea. However, this so-called residence time highly depends on the starting time and location of the water particle. During strong westerly winds, a water particle has a residence time of a couple of months through the center of the Channel. On the other hand, residence times along the coastal boundaries can range up to several years. The use of tracers makes it possible to monitor these time scales. A large amount of tracers is available, both natural and artificial. Several tracer based studies have been executed in the past for both the North Sea and the English channel. These studies investigated for example salinity and temperature distributions (Luyten et al. (2003)), fish larvae, suspended heavy metals (Van Pagee et al. (1986)) and dissolved nutrients (Salomon et al. (1991), Prandle (1984)). Based on spatial distributions they made a qualitative estimate on the residual circulation pattern, as well as typical resicence times in the studied regions. However, these estimates vary widely from one another. This is mainly due to the unknown origins of these tracers, from the observed distributions the ratio of sources is estimated with a significant uncertainty. For example, Prandle (1984) made an early estimate based on ^{137}Cs nuclides released from La Hague. He stated a residence time of one year between La Hague and the Strait of Dover. Later studies, such as Salomon et al. (1995), suggested the residence time to be only 4 months based on ^{125}Sb release. More distant locations in the North Sea also have a wide variation. For example, residence times for the Baltic entrance range from 15 to 23 months.

In the beginning of the 1980's a leakage from a nuclear power plant at La Hague, France, occurred. As a result, several radionuclides were released into the English Channel. Even though this leakage was considered as a pollution for the oceanic water, monitoring the distribution of these nutrients became very valuable for oceanographers. For the different types of nuclides, the radioactive Antimony-125 (^{125}Sb) was considered as remarkably useful as an oceanographic tracer. This is because it is regarded as a specific marker of discharges from La Hague since it is absent in the seawater background. In addition it has, at least for the English Channel, a more or less conservative behaviour. Its nuclear decay rate is considerably smaller compared to its residence time in the English Channel.

In this section, the release of Antimony-125 has been simulated to obtain a better insight in the different time scales and mean trajectories of the water particles in the English Channel and southern North Sea. Limitations of the DCSM models should be taken into consideration when results are compared to previous studies. The English channel is in general well mixed over the vertical, therefore baroclinic induced flow becomes negligible. Hence, representations of the movement of tracers should be reasonably well. However, this approximation fails at two areas in the English channel. First there is the western part, which stratifies during summer. Since only a small fraction of Anitomy-125 released from La Hague reaches this area it should not affect the general pattern of the distribution in a significant way. The other areas are the ROFI's at the French and English coastal boundaries. Especially the Seine has a significant fresh water outflow and creates a relative strong current along the coast. It is expected that the model will behave relatively slowly at these areas, comparison between results at these locations is therefore of lesser value.

For a fluid in motion, dissolved materials transport due to both convection as well as dispersion. This means there is no one-to-one relation between the fluid' s residual velocity and particle displacement in time. For this reason, results given in this section only give a rough estimate on the residual water circulation. To monitor the leakage of the tracer from La Hague three new time scales are introduced. Consider a bounded region in which a tracer (c) is added at a certain time (t_0) and location (x_0, y_0). Now we can define:

1. The 'residence time' τ_r as the time needed for $c(x_0, y_0, t_0)$ to leave the system at any boundary of the region.

2. The 'transit time' τ_a as the time needed for $c(x_0, y_0, t_0)$ to travel to any location (x, y) within the region.

3. The 'half-life' $\tau_{1/2}$ as the time needed for a total amount of radioactive substance to decay to half of its initial value.

The half-life of ^{125}Sb is known to be 2.7 years. The residence time in the English Channel from Cap de la Hague is in the order of 5 months. Therefore the decay rate is not significant in this region, as mentioned before. However, in this section trajectories are monitored up the Kattegat. The corresponding transit time is at least one year, dependent on the time of release. For this reason a nuclear decay rate is implemented into the model. In case of a closed system, i.e. the substance does not leave the system and no extra substance is added, the concentration as a function of the decay rate is given as:

$$\frac{\partial \langle c(t) \rangle}{\partial t} = -\lambda \langle c(t) \rangle \tag{5.1}$$

Where λ is the decay rate and $\langle c(t) \rangle$ is the spatial averaged concentration over the whole region. Under the assumption of exponential behaviour $c(t) = c_0 e^{-\lambda t}$ with c_0 as the initial concentration, the decay rate is proportional to the half life by $\lambda = -\frac{\ln 1/2}{\tau_{1/2}}$. For Antimony-125 the corresponding decay rate is $7{\cdot}10^{-4}$ s^{-1}. For the current model, the term $\lambda c(x, y, t)$ is added as a sink term on the right hand side of the transport equation 4.6.

For this thesis, three experiments on the release of radionuclides have been done. In all cases, simulations are done for the period of the leakage; 1984 till 1993. Since meteorological forcings may differ substantially over the years, the choice of a simulation of the same period is important for an accurate comparison. Note that every simulation first starts with a spin-up time of 14 days in which no radionuclides are released. In the first experiment, a stationary release of Antimony-125 is simulated for three years. Based on this study the mean trajectories from Cap de la Hague are monitored and visualized. The second experiment is similar, but in this case only a short, concentrated, release of 1 week is simulated. The high concentration cloud is followed to give an indication of the spatial varying transit time. In the third experiment the actual La Hague leakage with varying discharges is simulated and compared to measured concentrations from Guéguéniat et al. (1994). Most of the simulations are done in DCSMv5, since this computation time is relatively small. There was unfortunately not enough time to compute the same experiments in DCSMv6. However, the first experiment was also simulated in DCSMv6, and it showed similar results.

5.3.1 Experiment I: Mean trajectories

The first experiment is a theoretical approach, where the focus lies on general stream patterns. Time scales are discussed in the next two experiments. A constant discharge of $4{\cdot}10^9$ Bq/s Antimony-125 is released from La Hague. To bypass time dependencies, the model is forced by a spatial uniform and stationary wind field. A moderate west southwest wind velocity of $\hat{W} = 7.33$ ms^{-1} is chosen, equivalent to a shear stress of $\hat{\tau}_w = 0.074$ Nm^{-2}. The residual flow through the Strait of Dover is 79000 m^{3}s^{-1}. This is in the same order of the actual flow through the Strait of Dover when forced by a time and spatial varying wind field, as will be shown in the next section. Concentration distributions of Antimony-125 are presented in figure 5.3 for 4 different moments. For the first few months the concentration cloud moves into two distinct branches. One moves south along the coast of Normandy, where the second branch spreads out in northwest direction (fig. 5.3a). After more or less three months the concentration of Antimony-125 in the cove between Bretagne and Normandy stays more or less equal, it has reached its dynamic equilibrium. North of La Hague the cloud moves to the East in the direction of The North Sea with the largest displacements in the center of the Channel (fig. 5.3b). Concentrations at the Bay of Seine are still relatively low. Near the Strait of Dover, the largest velocities are reached at the French and Belgian border (not visible in this figures). After the cloud has moved through the Strait of Dover, it travels along the Dutch coast to the North. It does not reach points northwest of the ampidromic point located at 2.9°E, 52.5°N. The main stream is located several kilometres from the coast, leaving low concentrations near the Dutch coast (fig. 5.3c). After two years the English Channel and southern North Sea have reach their dynamic equilibrium with high concentrations northeast of La Hague and along the French, Belgian, Dutch and German borders. North of here water is flowing into the Kattegat, where it rotates in a cyclonic way along the land boundaries to the Norwegian coast (fig. 5.3d).

5.3.2 Experiment II: Transit time

In the second experiment, a quasi-punctual release of 10^9 Bq/s during the first week of January 1984 (a total of $6{\cdot}10^{14}$ Bq) has been simulated for three years. A time and spatial varying windfield is imposed obtained from ERA-Interim data. The high concentration cloud will propagate in time and space in a similar matter as discussed in previous section. However, since the release is only for a short time, each location will show a concentration peak of Antimony-125 at a certain time. This represents the passing of the puntual release of Cap de la Hague. Based on time differences between concentration peaks at various locations an estimate can be done on the spatial transit time. The Antimony-125 starts as a highly concentrated cloud at La Hague, and moves away as a function of time. However, due to both convection and dispersion of the dissolved material, the shape of the cloud becomes distorted. Due to constantly changing meteorological forcings and nuclear decay, the initial peak may be flattened, damped and separated into different parts. This makes

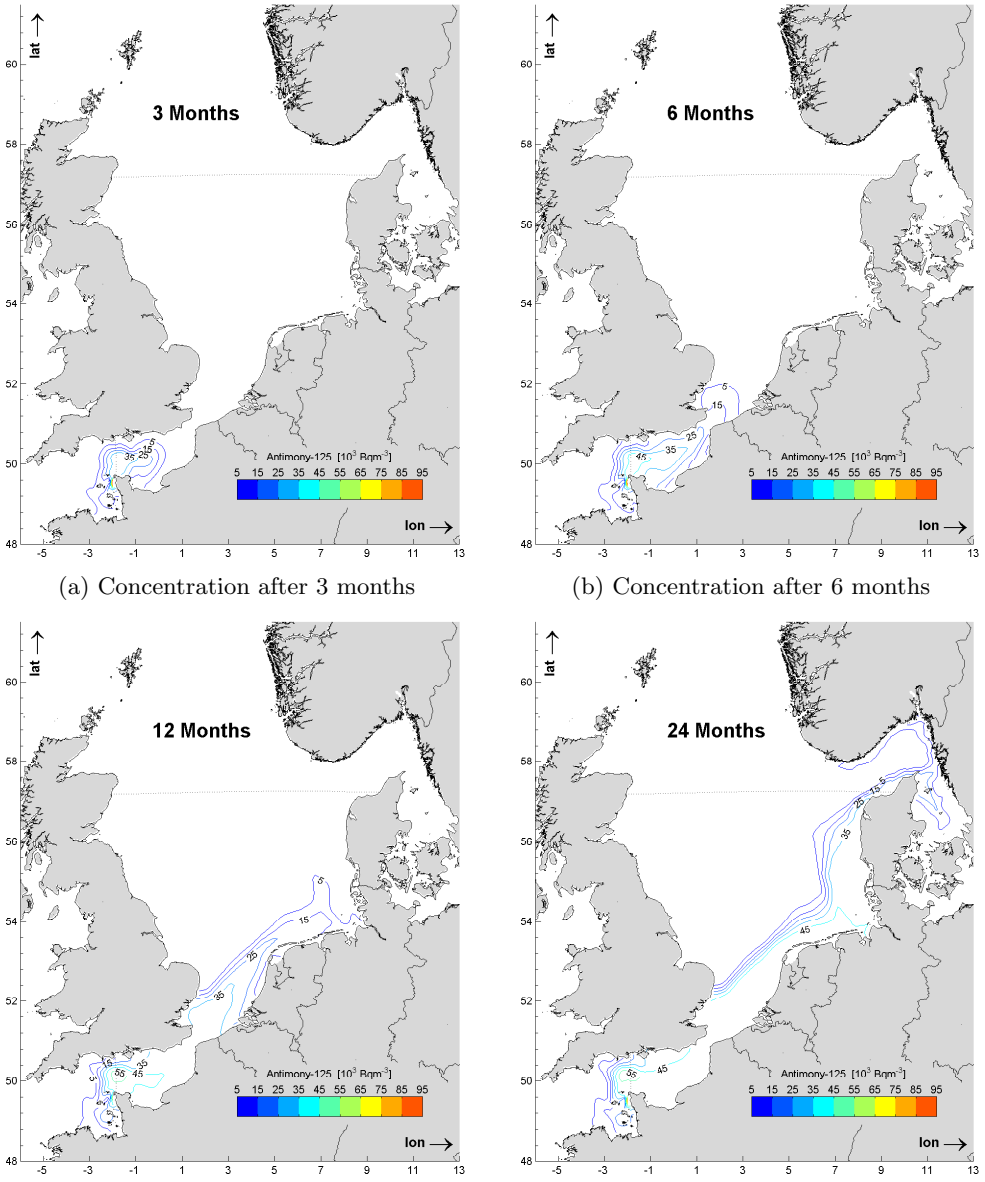

(a) Concentration after 3 months

(b) Concentration after 6 months

(c) Concentration after 12 months

(d) Concentration after 24 months

Figure 5.3: Simulation of Antimony-125 displacement with a permanent discharge from La Hague. The model is forced by a west southwest wind with a corresponding shear stress of $\hat{\tau}_w = 0.074$ Nm^{-2}.

it a challenge to define the exact time lag between two distinct locations.

At first, 11 monitoring stations (see fig. 5.4) are investigated in detail on their time dependent concentrations. A similar simulation has been executed by Salomon et al. (1995), who validated his output with measurements. Results of both tests are shown in figure 5.5. Two major differences can be observed. First of all, a clear time lag occurs starting from station E up to the last station K. While concentration peaks close to La Hague occur on similar time events, further away from La Hague the transit time between Salomon et al. (1995) and the present model behaves on a ratio 1:1.8 (fig. 5.4 bottom-right). Hence the present model behaves almost two times slower considering residual circulation. The second notable difference is the shape of the curve after the peak has passed by (the tail). After the peak has passed by, Salomon et al. (1995) suggests a much faster decay than the present model. In other words, it takes longer for the concentration cloud to completely pass through a station. This again suggest the model to behave more slowly.

The complete spatial variability of transit times from La Hague is shown in figure 5.6b. Again, the time of maximum concentrations are compared to the time of release from Cap de la Hague. Note that this is still the same simulation, only in this case the transit time is shown over the whole domain. Values obtained from Salomon et al. (1995) are shown in figure 5.6a. Especially in the English Channel the model behaves much more slowly. Salomon suggests a transit time of around 3,5 months at the Strait of Dover, where the present model computes it to be 7 months. This ratio (1:2) corresponds to the ratio found by the monitoring stations (1:1.8). However, in the North Sea, the difference in transit time between Salomon en DCSM stays more or less equal. For example, the region 1°North of the Dutch coast is reached after 8-10 months by Salomon, where the present model suggests 11-13 months. The corresponding ratio (1:1.4) is much smaller than the ratio found by the monitoring stations. This is mainly because of the transit times obtained from station J and K. In the present model, the largest mean residual current flows along the Dutch coast, and deflects to the north at 7°E, more or less above the border between Germany and the Netherlands. Salomon suggests this deflection to be more to the east, at around 8°E. Stations J and K lie East of this main stream, close to the Danish coast. Therefore it takes much longer for the Antimony-125 to get here, transit times are significantly larger increased. When additional stations would be placed more to the West, the difference between Salomon and DCSM would be much smaller. Based on this analysis, the conclusion can be drawn that especially in the English Channel the present model behaves very slow. Once the stream has reached the North Sea, the representation of transit times is much better except for specific regions like the region in front of the Danish coast.

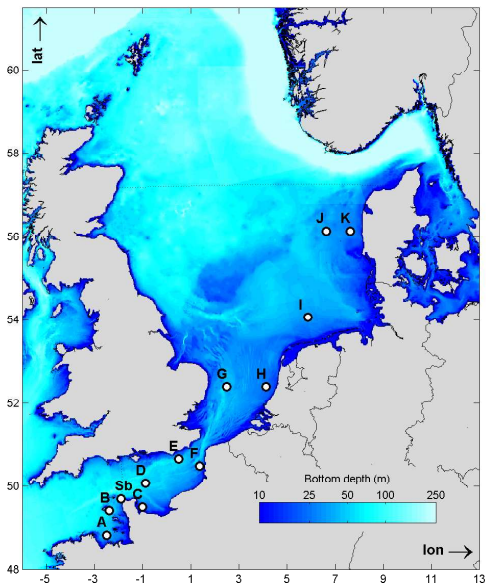

Figure 5.4: Monitoring stations for Antimony-125 concentrations.

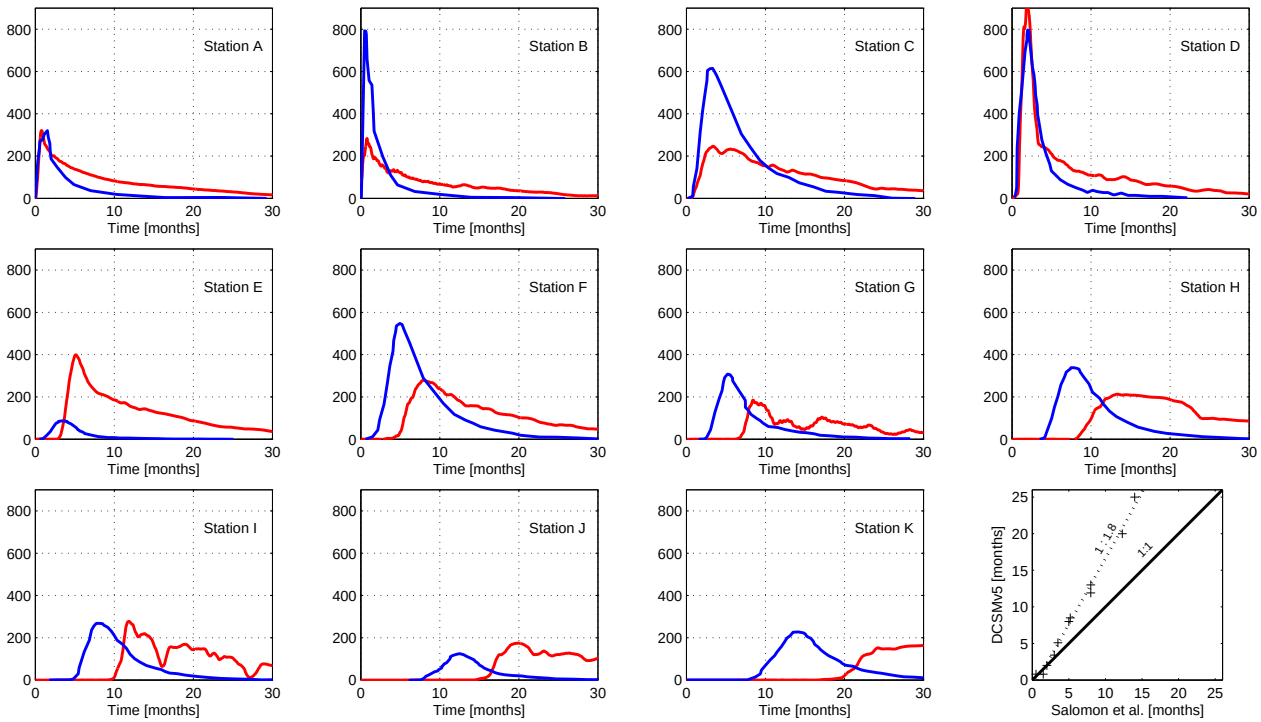

Figure 5.5: Concentrations of Antimony-125 (Bq m^{-3}) for the present model (red) and results obtained from Salomon et al. (1995) (blue) at the different monitoring stations from figure 5.4 as a function of time.

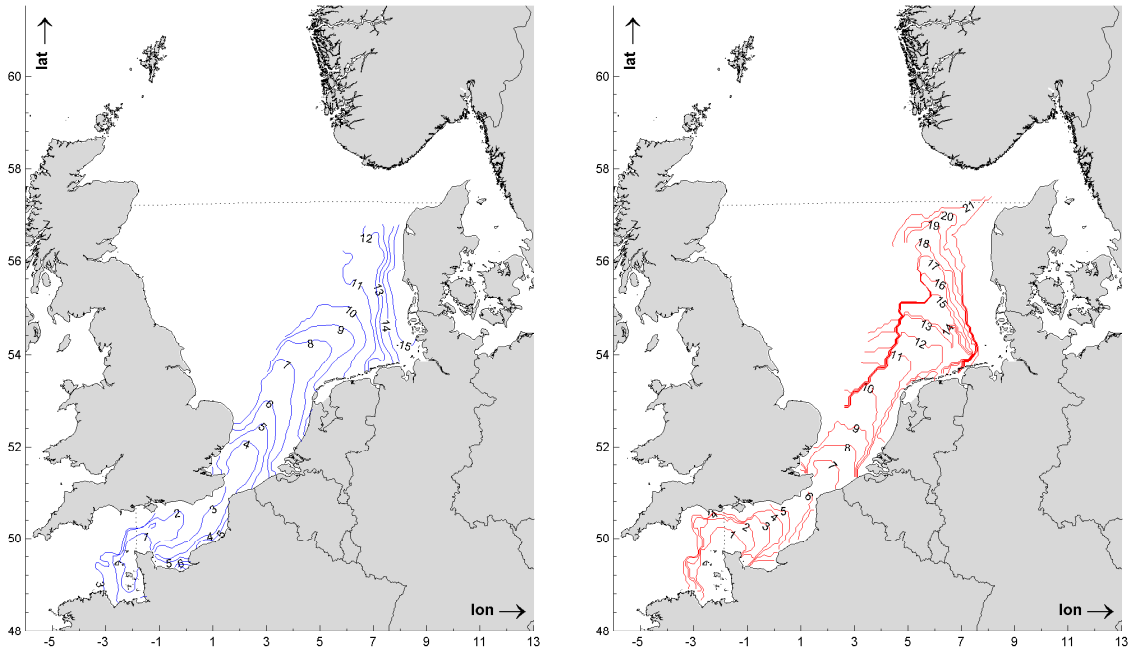

(a) [After Salomon et al. (1995)]

(b) DCSMv5

Figure 5.6: Estimated transit times from La Hague in months. Based on (a) the dispersion of Technetium-99 in the period 1983 to 1992. and (b) the dispersion of Antimony-125 in the period 1983 to 1986.

5.3.3 Experiment III: Data comparison

In this final experiment a simulation of the actual leakage at Cap de la Hague is executed. The model results are compared to measurements, obtained from research based cruises. In the early 90's ten cruises were done covering the English Channel, North Sea, Skagerrak and Kattegat. On these cruises, four radionuclides were measured, namely ^{137}Cs, ^{99}Tc, ^{125}Sb and ^{90}Sr. Results on the trajectories of these cruises, as well as their obtained concentrations, are presented in Herrmann et al. (1995). An extensive data analysis has been executed by Guéguéniat et al. (1994). In this final experiment a time varying amount of Antimony-125 is released for the period of 1984 till 1993. Figure 5.7 shows the monthly discharges from La Hague. Between August 1988 and May 1989 the amount of Antimony-125 released form La Hague is relatively low in comparison with both previous as well as following periods. During these months, a low amount of Antimony-125 travels towards the North Sea. On June 1989, this so-called "low concentration cloud" is passing through the Strait of Dover. The scatter plot in figure 5.8a shows the observational data as published by Guéguéniat et al. (1994). The cloud is clearly present around the Strait of dover between 1°E - 3°E and 50°N - 52°N with a concentration of around 10 Bqm^{-3}. More to the North concentrations are higher, also close to La Hague concentrations are significantly higher due to the large amount of release on June 1989. In the same figure the model output on June 1989 is shown with an area plot. The low concentration cloud is still very close to La Hague between 3°W - 1°E and 49°30'N - 50°30'N. Three months later the cloud is on the same position as the cloud from observational data. This is shown in figure 5.8a, where observational data on June 1989 (scatter plot) is compared with modelled data on October 1989 (area plot). More to the North, in front of the Danish coast, measurements suggest the concentration to be significantly lower than model results. The present model seems to trap the radionuclides within this region, and therefore let a much less amount pass though into the Skagerrak.

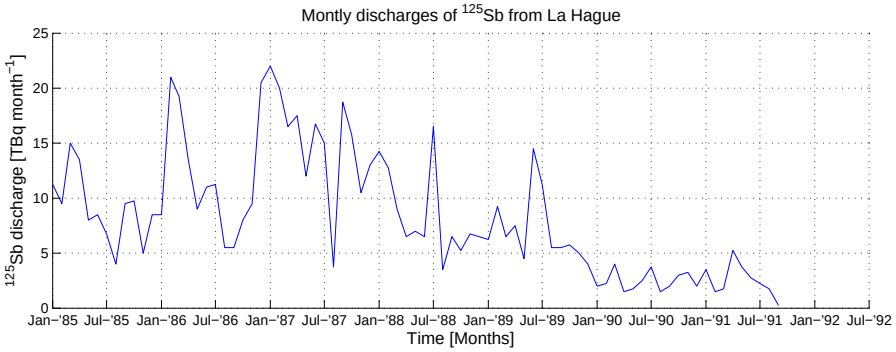

Figure 5.7: Monthly discharges of Antimony-125 from Cap de La Hague between 1985 and 1992, data obtained from Guéguéniat et al. (1994).

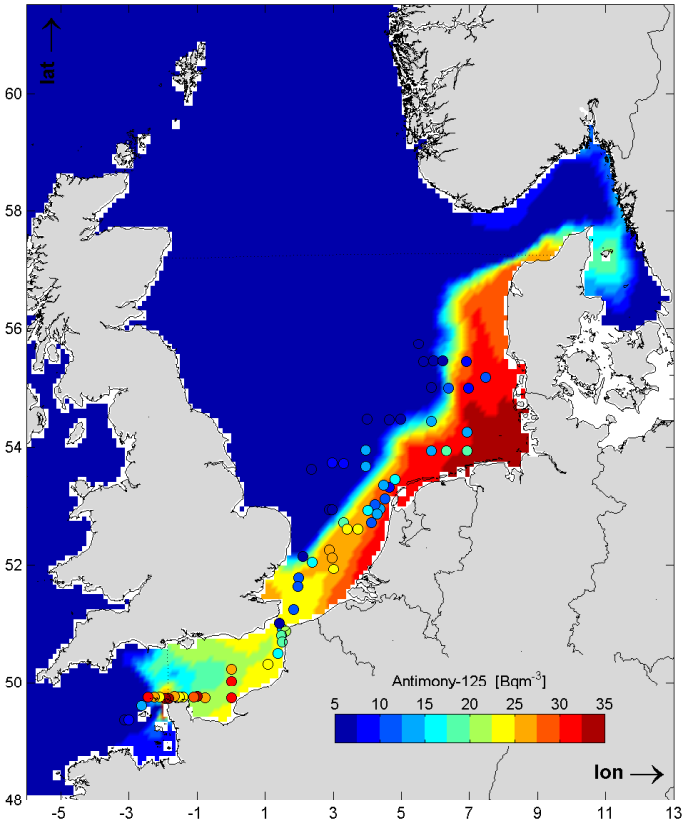

(a) Model on June 1989, measurements on June 1989.

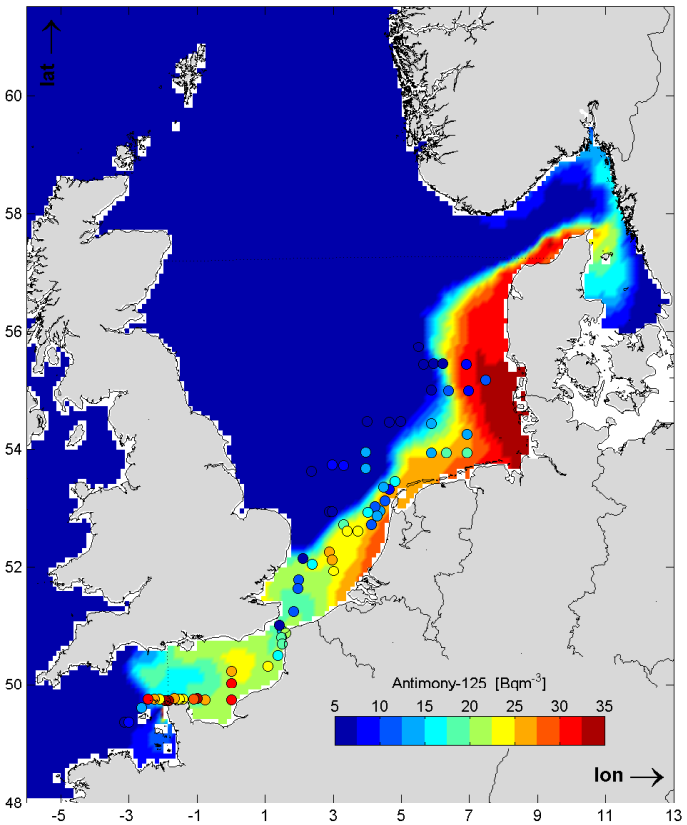

(b) Model on October 1989, measurements on June 1989.

Figure 5.8: Antimony-125 distributions based on model simulations (surface plot) and measurements (scatter plot). Colors indicate the concentration. Observational data is obtained from Guéguéniat et al. (1994).

5.4 Residual flow through Strait of Dover

In this section a quantitative analysis is executed on residual fluxes through the Strait of Dover. The fluxes are investigated as a function of tidal and meteorological forcings and compared to measurements and other modelling studies. A monitoring crosssection is placed between 1°E and 1°45' °on a latitude of 50°57'N which integrates the velocity over the whole crosssectional area. Throughout this section, several flow related quantities are used to determine the residual flow through the Strait of Dover. In all cases, positive values are considered as an inflow into the North Sea. They are defined as

1. the 'discharge' $Q(t)$ as the total water flux at a certain time t. Taking A as the crosssectional area of the Strait of Dover, the discharge is related to the spatial varying velocity with $Q(t) = \int u(x, y, t)\mathrm{d}A(t)$.

2. the 'cumulative flow' $M(t)$ as the total water transport between a certain time interval Δt. It is a time integration of the discharge with $M(t) = \int Q(t)\mathrm{d}t$.

3. the 'gross transports' $G^{in}(t)$ and $G^{out}(t)$ as the mean in- and outflow of water between a certain time interval Δt. They are defined as

$$G^{in}(t) = \frac{\int Q^{in}(t)\mathrm{d}t}{\Delta t}, \quad \text{and} \quad G^{out}(t) = \frac{\int Q^{out}(t)\mathrm{d}t}{\Delta t}$$

4. the 'net transport' or 'residual flow' $Q_r(t)$ as the time averaged water transport between one or more complete tidal cycles. In case the 'gross transports' have been calculated in between one or more tidal cycles, the residual flow becomes $Q_r(t) = G^{in}(t) - G^{out}(t)$.

In the previous sections, time varying residual currents and mass fluxes were not taken into account. Since this section only looks at a single signal through a cross-section, it becomes possible to investigate time varying residuals. The residual flow $Q_r(t)$ can be defined as a superposition of different components:

$$Q_r(t) = Q_r^{\mathrm{O}} + Q_r^{\mathrm{W}}(t) + Q_r^{\mathrm{IBM}}(t) + Q_r^{\mathrm{D}}(t) \tag{5.2}$$

The first component is the so-called oceanic residual. This is induced by the interaction of tide induced flow, local geometry and the earth's rotation. When a single tidal constituent is considered, the resulting oceanic residual is constant in time. The interaction with different tidal constituents introduces a small time dependency. However, this variation is negligible. The second and third component are meteorological components induced by wind and atmospheric pressure via the inverse barometer effect (IBM). Meteorological forcings vary on the time scale of several days. Therefore the variations of these components become highly significant and hence time variations should be taken into account for these components. The fourth component is induced by density variations due to fresh water inlets, surface heating during summer and other density related variations of the water body. The time scale of these forcings is dependent on the buoyancy source, it can vary from several days to annual variations. It should be noted that the last component is not yet taken into account in this chapter. The superposition of the above mentioned components does not take into account nonlinear effects, which might become quite significant for certain cases. For example, the hydrodynamic structure around river mouths is a highly nonlinear interaction between tide, wind and stratification (see e.g. Simpson (1997)). Therefore the components are only considered as a rough approximation to give an idea on the degree of importance of each forcing.

5.4.1 Low-pass filtering

The time scale of tidal and inertial oscillations is small compared to the time scale of residual circulation due to for example meteorological conditions. In addition, the magnitude of these oscillations is in general much larger than those of the residuals. For a proper analysis of large scale motions tidal and inertial oscillations are considered as strong, high-frequency, noise. They need to be filtered out of the signal to obtain a clear view of the desired output.

In an ideal situation, all tidal constituents are known, as well as the inertial oscillations. Removing these fluctuations from the signal results by definition automatically in a residual signal. However, in practice this is not possible because either the constituents are unknown, the simulated signal contains a certain bias with the measured data, or both. An alternative way is to apply a filter on the signal to a certain extent that tidal and inertial frequencies are taken out of the signal. By applying a low-pass filter, high-frequency motions are damped to a certain extent, dependent on the filter type. Most filters use a weighting factor over the original time series, the general structure of this filter is

$$y(t_k) = \sum_{i=-n}^{n} w_i x(t_{k+i}) \tag{5.3}$$

$$\sum_{i=-n}^{n} w_i = 1 \tag{5.4}$$

Here the filtered output signal $y(t_k)$ at time $t_k = k\Delta t$ is obtained from the input signal $x(t)$ and symmetric filter weights w_i. The most simplified way is by applying a moving average over the time series, hence each weighting factor is given as $w_i = 1/(2n+1)$. However, this can result in aliasing problems in case of a poorly chosen time interval. To tackle this problem, Godin (1972) suggested an improved method, which he defined as the "tidal killer". It takes three times the moving average of a signal, where the first two times are a moving average of a 24 wide band and the third time a 25 wide band. The filter completely eliminates diurnal constituents and higher frequencies. However, it also damps the signal of lower frequency signals (Walters and Heston (1982)) in which residual flows might be present. Better results can be obtained when the filter weights w_i are freely chosen. A variety of these filters has been published in the past. For a brief review one is referred to Thompson (1983). According to Thomson, the so-called "120i913" filter completely blocks the diurnal tidal constituents O1, K1, Q1 and P1, the semi-diurnal constituents M2, S2 and N2 and the inertial frequency[2] of $\omega_0 = f = 16.7°\text{h}^{-1}$.

An alternative way of low-pass filtering is to adjust the frequency spectrum with the use of a Fourier transform. The frequency spectrum can be described in its most general form by the equation below. Here, the Fourier transform $X(\omega)$ of $x(t)$ is multiplied with a frequency response factor $R(\omega)$ to obtain the Fourier transform $Y(\omega)$ of $y(t)$. After filtering the signal, an inverse Fourier transform results in a filtered signal based on its frequencies.

$$Y(\omega) = R(\omega)X(\omega) \tag{5.5}$$

It is desired to obtain a filter which gives a frequency response factor near unity at low frequencies, but a small response at higher frequencies. The easiest way is to use a single low-pass filter which defines a response factor of zero for all frequencies above a user defined value. However, there is an overlap in frequencies between tidal constituents and residual flow. This ratio, as well as the exact frequencies, are not known on forehand. A better approach is to estimate the tide induced signal with the use of tidal potentials as described by Doodson (1954). Subtracting this tidal signal from the frequency spectrum still retains high-frequency residuals. A package for this frequency filtering is made available under the name T_TIDE, it is well documented by Pawlowicz et al. (2002).

The filters as described above have been applied on a one year simulation with tidal and meteorological forcings. A Fast Fourier transform has been applied to investigate the frequency response of each filter. This is shown in figure 5.9. The frequency response of the "tidal killer" clearly shows the damping of periods of less than one day. Even for frequencies of for example 0.2 d^{-1}, i.e. a period of 5 days, the filter response is only 80%. This frequency certainly consist of almost entirely residual signals, which makes the frequency response of the tidal killer to low. Both the Thompson filter as well as the T_TIDE filter show better results. The major difference between the two is the starting frequency from where the filters give a smaller response. Where T_TIDE still allows signals with a period just larger than one day, the Thompson filter only allows periods of two days and up. Figure 5.10 shows the filtered signals compared to the unfiltered signal for January 2007. High-frequency peaks

[2]Since inertial frequencies depend on Latitude, Thompson applied his filter at Sydney, Australia. For the North Sea the inertial frequency exceeds $20°\text{h}^{-1}$.

of around 1 day periods are partially damped out by the Thompson filter. This can for example be seen on day 10 where the filtered signal of the T_TIDE signal is twice as large as the Thompson filter. Still, when looking at periods longer than a few days, the mean filtered signal of the three considered filters is comparable with a deviation of around 1% between the different filters and the unfiltered signal. Throughout this thesis both the Thompson filter as well as the T_TIDE filter are used, depending on the amount of detail which is required in the residual signal.

5.4.2 Oceanic residuals

In the first simulation the model is solely forced by tide induced water elevations at the boundaries, in combination with tide generating forces over the whole domain. In the North sea, the dominating tide is the semi-diurnal M2 tide. Several studies on residual flow therefore only took into account this M2 tide. A motivation for this simplification is stated by the Stokes transport (eq. 3.29); tidal driven residuals are proportional to the product of the horizontal and vertical tidal amplitude. Additional tidal constituents do increase the maximum amplitude. However, the mean amplitude is similar to the amplitude due to the single M2 constituent. To investigate the differences in residual flow, an additional simulation has been computed where only the M2 constituent is implemented. Comparison with the complete tidal forcing simulation puts the available literature in perspective of these results. Discharges through the Strait of Dover are shown in figure 5.11. Here it can be seen that both the M2 forced, as well as the complete tidal forced simulations, give a varying discharge with an amplitude of about 1500 m^3s^{-1}. This confirms the argumentation of M2 being the dominant constituent.

A gross transport of 432000 m^3s^{-1} flows into the North Sea during flood periods, while 387000 m^3s^{-1} is flowing out. This results in a net transport of 45000 m^3s^{-1}. The residual flow is therefore an order of magnitude smaller than the gross transports. The M2 forced

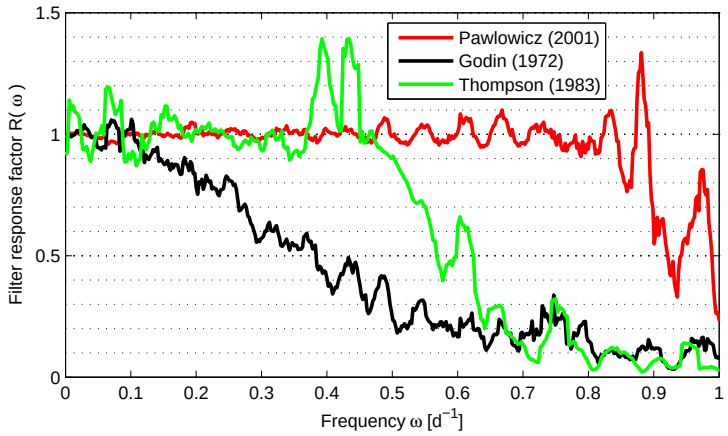

Figure 5.9: Frequency response factor for differen low-pass filters.

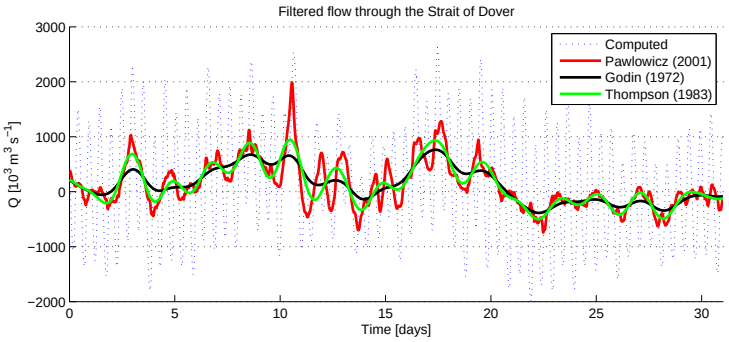

Figure 5.10: Comparison of filtered signals with original signal for January 2007.

Model	Source	Q_r^{O} ($10^3 \mathrm{m}^3\mathrm{s}^{-1}$)
Cartwright (1961)	Cable	50
Prandle (1978a)	model (10' x 6,5')	82
Pingree and Griffiths (1980)	10' x 5'	30
Prandle (1984)	model (30' x 20')	50
Prandle et al. (1996)	HFR+ADCP	41
Salomon et al. (1993)	model (10' x 6')	37
DCSMv5	model (7.5' x 5')	26
DCSMv6	model (1.5' x 1')	45

Table 5.1: Tide induced residual estimates through the Strait of Dover

simulation results in a comparable residual flow of 47000 $\mathrm{m}^3\mathrm{s}^{-1}$. Again, this confirms the dominance of the M2 tide with a difference of only 2%. The courser DCSMv5 model gives a smaller net transport of only 26000 $\mathrm{m}^3\mathrm{s}^{-1}$, together with gross transports of 400000 $\mathrm{m}^3\mathrm{s}^{-1}$ in and 374000 $\mathrm{m}^3\mathrm{s}^{-1}$ out of the North Sea. The DCSMv5 model allows less water to flow through the crosssection which may be due to the course grid structure. This could also be seen in figure 5.11, here the sinusoidal amplitude of DCSMv5 is being 20% smaller than the DCSMv6 model. Based on equation 3.29 a smaller flow velocity, which is directly related to the discharge, results in a smaller residual flow. The estimated residuals are in line with modeling studies (see table 5.1).

5.4.3 Stationary meteorological residuals

In contrast to tidal residuals, meteorological induced residuals are highly time dependent. Time scales vary from a single day (due to, for example, a single storm event for example) up to a couple of years (North Atlantic Oscillation). By comparing residual flows of different periods, a bias will occur, since the meteorological forcings differ significantly. Therefore, it is useful to investigate the response of the numerical models to meteorological forcings. This is done by forcing the model with steady, uniform, meteorological forcing. The latter will be the subject of this section. Obtained results are compared to other modeling studies which did similar investigations. In the next section time and spatial varying wind and pressure fields are examined.

Wind velocities act as an external force in the form of a shear stress. They are found on the RHS of the governing equations in the $\vec{\tau}_w$ term. Since there is no analytical relation between wind and shear stress, empirical formulations are used[3]. To obtain a clear comparison between different modeling studies, the wind induced residuals are described in terms of the shear stress and wind direction; $Q_r^{\mathrm{W}}(|\tau_w|, \theta_w)$. A linear behaviour is expected for both the wind stress and direction. This assumption can be justified by a scaling analysis

[3]The relation between wind speed and shear stress for the current models is given by equation 4.5

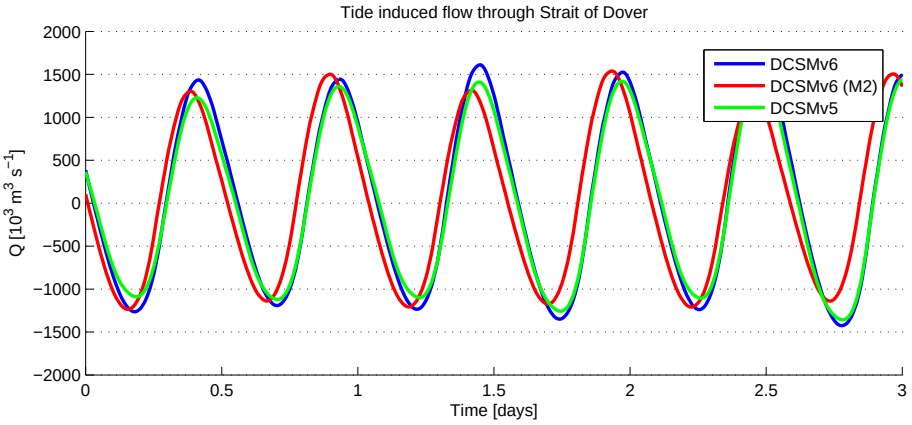

Figure 5.11: Tide induced flow through the Strait of Dover for 1 till 3 January 2007.

Model	Grid (lon x lat)	Q_r^O	α (10^6)	θ_{max} (°)	rms
Prandle (1978a)	10' x 6,5'	82	0.67	201	
Pingree and Griffiths (1980)	10' x 5'	30	1.2	187	
Prandle (1984)	30' x 20'	50	0.8	196	
Salomon et al. (1993)	10' x 6'	37	1.1	186	
DCSMv5	7.5' x 5'	26	0.91	195	3.2
DCSMv6	1.5' x 1'	45	1.53	190	4.5

Table 5.2: Constants found in literature and model simulations for equation 5.7. The rms value is the root mean square of the difference between computed flow of each simulation and the deduced formulation. Discharges are given in $10^3 m^3 s^{-1}$.

of the nonlinear governing momentum equations at the Strait of Dover. They are repeated below in their vectorized form.

$$\frac{\partial \vec{u}}{\partial t} + \vec{u}\nabla\vec{u} = -g\nabla\vec{\eta} - f \bullet \vec{u} - \frac{\vec{\tau_b}}{\rho h} + \frac{\vec{\tau_w}}{\rho h} - \frac{\nabla \vec{p_a}}{\rho} + \nu_H \nabla^2 \vec{u} \tag{5.6}$$

Since the model is only forced by a stationary wind field, the time derivative equals zero under the assumption that the model has reached its dynamic equilibrium. Horizontal diffusion is considered small in comparison with convection, neglecting this term is therefore acceptable. The relation between convection and Coriolis is given by the Rossby number $\mathrm{Ro} = U/Lf$. Even in the Strait of Dover where velocities can reach up to 1 m/s the Rossby number stays small ($\mathcal{O}[10^{-1}]$). Convection is small compared to inertial oscillations and can therefore also be neglected. Prandle (1978a) derived a linear approximation for the non-linear friction term which is valid for tide dominated flows. He defined $\vec{\tau_b} = k_1 \vec{U}|\vec{U}| \approx k_2 \vec{U}$. Where k_1 is an empirical coefficient and $k_2 = (8/3\pi)k_1 \hat{U}$. By applying all the above mentioned simplifications, the remaining terms have a linear interaction. Hence a linear relation between wind stress and residual currents should give reasonable values.

The model has been forced by a stationary, uniform, wind field of 10 ms^{-1},equivalent to a wind stress of $\tau_w = 0.16$ Nm^{-2}. Eight simulations have been executed, where for each simulation the wind direction is increased with 45°. An expression for the residual flow has been found by a least square-fitting with the expression

$$Q_r(|\tau_w|, \theta_w) = Q_r^O + \alpha|\tau_w| \cos(\theta_w - \theta_{w,\max}) \tag{5.7}$$

Obtained values are shown in table 5.2 and figure 5.12, together with values obtained from other literature studies. The sensitivity to tidal and wind induced forcings are given by the values of Q_r^{Ocean} and α respectively. When the present models are compared, the DCSMv6 model gives a much larger response to both tidal and wind induced forcings. Under a wind direction of maximum angle the flow is almost twice as large as DCSMv5. A plausible

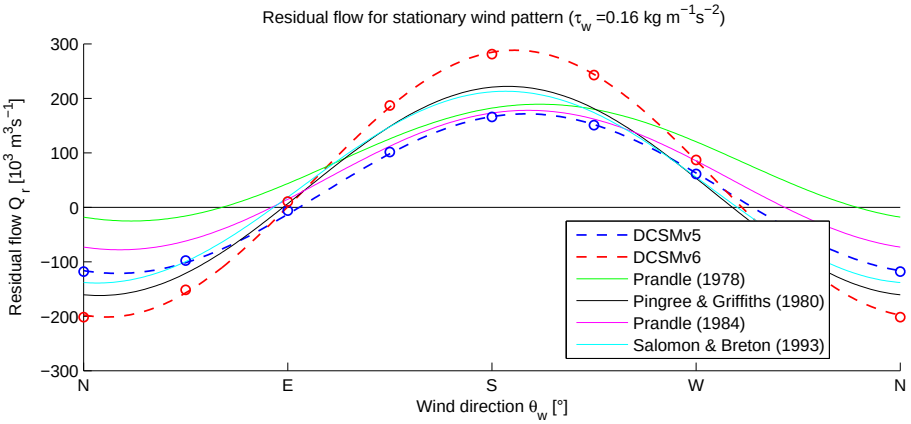

Figure 5.12: Residual flow as function of wind speed and direction based on 8 different simulations (scatter points). Solid lines are obtained by least-square fitting.

Year	Q_r	G^{in}	G^{out}
2003	36	418	-382
2004	51	423	-372
2005	29	411	-382
2007	47	422	-375
2008	78	440	-362

Table 5.3: Yearly average flow through the Strait of Dover. Residual flow is a summation of the gross in- and outflow into the North Sea ($Q_r = Q_{in} + Q_{out}$). Units are in $10^3 \mathrm{m}^3\mathrm{s}^{-1}$

cause to these differences may again be attributed to the number of grid cells between Dover and Calais. DCSMv6 contains more than 30 grid cells, while DCSMv5 only has 4 grid cells at this location. Since both models compute on a rectangular grid, the land boundaries are staircase typed. This induces a large amount of energy loss caused by artificial boundary effects (Kramer and Stelling (2008)) at cells' close to these boundaries. The few grid cells in DCSMv5 all undergo these boundary effects, this explains the smaller sensitivity to external forcings. Differences with other modelling studies show even larger deviations in sensitivity. Besides the reason as just mentioned, the large deviations between these variables may also be attributed to numerical different approaches and different formulations for forcings like bottom friction and water levels. The difference in maximum angle of response might be found in the wind induced surface elevation changes. The first model of Prandle for example only covers the North Sea, whereas the models in this thesis cover the whole continental shelf. Surface elevations therefore can adjust in a physically better way to the wind forcings. This has a significant effect on the maximum angle of response.

5.4.4 Time and spatial varying meteorological residuals

For this thesis, the year 2007 has been chosen as simulation period. The amount of available data on residual flows is scarce, as discussed in section 2.3. It becomes inevitable to compare the present model results with measurements and modelling studies from different years. Since residual flows are highly dependent on meteorological forcings, and the latter may vary over the years, it is wise to investigate the difference between various years. To minimize computation time, only simulations have been done for the DCSMv5 model. Simulations are done from January 2003 up to December 2008 with a gap in 2006. As shown in figure 5.13, the annual cumulative flow roughly varies between 1000-1500 km^3, with the exception of 2008, where it reaches up to 2500 km^3. An overview of the corresponding gross and net transports is shown in table 5.3. Daily residuals vary widely throughout the months and years. However, on large scale a general structure can be seen with relative large residual amplitudes between November and January and smaller amplitudes during summer. An average residual current of 48000 $\mathrm{m}^3\mathrm{s}^{-1}$ is found. Since 2007 gives an annual flow of 47000 $\mathrm{m}^3\mathrm{s}^{-1}$, it is considered to be a representative year for the whole period. Figure 5.14 compares the monthly mean values between the present model and estimates on residual flow by Salomon and Breton (1993). These estimates were based on a similar equation as equation 5.7, which he constructed by fitting with simulated residuals of a shorter period. From all the 108 estimates, only for a single month the flow is in opposite direction. The majority varies around 100000 $\mathrm{m}^3\mathrm{s}^{-1}$. The present model simulations give, on average, a lower monthly mean value. The monthly variations are larger, and also more flows are in opposite direction.

In section 5.4.3 an equation was derived based on stationary and uniform wind forcings (see eq. 5.7). With the obtained coefficients, this equation has been applied on the actual wind field. The computed residual flow, based on this equation, is compared with the actual model results. Since the stationary equation only contains a single wind direction and magnitude, a representative value has to be found for the spatial varying wind field. This is done by taking the average of a certain bounded wind field around the Strait of Dover, therefore two steps are taken. In the first step a land mask has been put over the wind field, hence only wind velocities above the water columns are taken into account. Secondly, the average of a rectangular bounded region around the Strait of Dover is taken. Because equation 5.7 assumes a system in equilibrium state, one needs to take into account

the adaptation time of the system to a changing wind field to determine the size of the region. For example, short scale variations are only due to wind forcings close to the Strait of Dover. Wind induced residual variations have a time scale T_r of several days to one week. Residual flows have a typical velocity U_r of about 0.1 m^1s^{-1}. On first approximation the spatial scale would be in the order of $L_r = U_r T_r$. This results in an area of 120x120 km^2. A correlation analysis has been executed in which the size of the region was taken as a variable, with the just mentioned area size was taken as starting point. Therefore, the calculated residuals with the stationary equation were compared to the computed residuals. The chosen area of 120x120 km^2 appeared to be a factor two smaller than the area with highest correlation. Larger areas still gave comparable correlations, since the average wind vector stayed more or less equal. When smaller areas were chosen, the stationary calculation became very sensitive to locally varying wind at the expense of the dominating large scale wind pattern. For this reason, the area has been increased to 250x250 km^2. The approach appears to give a good estimate on the daily residual flow (correlation $r = 0,72$) as is

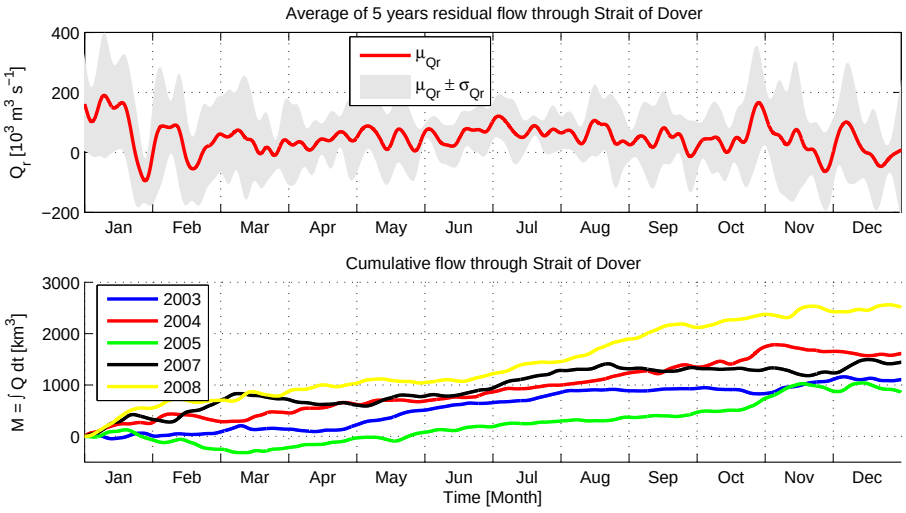

Figure 5.13: Mean residual flow through the Strait of Dover over 5 years of modeling (top). Standard deviation is shown by the gray area. Cumulative transports are shown on the bottom.

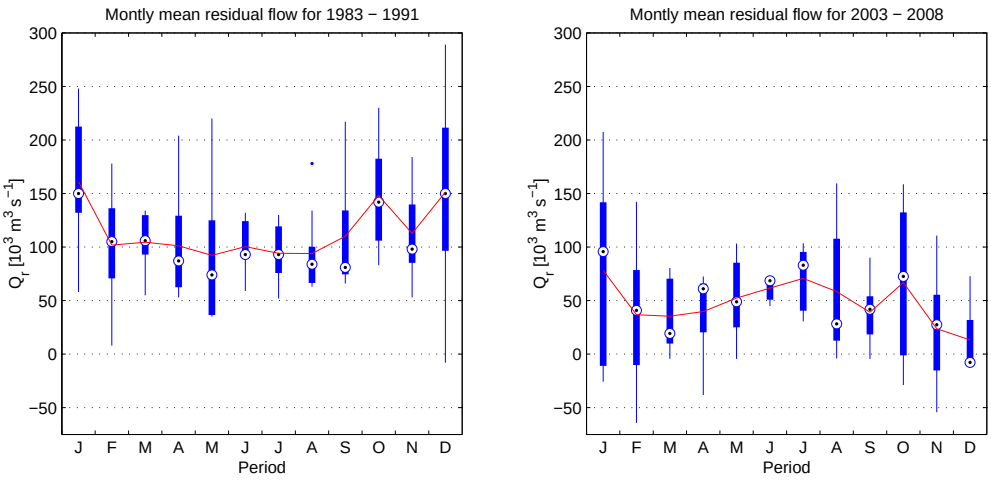

(a) Salomon and Breton (1993)

(b) DCSMv5

Figure 5.14: Monthly mean residual flows based on two different approaches in different periods. Blue bars show a box plot, red line shows the mean value per month.

shown in figure 5.15, the adaptation time to varying wind fields is in the order of several hours. Since the approach assumes equilibrium flow while this is practically never the case, a significant overestimate in magnitude is done in case of rapidly varying wind fields. This is clearly visible at day 10 and 17. In addition, when the wind field is rapidly changing, the approach fails to give a proper time varying behaviour. See for example days 10 to 15, where the flow directions can even be in opposite direction.

Up till now surface level elevations between the North Sea and English Channel have not been taken into account yet. Although the main structure of daily residuals can be explained by wind and tide induced forcings, surface elevations also have a certain amount of influence on the residuals. Especially at periods where the stationary approach fails, as described above, variations in surface elevations can give an explanation for this wrong approximation. To investigate this influence, a proper definition of the surface level difference between the English Channel and the North Sea needs to be found. Therefore two monitoring stations on each part are compared with one another. For the English channel water levels in New Haven and Dieppe are monitored. While the same is done in the North Sea for Lowesoft and Vlissingen. Since tidal fluctuations are not valuable for this analysis, residual elevations are obtained with the application of the Thompson filter in the same manner as is done with transports. The signals of the two stations in the North Sea are subtracted from the ones within the English Channel. During the whole simulation, this gives a mean water level differences which varies between -1 and 1 meter. It is worth mentioning that without meteorological forcings this difference is only about 1 cm. These relatively large variations are a superposition of surge levels and inverse barometer effects. A qualitative representation of the residual water level elevations is shown in the upper part of figure 5.15. It is shown that at times were the stationary wind driven approach fails to give good estimates, surface level elevations are highly fluctuating. Most obvious are the southward directed currents at day 26 and 28 where wind velocities are small. Here, the surface level difference changes in two days almost complete from sign. Hence the water level in the North Sea largely increases (or in the Channel decreases). On day 24, water levels are higher in the channel while on day 26 the opposite is true. Under the assumption of the transports initially being in equilibrium with the water levels, the increased water level in the North Sea acts as a kind of barrier. It reduces or even reverses the flow into the North Sea. In the case of no or small varying water level differences, the effect is very small. This can for example be seen in the first 8 days of January. Even though high water levels are observed in the North Sea, the model seems to fully adapt to the wind field and neglecting large surface level differences.

The mean residual flow for the period as shown in figure 5.15 is 100000 m^3s^{-1}. The stationary approach substantially overestimates this value with 166000 m^3s^{-1}. Therefore a new approach has been set up by a least square fitting between equation 5.7 and the computed residuals. The surface elevations are not taken into account since it's behaviour

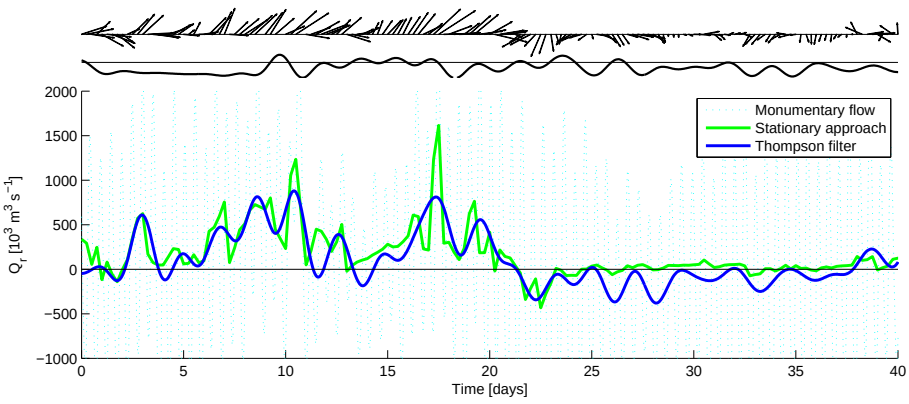

Figure 5.15: Residual flow for 1 January till 9 February 2007 as calculated by DCSMv6. The top vectors give an indication of direction and magnitude of the wind field. The black line indicates surface level elevations between the North Sea and the English Channel

is non-linear, while the stationary approach is linear. Similar values are obtained with $\alpha = 1400000$ and $\theta_{w,\max} = 194$. The correlation for these values in comparison with the computed signal is $r = 0,79$. The mean residual flow for the same period is a bit smaller; 153000 m^3s^{-1}.

For the year 2007 no measurements are available on residual flows through the Strait of Dover. Therefore, for comparison, the present model results are compared with model results from the NOOS working group on transports. From the NOOS working group the results from two of their numerical models were used. Their first model is the three-dimensional baroclinic model BSHcmod (Dick et al. (2001)) from the German member BSH. It covers the North Sea from the English channel (4°W) up to the northern North Sea (60°N) and the Baltic sea. Grid cells have a spatial resolution of 5 km. Water levels are imposed at the boundaries based on 14 harmonic tidal constituents and external surges provided by a northeast Atlantic model. The second model is a nested model provided by the Belgian member MUMM (Luyten et al. (1999)). The largest model domain covers the whole Northwest European Continental Shelf. It calculates barotropic flow on a single layered grid with a horizontal spatial resolution of 6 km. The model is forced at its boundaries by 8 (diurnal and semi-diurnal) tidal constituents. For the North Sea a three dimensional baroclinic model of 20 sigma layers is used. The spatial resolution is identical. It ranges from the English channel (4°W) up to the northern North Sea (57°N). In front of the Belgian coast a detailed 3D baroclinic model is nested but is of no importance for this research.

The yearly averaged residual flows show big differences. Both DCSM models give similar results with an annual flow of 45000 $m^{3\text{-}1}$ (v5) and 56000 $m^{3\text{-}1}$ (v6). Different results are obtained from the NOOS models. The BSH model gives an annual averaged inflow of only 29000 $m^{3\text{-}1}$ while MUMM gives an inflow of 85000 $m^{3\text{-}1}$. Daily variations for the first 40 days of 2007 are shown in figure 5.16. As it was suggested in section 5.4.3, the sensitivity of DCSMv6 to meteorological forcings is much larger than the older DCSMv5 model. This is clearly visible in the amplitude of daily variations. The adaptation time from BSH and MUMM are shown to be in the same order. Where the MUMM model gives comparable magnitudes in daily residuals, the BSH model shows a much larger response for both in- and outflows in the North Sea. Especially for negative flows BSH gives relatively large responses. The latter is the main reason for the annual residual flow to be very low. The effect of atmospheric pressure is not implemented in the BSH model. For comparison, an additional simulation for DCSMv6 has been executed where this IBM effect is not taken into consideration. Without IBM the overall daily magnitude increases, especially for negative flows. The annual averaged residual flow reduces to 29000 $m^{3\text{-}1}$, which is in very good agreement with the BSH model. Correlation between the different model results varies between 0.81 for BSH and 0.99 for DCSMv5 (see 5.16).

5.4.5 Concluding remarks

In section 5.2 modelled large scale circulation pattern was analysed. It was shown that the general circulation structure is presented quite well. Only currents which are for a large part density driven are not, or in a less extent, represented by the model. In section 6.5 and 5.3 the magnitude of the residual flow was studied in more detail. The Cap de la Hague experiment showed the transit time in the English Channel to be rather low. In comparison with both modelling studies and measurements the residence time in the English Channel is almost twice as large. When the water has passed through the Strait of Dover, transit times are more or less in the same order. The modelled annual residual flow through the Strait of Dover is approximately 50000 m^3s^{-1}. Previous measurements and modelling studies suggest an annual transport starting at about 100000m^3s^{-1} up to almost 250000m^3s^{-1}(see section 2.3). The modelled transport is therefore approximately twice as small as other studies suggest. This strengthens the statement of the residence time in the English Channel being twice as large. It is interesting to see that the models from the NOOS group seem to have similar problems. The BSH model estimates an annual transport of only one third of the desired value. A complete overview of transports through the Strait of Dover is shown in figure 5.18.

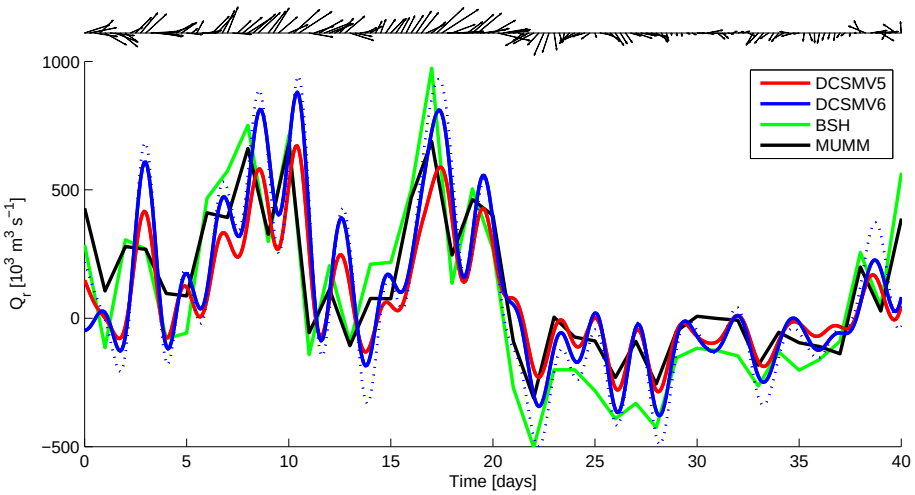

Figure 5.16: Residual flow for January 2007 as calculated by different models. The top vectors give an indication of direction and magnitude of the wind field. The dashed line indicates a simulation without the IBM effect.

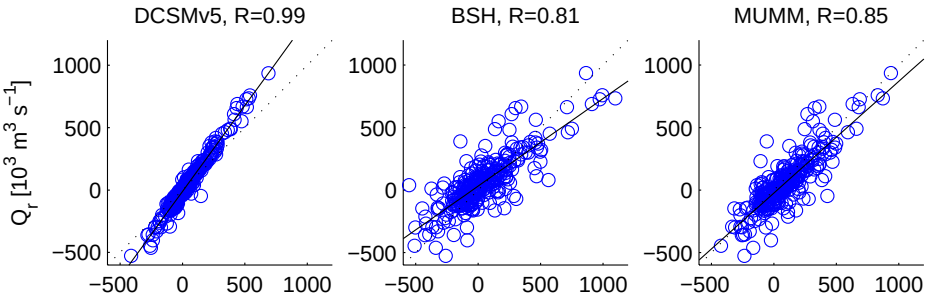

Figure 5.17: Correlation of DCSMv6 with other models.

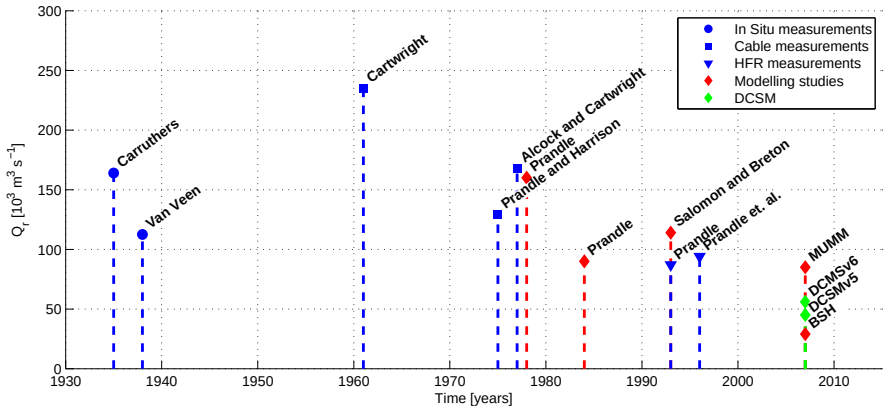

Figure 5.18: Residual flow through the Strait of Dover based on historical measurements and numerical modelling. Model results of the present models are shown for the year 2007.

6 Sensitivity analysis

In the previous section a thorough analysis was executed on the behaviour of the current DCSM models in respect to known theory, available measurements and other modelling studies. It was shown that the models give a relative low residual current through the Strait of Dover in comparison with previous studies. Therefore, the conclusion can be drawn that either important physical processes are missing, or the numerical approaches from Delft3D-FLOW does not represent the physics in a proper way. In this section several adjustments are made on the DCSMv6 model. The sensitivity of the present model on these adjustments is investigated.

6.1 Bottom roughness

The used bottom roughness in this study is constructed with the use of an extensive calibration. This calibration was based on water levels. However, the effect on transports were (to a certain extent) not taken into account. By reducing the bottom friction in the area around the Strait of Dover the passage becomes more smooth, this will result in larger oscillating flows. Due to larger oscillations the "tidal stress" (Nihoul and Ronday (1975)) increases, this directly results in a larger residual flow (see also equation 3.29). In case of wind driven transports, the magnitude of daily residual flow increases for both in- and outflow of the North Sea. Since the largest part of the daily residuals is in the directed into the North Sea, the effect will be in favour of inflowing residuals. Therefore, a reduced bottom friction increases both the tidal and meteorological residual flow. In figure 6.1 results are shown for the case of a reduced bottom roughness around the Strait of Dover. It clearly shows an increase in daily residuals. For this particular situation where the bottom friction is reduced with 30%, the daily residual flow has increased with 29%. On annual scale the residual flow increases with 6%.

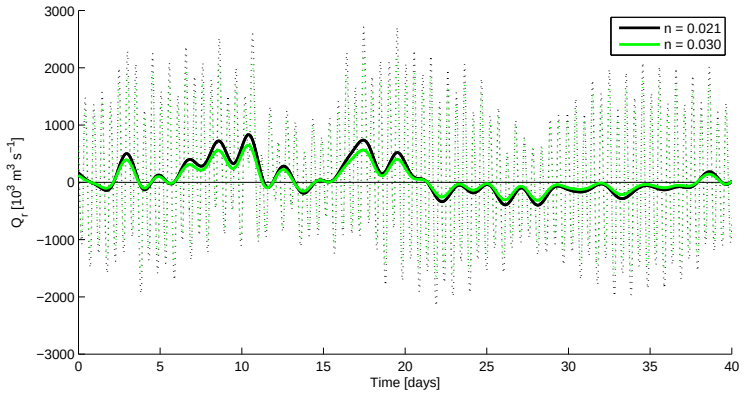

Figure 6.1: Decreased bottom roughness for January 2007

6.2 Model boundary conditions

At the model boundaries a water level has been imposed based on tidal constituents and the inverse barometer effect. Since the model boundaries are located in deep water, the surge component is assumed to be negligible. The density driven component, defined by the steric height, is not implemented yet in the present models. However, it can have an surface elevation of up to 10 cm. It has been shown in previous sections that surface elevations can have a significant amount of effect on the residual flows. Especially when surface level differences are rapidly changing, their effect on residual flows can be very significant. Although the steric height is a slowly varying variable, it still can introduce a certain amount of residual flow. Since Delft3D does not provide a direct method to implement steric heights, a zero-frequency component "A0" has been imposed on the boundaries of the model domain to simulate the effect of a constant surface level elevation. The data was based on TOPEX/Poseidon altimeter data, which provides a monthly mean surface

elevation in relation to the geoid. It is worth mentioning that the reference plane of DCSM is MSL (mean sea level) instead of the geoid. A certain bias will is introduced due to different referencing. However, this bias is supposed to have negligible effect on the residual transports. The altimeter data also contains the inverse barometer effect. Therefore, the annual mean water level based on the IBM has been subtracted from the altimeter data. In this way, the time varying IBM can still be used as a water level forcing at the boundaries. The final added zero-frequency gives a surface elevation of 50 cm along the western boundary for DCSMv6 and 25cm for DCSMv5. Its effect on the general circulation pattern in the North Sea is negligible. When zoomed in on the Strait of dover, the residual transports increase with only 1% for both models. The mean surface level difference has decreased with a factor 2. The biggest influence occur outside the continental shelf, in the deeper parts of the ocean. Most of the increased water transports happen in this area.

6.3 Depth averaged baroclinic simulations

In previous sections density variations, as well as river and Baltic inflows, were not taken into account. When the complete model domain is considered, there are various locations where density driven components have a significant influence. In section 5.2 it has been shown that the model fails to properly represent the actual residual circulation pattern at certain locations. Good examples are the Norwegian Coastal current where the magnitude of the flow is rather low and the density driven current around the Dogger bank which is completely absent. When one is interested in the more detailed residual structures, also the areas around river outlets are not represented properly such as the several ROFI regions in the North Sea. The effect of density variations on the flow structure can, in most cases, only be described properly in three dimensions. Even though the present models compute on a two-dimensional, depth averaged, grid. An attempt is made to implement density variations within the present models. The models are tested on their numerical stability, the representation of missing currents from the barotropic simulations, and the quantitative residual flow through among others the Strait of Dover. In chapter 4 the implementation of density variations due to salinity and temperature variations has been elaborated. River discharges from the ZUNO-DD model are implemented into the current models. Since the Baltic entrance lies outside the ZUNO-DD domain, crosssectional model results from NOOS are imposed at the Baltic Sea. Baroclinic simulations were done for both model versions. Since both models behave in similar ways, only the DCSMv6 model is treated below.

On first approximation, the impact of density variations on residual transports can be found with the use of the potential energy anomaly, defined as

$$\phi = -\frac{g}{h}\int_{-d}^{\eta} z(\rho(T,S) - \rho(\overline{T},\overline{S}))\mathrm{d}z \tag{6.1}$$

It represents the energy required to completely mix the water column over the vertical. Horizontal gradients in the potential energy anomaly give an indication of the strength of density-driven circulations. Pingree and Griffiths (1978) stated that frontal positions closely match the "$h/\hat{U}^3$" criteria. Figure 6.2 shows this criteria based on a barotropic simulation of the present model. Here it can be seen that large fronts are present at, among others, the Norwegian trench and Dogger bank. These currents were indeed small, or missing, in the barotropic simulations. Horizontal gradients are small around the Strait of Dover, which indicates that errors related to stratification are small in this area. Note that since river outflows are not simulated in this model, fronts around ROFI regions are not presented here, although they do exist. One is referred to Simpson and Bowers (1981) or De Boer et al. (2008) for a more thorough review on the relation between potential energy anomaly and tidal and wind induced flows in stratified areas.

In a modelling study by Holt and Proctor (2008) the residual circulation has been divided into three separate components; a density, barotropic-wind and barotropic-ocean driven part. In this study it was shown that, on average, the magnitude of density driven transports is of the same order magnitude as the barotropic components. However, density driven transports show much more fine scale structure while wind and oceanic driven transports behave on a much larger scale. A good example is the amphidromic system which is a complete oceanic driven component which behaves on a relative large scale. Concerning the

Strait of Dover, opinions on density driven components differ. Prandle (1978a) argues the component to be negligible with a contribution of less than 1% directed towards the North Sea. Holt and Proctor (2008) claim the density component to be much larger, varying from 10 to 50%, dependent on the season. In most cases, the density component acts as an outflow, therefore counteracting from the other two components.

Results of the baroclinic simulation are shown in figure 6.3 and 6.4. Some very contradictory results are obtained when zoomed in on the region around the Skagerrak (figure 6.5). For the previous barotropic simulation, a relative good estimate on the circulation pattern was made, even though this region is highly stratified (McClimans et al. (2000)). However, when density differences are introduced, the circulation pattern at the Skagerrak does not give a good representation of the density driven circulation in this area. In fact, the barotropic simulation gave better results than the baroclinic simulation. This wrong representation is due to the absence of vertical stratification. When depth variations are taken into account, the brackish water from the Baltic sea flows only in the top layer of the water column along its land boundary on the right and follows the Norwegian coast. However, in the present depth averaged simulation the outflow from the Baltic sea gets topographically steered to the left due to large depth variations (f/h=constant). As a consequence, the Baltic water clashes with the Atlantic water, which originates from the Dooley current and northern boundary. The Atlantic inflow can't develop properly and turns towards the North at a latitude of 58°N. The flow pattern in the Skagerrak and southern Norwegian trench is completely reversed. Water along the Norwegian boundary now flows to the south and enters the Skagerrak along the Norwegian landboundary. Other areas show better results, the difference between both simulations has been shown in figure 6.6. Here it can be seen that a small flow around the dogger bank is present, although it's magnitude is still relatively small. In the southern bight a southward directed density driven current is introduced as also suggested by Holt and Proctor (2008). This results in an annual decrease of transport through the Strait of Dover of 15%.

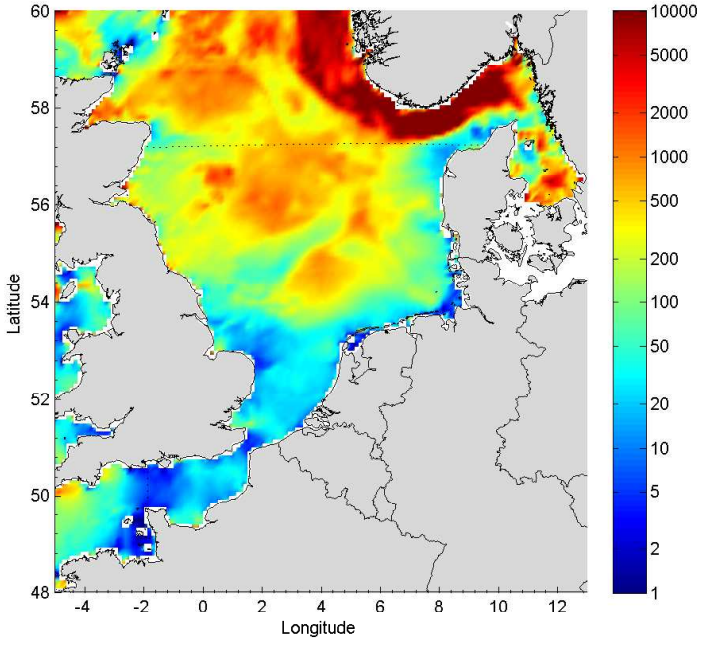

Figure 6.2: "$h/\hat{U}^3$" criteria based on a barotropic model simulation.

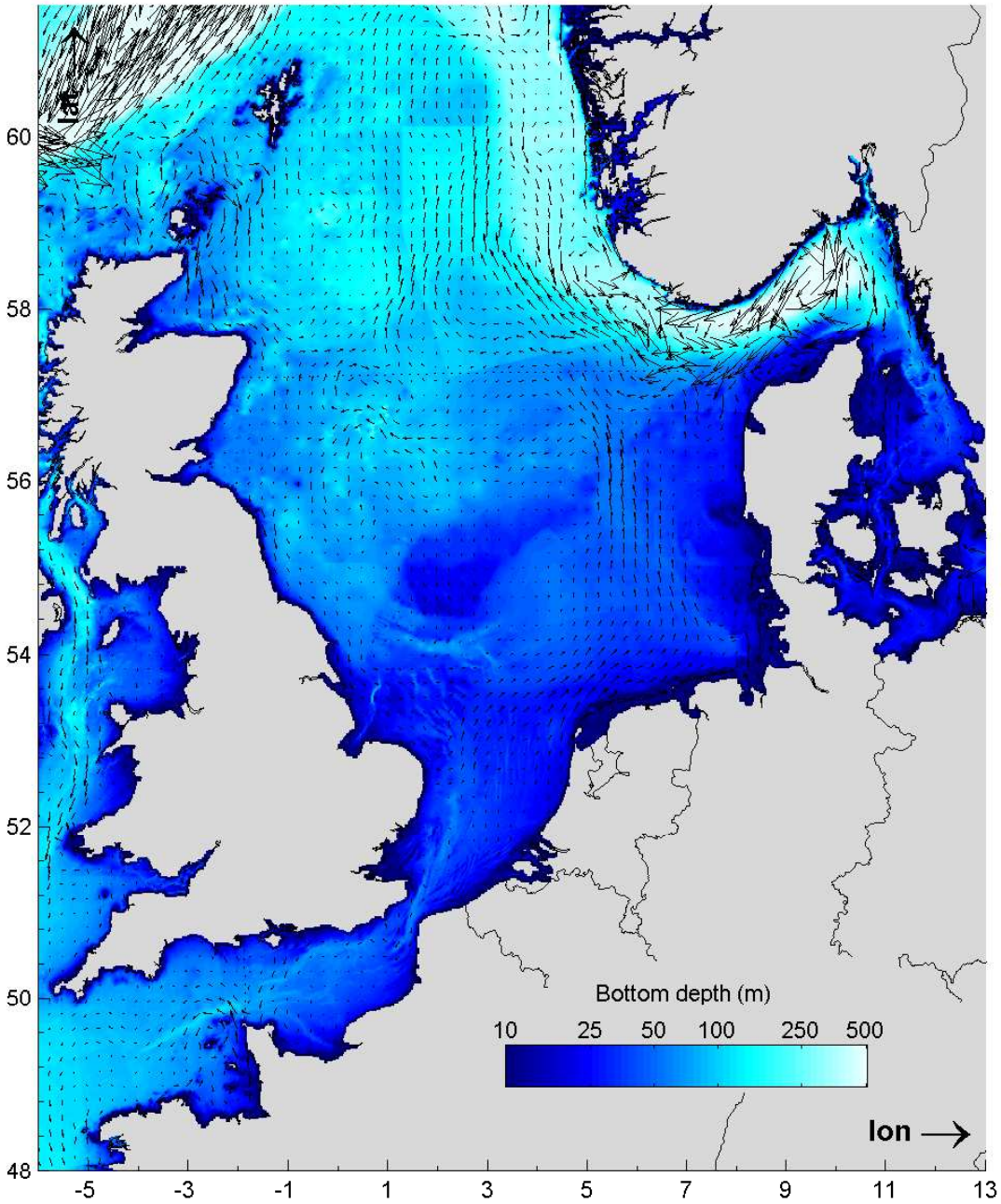

Figure 6.3: Annual mean, depth averaged, horizontal velocities for baroclinic flow. For clarity only vectors are shown at every tenth grid cell. Magnitude is indicated with the vector length on square root scale. Bottom depth is plotted on a logarithmic scale.

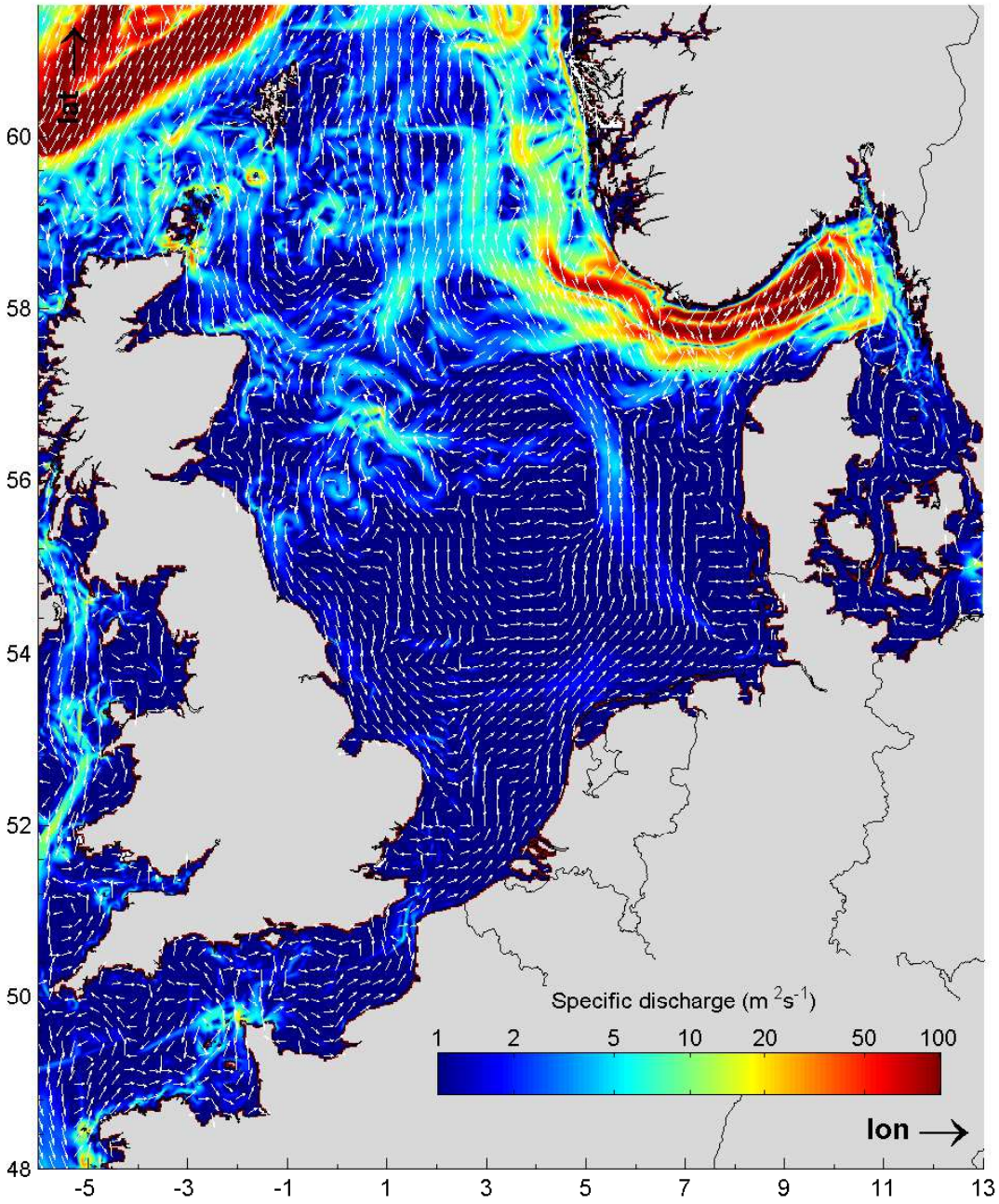

Figure 6.4: Annual mean, depth integrated, volume fluxes for baroclinic flow. For clarity only vectors are shown at every tenth grid cell. Magnitude is indicated with the color map, direction is shown by the corresponding vectors.

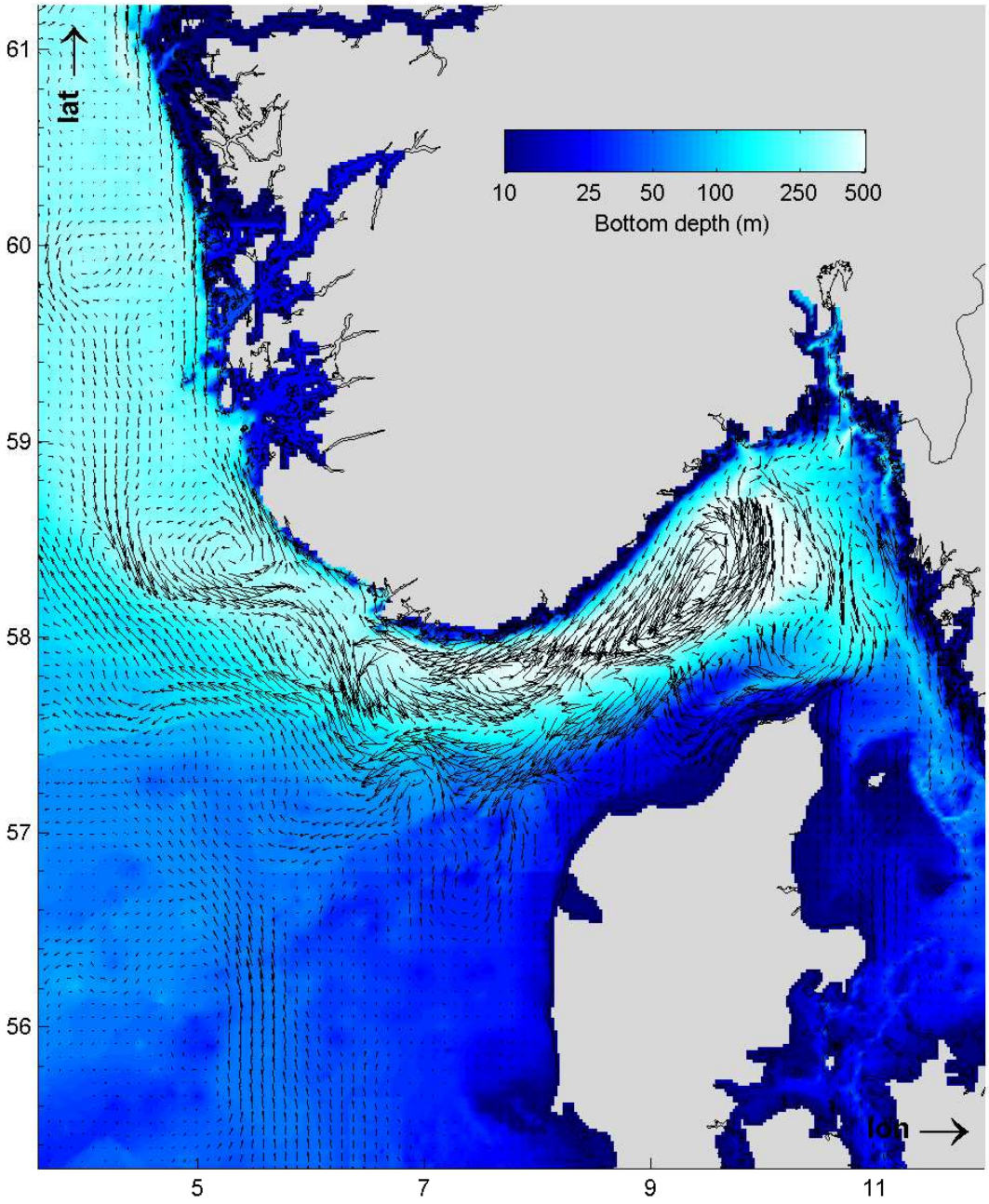

Figure 6.5: Annual mean, depth averaged, horizontal velocities for baroclinic flow. Zoomed in on Skagerrak and Norwegian Coastal current.

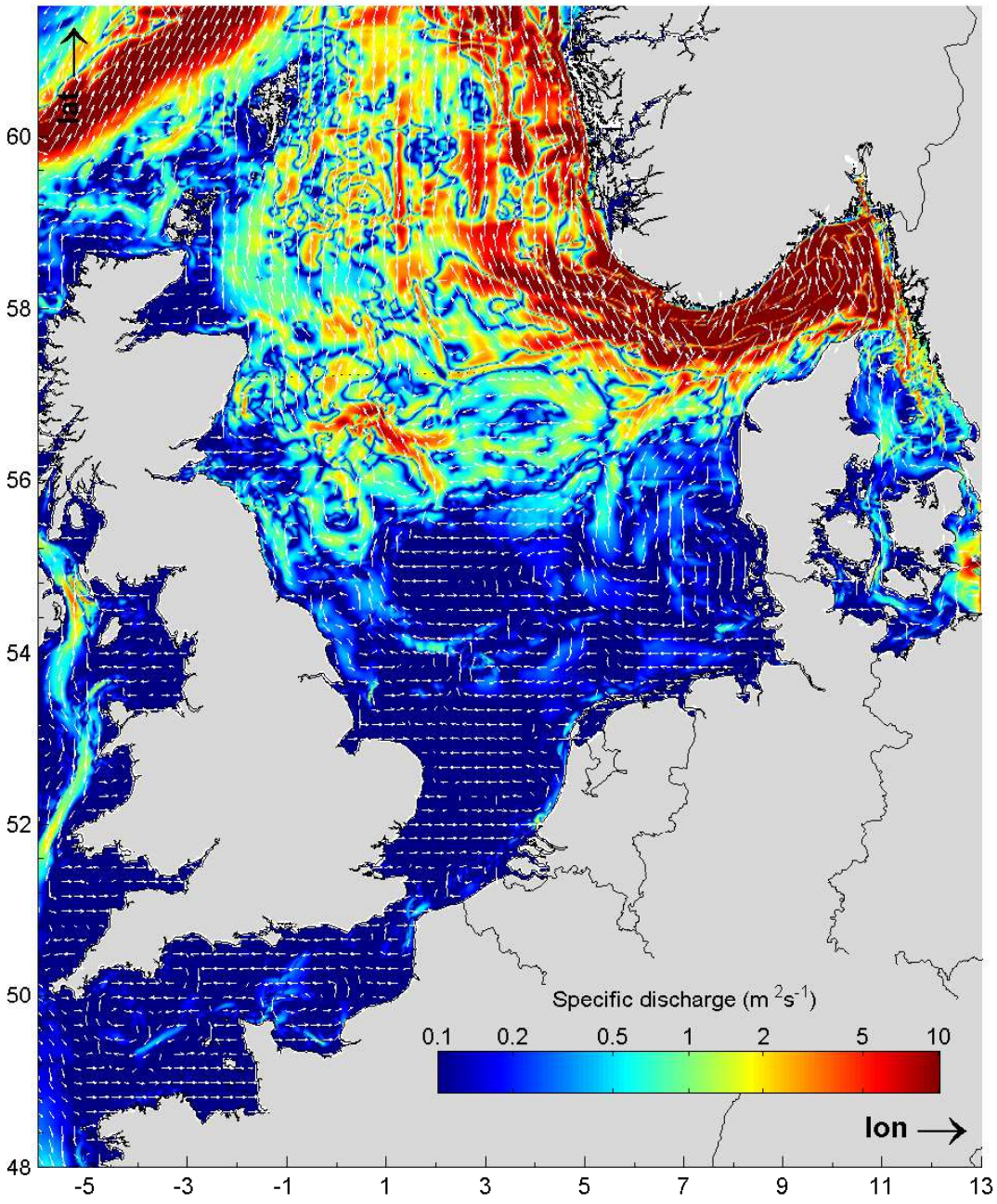

Figure 6.6: Difference between baroclinic and barotropic transports.

6.4 Numerical adjustments

In previous sections several adjustments were made on the DCSMv6 model. Here, each adjustment was related to a certain physical process. In this section the effect of various numerical adjustments is investigated. First, the present model is converted into a three dimensional layered system. Thereafter, some small adjustments are made within the Delft3D-FLOW package based on different discretization scheme's. Finally, a simulation of the present model is done in a new developed simulation package called DFlow-FM.

6.4.1 3D barotropic flow

A depth averaged simulation is known to overestimate the amount of bottom friction. This results in a reduction of the magnitude of the flow. The DCSMv6 model has been made three-dimensional by implementing 20 sigma layers into the domain. The amount of computational grid cells logically increases with a factor 20. As a results, the computation time becomes much larger. Therefore, only a single month has been simulated to investigate the significance of a layered system. The residual flow through the Strait of Dover shows an increase of 2% in relation to the depth averaged simulation. Unfortunately, a baroclinic simulation appeared to be unstable.

6.4.2 Advection discretization

The advection term in the momentum equations is solved with use of the so-called ADI-method. A full explanation of this method is beyond the scope of this thesis. The basic idea is that the time step used to solve the advection term is split up in two stages. First the term is solved in x-direction, and thereafter in y-direction. For the spatial discretization, two numerical methods are built in Delft3D-FLOW which use the ADI-method. These are the WAQUA and cyclic method. For a full explanation of these methods one is referred to Stelling and Leendertse (1992). The sensitivity of residual circulation on both methods is tested with two similar simulations. The difference between both methods appeared to be negligible, and therefore is of no further importance in this thesis.

6.4.3 Coriolis discretization

The momentum equations solve the velocities normal to the grid cell boundaries. For a certain grid cell center i, j the normal velocities are defined at $i, j \pm \frac{1}{2}$ for the velocity component u and at $i \pm \frac{1}{2}, j$ for the velocity component v. The Coriolis term contains a tangential velocity term, which is not defined on the same grid boundary as the normal velocity. In Delft3D-Flow, this problem is solved by a linear interpolation of the four surrounding cell normal values. For the Coriolis term fu, the discretization becomes

$$(fu)_{i+\frac{1}{2},j} = f_{i+\frac{1}{2},j} \cdot u_{i+\frac{1}{2},j} \tag{6.2}$$

$$u_{i+\frac{1}{2},j} = \frac{1}{4}(u_{i,j-\frac{1}{2}} + u_{i,j+\frac{1}{2}} + u_{i+1,j-\frac{1}{2}} + u_{i+1,j-\frac{1}{2}}) \tag{6.3}$$

In case of large depth variations, the interpolated velocity introduce errors or even numerical instabilities. These errors reduce significantly when depth variations are taken into account within the linear interpolation. The method is described by for example Kleptsova (2013), the Coriolis term now is defined as

$$u_{i+\frac{1}{2},j} = \frac{1}{4}\left(\frac{h_{i-\frac{1}{2},j}}{h_{i,j}}u_{i,j-\frac{1}{2}} + \frac{h_{i+\frac{1}{2},j}}{h_{i,j}}u_{i,j+\frac{1}{2}} + \frac{h_{i-\frac{1}{2},j}}{h_{i,j-1}}u_{i+1,j-\frac{1}{2}} + \frac{h_{i+\frac{1}{2},j}}{h_{i,j-1}}u_{i+1,j-\frac{1}{2}}\right) \tag{6.4}$$

This improved method is implemented on the present DCSM models. Its effect is indeed significant at locations with large depth variations, such as the southwest border of the northwest European continental shelf. Since depth variations in the North Sea and English Channel are much smaller, the errors made with the default interpolation method are small. The improvement of the improved method is negligible in this region, residuals through the Strait of Dover not affected.

6.4.4 An application in DFlow-FM

Delft3D-FLOW computes its hydrodynamic structure on a curvilinear-grid; it requires the numerical grid to be orthogonal and well-structured. The advantage of this grid structure is the second order accuracy. However, the amount of freedom in the choice of grid shapes is limited. In case of DCSM, all grid cells are of a rectangular shape. As a results, land-water boundaries have a shape similar as a staircase profile. Kramer and Stelling (2008) showed that these type of boundaries may introduce a large amount of energy loss, caused by artificial boundary effects. When the flow through the Strait of Dover is considered, a reduction of this energy loss could lead to a significant increase of residual transport. However, since Delft3D-FLOW requires the grid to be orthogonal, a smoothing of the land-water boundaries is not possible. The use of another simulation package, which does not require the grid to be orthogonal, might give a solution to this problem. An example of such a program is the recently developed DFlow-FM package. DFlow-FM computes on an unstructured grid, based on the orthogonal unstructured mesh approach as stated by Casulli and Walters (2000). A full transformation and adaptation of the present DCSM model to DFlow-FM is beyond the scope of this thesis. However, a first preliminary simulation has been done in DFLow-FM. The representation of the DCSM model in DFlow-FM is compared to the output from Delft3D-FLOW to check if both models show a similar behaviour. The converted DCSM model used for this simulation is kept as identical as possible to the model as it was used in Delft3D-FLOW. Therefore, the model computes on a similar grid with rectangle grid cells. Both models give similar residual fluxes though the Strait of Dover with a difference of only 5%. Unfortunately it was not possible to smoothen the boundaries around the Strait of Dover due to lack of time. In case of further research, it is highly recommended to perform this smoothing, since it is expected to have a significant amount of influence.

6.5 Concluding remarks

In previous sections the influence of different processes on the residual flow through the Strait of Dover were examined. In section the effect of tidal en meteorological induced forcings were investigated for the year 2007. It was shown that the tide induced flow was responsible for the largest part of the transport with a contribution of more than 80%. The other 20% was due to meteorological forcings. Here the interaction between wind and atmospheric pressure is of great importance. In case the atmospheric pressure is not added as an external force the wind induced residual acts in contrary direction. In the current chapter, several adjustments were made with either a physical or numerical motivation. Their influences appeared to be small in comparison with the contribution of the tide and meteorological induced residuals. These contributions are summarized in table 6.1.

Process	Contribution
Tidal residuals	82%
Meteorological residuals	18%
- Wind	-30%
- IBM	48%
Bottom friction	6%
A0 component	1%
Baroclinic flow	-15%
Barotropic 3D	2%
WAQUA/Cyclic	0%
Coriolis discretization	0%
DFlow-FM	5%

Table 6.1: Contributions to residual flow for DCSMv6 for 2007

7 Conclusion & recommendations

The construction of Maasvlakte 2 releases a certain amount of SPM into the North Sea. The Port of Rotterdam is required to monitor this distribution. The MoS^2 has been set up by Deltares to investigate this distribution with the use of numerical modelling. The three-dimensional ZUNO-DD model has been set-up. However, the modelled residual circulation appeared to be significantly low in comparison with measured distributions. It is desired to improve this residual representation to gain optimal insight in the water quality of the North Sea. The residual circulation is for a large part determined by the in- and outflow of water at the North Sea boundaries. Since the ZUNO-DD obtains these values from a larger continental shelf model called DCSM. The focus of this thesis is also on the larger continental shelf model, since a good residual representation in ZUNO-DD can only be obtained when the obtained boundary conditions are correct. The state-of-the-art DCSMv6 model has a large computation time, therefore the former DCSMv5 model is used for preliminary simulations.

The time and spatial scales of residual currents are large. Time variations range from a few days to several years. For the large scale North Sea circulation horizontal variations of less than a few kilometres are insignificant. Accurate measurements on residual circulations are difficult to obtain. The main reason for this is that these currents are an order of magnitude smaller than fluid motions of shorter time scales, such as tidal fluctuations. Since the Strait of Dover is a relative narrow channel, measurements at this location are the most accurate one can obtain for the North Sea. This makes the Strait of Dover an extensively studied area. During the last century, many attempts were made to quantify the residual flow through the Strait of Dover. The first measurements date back to the late 1920's. Velocities were measured at different locations and integrated over the wet crosssection between Calais and Dover. Between 1955 en 1965, electric potentials through a telephone cable between Calais and Dover have been analysed. These potentials were related to a crosssectional mean velocity according Faraday's law of induction. With the introduction of high frequency radars, it was possible to monitor the spatial varying surface current of a certain area. Even though many different measurement techniques are used, their results show large deviations, ranging from 87000 to 235000 m^3s^{-1}. Starting from the late 1970's, numerical models made it possible to investigate the importance of different forcings on residual currents. Tidal transports are found to be approximately 30000 to 50000 m^3s^{-1}. Meteorological induced currents are in the same order of magnitude. Density driven residuals appeared to be rather low with a contribution of an order of magnitude smaller than tide driven transports.

A barotropic, depth averaged, simulation has been performed to investigate the representation of the general circulation pattern in the North Sea. Based on a zero-frequency Fourier analysis, it was shown that the general behaviour is similar as the pattern described by various authors. Some specific density driven flows, such as the current around the Dogger bank, are absent. However, other typical density driven currents like the cyclonic circulation pattern in the Skagerrak is clearly present. Boundary in- and outflows are relatively small at the Norwegian Coastal current and Strait of Dover. The age distribution of English Channel water has been investigated with the use of the Cap de la Hague experiment. The leakage of the radioactive nuclide Antimony-125 from La Hague has been simulated for the years 1985 and 1993. Results were compared to both measurements and other modelling studies. It was shown that especially in the English Channel the transit times are considerably large compared to measurements. The residence time from La Hague to the North Sea is approximately 7 months while other validated modelling studies suggest a residence time of only 3,5 months. After the English Channel water has reached the Dutch coast, the simulated transit time is represented in a much better way since they are comparable with other studies.

A quantitative analysis on residual flows through the Strait of Dover has been performed. The representation of the present model of tidal and meteorological induced residuals is investigated. A low-pass filter on the instantaneous discharge made it possible to properly

analyse the different residual components, including their time variations. For DCSMv6, a tidal residual flow of 45000 $m^3s^{-1}$was found. A linear approximation of wind induced residuals has been found by forcing the model with a uniform, stationary, wind velocity. A scaling analysis showed that linear approach to be legitimate. It can be used as a first approximation on residual flow. In addition, it can be compared to studies which did a similar analysis. The sensitivity to wind shear for the present model appeared to be larger than other modelling studies. A comparison between the stationary approach and the actual model simulation showed that the stationary approach gives comparable values on a daily scale with a correlation of 0,79. However, on annual scale, the approach overestimates the average flow with a factor two. Rapidly varying surface level differences between the North Sea and English Channel have a significant effect on the residual flow. A rapidly increasing North Sea water level reduces the net inflow, or can even reverse the direction of the flow. A combination of the meteorological and tidal forcings gives an annual flow of 56000 m^3s^{-1}. Daily and annual obtained results were compared to two models from the NOOS working group. These models are three dimensional and compute baroclinic flow. The two models, in combination with the present models, showed very different values ranging from a yearly average of 29000 to 85000m^3s^{-1}.

Several adjustments were made to the DCSMv6 model in order to obtain an increased residual flow through the Strait of Dover. A decrease in bottom friction gives a daily increase in magnitude of 29%. However, since daily transports can be either be flowing in or out of the North Sea, this increase reduces to only 6% on annual scale. A annual mean water level is imposed at the model boundaries to include the effect of steric height. However, since the model boundaries lie outside the continental shelf, its impact on the strait of Dover is small with only a 1% increase. Most of the increased mass transport travels along the continental shelf edge to the north. The effect of density variations is implemented in the depth averaged models. Initial North Sea density differences and fresh water inflows are introduced. Over the whole domain, the model fails to properly represent the hydrodynamic circulation at locations were currents are highly stratified in reality. This is for example clearly visible at the Skagerrak and Norwegian Coastal current, which are stratified density driven flows. Since the southern North Sea is in general well mixed, the hydrodynamic representation is much better represented. A small southward directed density component is introduced. It reduces the annual inflow though the Strait of Dover with 15%. Several numerical adjustments which are available within the Delft3D-FLOW package were made to the present model. Their effects on the transports through the Strait of Dover are negligible. Since also physical adjustments gave insignificant differences in transports, the conclusion can be drawn that the residual circulation cannot be improved within the Delft3D-FLOW package due to its numerical limitations.

Land-water boundaries have a shape similar as a staircase profile. Previous studies showed that these boundaries introduce a large amount of energy loss caused by artificial boundary effects. A reduction of this energy loss could lead to a significant increase of residual transport through the Strait of Dover. However, this is not possible in the present Delft3D-FLOW package. Another recent developed simulation program called DFlow-FM computes on an unstructured grid. One big advantage of this computation method is the ability of smoothing the land-water boundaries. Due to time limitations of this project a complete conversion and adaptation of the model to DFlow-FM was not possible. Therefore only a preliminary computation has been performed. The converted model was kept as close as possible to the Delft3D-FLOW version. A comparison between both models was done to investigate the difference in represented residuals due to different numerical approaches. Both programs gave similar residual fluxes through the Strait of Dover with a difference of only 5%. For further research it is highly recommended to investigate the effect of smoothened land-water boundaries around the Strait of Dover.

References

G.A. Alcock and D.E. Cartwright. An analysis of 10 years' voltage records from the dover-sangatte cable. *Deep-Sea Research*, 1977.

M. Blaas, K. Cronin, G.Y. El Serafy, Y.F. Friocourt, I.D.T.F. Garcia Triana, S. Gaytan Aguilar, and G.H. Keetels. MoS2: Model setup, data assimilation and skill assessment. Technical report, Deltares, 2012.

K.F. Bowden. The flow of water through the straits of dover, related to wind and differences in sea level. *Philosophical Transactions of the Royal Society of London. Series A, Mathematical and Physical Sciences*, 248(953):pp. 517–551, 1956.

J.N. Carruthers. *The Flow of Water Through the Straits of Dover as Gauged by Continuous Current Meter Observations at the Varne Lightvessel, Etc.* 1928.

D.E. Cartwright. A study of currents in the strait of dover. *Journal of Navigation*, 14: 130–151, 4 1961.

V. Casulli and R.A. Walters. An unstructured grid, three-dimensional model based on the shallow water equations. *International Journal for Numerical Methods in Fluids*, 32(3): 331–348, 2000.

A.M. Davies, S. Kwong, and R.A. Flather. Formulation of a variable-function three-dimensional model, with applications to the m2 and m4 tide on the north-west european continental shelf. *Continental Shelf Research*, 17(2):165–204, 1997.

G.J. De Boer. *On the interaction between tides and stratification in the Rhine Region of Freshwater Influence*. PhD thesis, Delft University of Technology, 2009.

G.J. De Boer, J.D. Pietrzak, and J.C. Winterwerp. Using the potential energy anomaly equation to investigate tidal straining and advection of stratification in a region of freshwater influence. *Ocean Modelling*, 22(1):1–11, 2008.

W.P.M. De Ruijter, L. Postma, and J.M. De Kok. *Transport atlas of the Southern North Sea*. Tech. rept. Rijkswaterstaat tidal waters division and Delft Hydraulics., 1987.

Deltares. *Delft3D-FLOW, version 3.15, user manual*. Rotterdamseweg 185; P.O. Box 177; 2600 MH; Delft; The Netherlands, 2013.

S. Dick, E. Kleine, S.H. Mller-Navara, H. Keline, and H. Komo. The operational circulation model of BSH (BHCmod) - model description and validation. *Brichte des Bundesamtes fur Seeschifffahrt und Hydrographie*, 29:44, 2001.

A.T. Doodson. The harmonic development of the tide-generating potential. *International Hydrographic Review*, 31:pp. 37–61, 1954.

C. Eckart. Properties of water, part ii. the equation of state of water and sea water at low temperatures and pressures. *American Journal of Science*, 256:225 – 240, 1958.

G. Godin. *The analysis of tides*. Liverpool University Press, 1972.

P. Guéguéniat, P. Bailly Du Bois, R. Gandon, J.C. Salomon, Y. Baron, and R. Leon. Spatial and temporal distribution (1987-91) of 125Sb used to trace pathways and transit times of waters entering the north sea from the english channel. *Estuarine, Coastal and Shelf Science*, 39(1):59 – 74, 1994.

J. Herrmann, P.J. Kershaw, P. Bailly du Bois, and P. Guéguéniat. The distribution of artificial radionuclides in the english channel, southern north sea, skagerrak and kattegat, 1990-1993. *Journal of Marine Systems*, 6(56):427 – 456, 1995.

J. Holt and R. Proctor. The seasonal circulation and volume transport on the northwest european continental shelf: A fine-resolution model study. *Journal of Geophysical Research: Oceans (1978-2012)*, 113(C6), 2008.

M.J. Howarth. North sea circulation. *Proudman Oceanographic Laboratory*, 2001.

J.A. Johannessen, S. Sandven, K. Lygre, E. Svendsen, and O.M. Johannessen. Three-dimensional structure of mesoscale eddies in the norwegian coastal current. *Journal of Physical Oceanography*, 19(1):3–19, 1989.

O.S. Kleptsova. Unstructured orthogonal meshes for modeling coastal and ocean flows. Master's thesis, Delft University of Technology, 2013.

S.C. Kramer and G.S. Stelling. A conservative unstructured scheme for rapidly varied flows. *International journal for numerical methods in fluids*, 58(2):183–212, 2008.

A.J. Lee. Chapter 14 north sea: Physical oceanography. In *The North-West European Shelf Seas: The Sea Bed and the Sea in Motion II. Physical and Chemical Oceanography, and Physical Resources*, volume 24, Part B, pages 467 – 493. Elsevier, 1980.

M.S. Longuet-Higgins. On the transport of mass by time-varying ocean currents. In *Deep Sea Research and Oceanographic Abstracts*, volume 16, pages 431–447. Elsevier, 1969.

P.J. Luyten, J.E. Jone, R. Proctor, A. Tabor, P. Tett, and K. Wid-Allen. *COHERENS A Coupled Hydrodynamical-Ecological Model for Regional and Shelf Seas: User Documentation. MUMM Report, Management Unit of the Mathematical Models of the North Sea.* 1999.

P.J. Luyten, J.E. Jones, and R. Proctor. A numerical study of the long-and short-term temperature variability and thermal circulation in the north sea. *Journal of Physical Oceanography*, 33(1), 2003.

T.A. McClimans, J.D. Pietrzak, V. Huess, N. Kliem, J.H. Nilsen, and B. Olaf Johannessen. Laboratory and numerical simulation of the skagerrak circulation. *Continental Shelf Research*, 20(9):941–974, 2000.

J.C.J. Nihoul and F.C. Ronday. The influence of the "tidal stress" on the residual circulation. *Tellus*, 27(5):484–490, 1975.

L. Otto, J.T.F. Zimmerman, G.K. Furnes, M. Mork, R. Saetre, and G. Becker. Review of the physical oceanography of the north sea. *Netherlands Journal of Sea Research*, 26 (2-4):161 – 238, 1990.

R. Pawlowicz, B. Beardsley, and S. Lentz. Classical tidal harmonic analysis including error estimates in matlab using t_tide. *Computers & Geosciences*, 28:929–937, 2002.

R.D. Pingree and D.K. Griffiths. Tidal fronts on the shelf seas around the british isles. *Journal of Geophysical Research: Oceans (1978–2012)*, 83(C9):4615–4622, 1978.

R.D. Pingree and D.K. Griffiths. Currents driven by a steady uniform wind stress on the shelf seas around the british isles. *Oceanologica Acta*, 3(2):227 – 236, 1980.

R.M. Ponte and P. Gaspar. Regional analysis of the inverted barometer effect over the global ocean using TOPEX/POSEIDON data and model results. *Journal of Geophysical Research: Oceans*, 104(C7):15587–15601, 1999.

D. Prandle. Residual flows and elevations in the southern north sea. *Proceedings of the Royal Society of London. A. Mathematical and Physical Sciences*, 359(1697):189–228, 1978a.

D. Prandle. Monthly-mean residual flows through the dover strait, 19491972. *Journal of the Marine Biological Association of the United Kingdom*, 58:965–973, 11 1978b. ISSN 1469-7769.

D. Prandle. A modelling study of the mixing of 137Cs in the seas of the european continental shelf. *Philosophical Transactions of the Royal Society of London. Series A, Mathematical and Physical Sciences*, 310(1513):pp. 407–436, 1984.

D. Prandle. Year-long measurements of flow-through the dover strait by HF radar and acoustic doppler current profilers (ADCP). *Oceanologica Acta*, 16(5-6):pp. 457–468, 1993.

D. Prandle and A.J. Harrison. Relating the potential difference measured on a submarine cable to the flow of water through the strait of dover. *Deutsche Hydrografische Zeitschrift*, 28(5):207–226, 1975.

D. Prandle, G. Ballard, D. Flatt, A.J. Harrison, S.E. Jones, P.J. Knight, S. Loch, J. McManus, R. Player, and A. Tappin. Combining modelling and monitoring to determine fluxes of water, dissolved and particulate metals through the dover strait. *Continental Shelf Research*, 16(2):237 – 257, 1996.

J. Proudman and A.T. Doodson. The principal constituent of the tides of the north sea. *Philosophical Transactions of the Royal Society of London*, 224:pp. 185–219, 1924.

J.C. Salomon and M. Breton. An atlas of long-term currents in the channel. *Oceanologica Acta*, 16(5-6):pp. 439–448, 1993.

J.C. Salomon, P. Guéguéniat, and M. Breton. Mathematical model of 125sb transport and dispersion in the channel. In *Radionuclides in the Study of Marine Processes*, pages 74–83. Springer Netherlands, 1991.

J.C. Salomon, M. Breton, and P. Guéguéniat. Computed residual flow through the dover strait. *Oceanologica Acta*, 16(5-6):pp. 449–455, 1993.

J.C. Salomon, M. Breton, and P. Guéguéniat. A 2d long term advectiondispersion model for the channel and southern north sea part b: Transit time and transfer function from cap de la hague. *Journal of Marine Systems*, 6(56):515 – 527, 1995.

J.H. Simpson. Physical processes in the ROFI regime. *Journal of Marine Systems*, 12:pp. 3–15, 1997.

J.H. Simpson and D. Bowers. Models of stratification and frontal movement in shelf seas. *Deep Sea Research Part A. Oceanographic Research Papers*, 28(7):727–738, 1981.

J.H. Simpson, W.G. Bos, F. Schirmer, A.J. Souza, T.P. Rippeth, S.E. Jones, , and D. Hydes. Periodic stratification in the rhine ROFI in the north sea. *Oceanologica Acta*, 16(1):pp. 23–32, 1993.

D.C. Slobbe. *Roadmap to a mutually consistent set of offshore vertical reference frames*. PhD thesis, Delft University of Technology, 2013.

S.D. Smith and E.G. Banke. Variation of the sea surface drag coefficient with wind speed. *Quarterly Journal of the Royal Meteorological Society*, 101(429):665–673, 1975.

G.S. Stelling and J. J. Leendertse. Approximation of convective processes by cyclic AOI methods. *Estuarine and coastal modeling*, 91:pp. 771–782, 1992.

R.H. Stewart. *Introduction to Physical Oceanography*. Orange Grove Books, 2009.

G.I. Taylor. Tidal Oscillations in Gulfs and Rectangular Basins. *Proceedings of The London Mathematical Society*, s2-20:148–181, 1922.

R. O. R. Y. Thompson. Low-Pass Filters to Suppress Inertial and Tidal Frequencies. *Journal of Physical Oceanography*, 13:1077–1083, June 1983.

M.N. Tsimplis, A.G.P. Shaw, R.A. Flather, and D.K. Woolf. The influence of the north atlantic oscillation on the sea-level around the northern european coasts reconsidered: the thermometric effects. *Philosophical Transactions of the Royal Society*, 364:pp. 845–856, 2006.

J.A. Van Pagee, H. Gerritsen, and W.P.M. de Ruijter. Transport and water quality modelling in the southern north sea in relation to coastal pollution research and control. *Water Science & Technology*, 18(4-5):245–256, 1986.

J. Van Veen. Water movements in the straits of dover. *Journal du Conseil*, 13(1):7–36, 1938.

J. Van Wiechen. Modelling the wind-driven motions in the rhine ROFI. Master's thesis, Delft University of Technology, 2011.

J.J. Velema. On the tidal dynamics of the north sea. Master's thesis, University of Twente, 2010.

R.A. Walters and C. Heston. Removing Tidal-Period Variations from Time-Series Data Using Low-Pass Digital Filters. *Journal of Physical Oceanography*, 12:112–112, January 1982.

H. Wanner, S. Bronnimann, C. Casty, D. Gyalistras, J. Luterbacher, C. Schmutz, Stephenson D.B., and E. Xoplaki. North atlantic oscillation - consepts and studies. *Survays in Geophysics*, 22:321 – 382, 2001.

N.G. Winther and J.A. Johannessen. North sea circulation: Atlantic inflow and its destination. *Journal of Geophysical Research: Oceans*, 111(C12), 2006.

F. Zijl. Development of the next generation dutch continental shelf flood forecasting models. Technical report, Deltares, 2013.

List of Symbols

Roman Symbols

A	[L^2]	crosssectional or surface area
c	[ML^{-3}]	concentration
C	[$L^{1/2}T^{-1}$]	Chézy coefficient
C_D	[-]	wind drag coefficient
d	[L]	bottom depth
D	[L^2T^{-1}]	eddy diffusivity
Ek	[-]	Ekmann number
f	[T^{-1}]	Coriolis parameter
g	[LT^{-2}]	gravitational acceleration
G	[L^3T^{-1}]	gross transport
h	[L]	water depth ($h = d + \eta$)
k	[ML^{-3}]	friction coefficient
L_{Ro}	[L]	Rossby radius of deformation
M	[L^3]	cumulative flow
n	[$L^{-1/3}s$]	Manning's coefficient
p	[$ML^{-1}T^{-2}$]	pressure
q	[L^2T^{-1}]	specific discharge
Q	[L^3T^{-1}]	discharge
Ro	[-]	Rossby number
t	[T]	time
u, v, w	[LT^{-1}]	velocity in x, y, z direction, respectively
U, V	[LT^{-1}]	depth averaged velocity in x, y direction, respectively
W	[LT^{-1}]	wind velocity
x, y, z	[L]	spatial coordinates

Greek Symbols

η	[M]	surface level elevation
λ	[-]	longitude
λ	[T^{-1}]	decay rate of radioactive substance
θ	[-]	phase
θ_w	[-]	wind direction
φ	[-]	latitude
ϕ	[-]	tidal potential for equilibrium tide
Π	[$L^{-1}T^{-1}$]	potential vorticity
ν	[L^2T^{-1}]	eddy viscosity
ρ	[ML^{-3}]	density of water
ρ_a	[ML^{-3}]	density of air
τ	[$ML^{-1}T^{-2}$]	stress tensor
τ	[T]	time scale
ω	[T^{-1}]	vorticity, frequency

Additions

$\hat{n}$	amplitude
$\bar{n}$	time averaged quantity
$\langle n \rangle$	spatial averaged quantity
$\vec{n}$	vectorized unit
$\lvert n \rvert$	magnitude

Abbreviations

DCSM	Dutch Continental Shelf Model
NWECS	Northwest European Continental Shelf
MoS^2	Model-Supported Monitoring of SPM
MV2	Maasvlakte 2
ROFI	Region of Freshwater Influence
SPM	Suspended Particulate Matter
ZUNO-DD	Zuidelijke Noordzee Domain Decomposition

List of Figures

List of Tables